CARDIORESPIRATORY AND VASCULAR FUNCTION DURING STRESS

by

CARL JACOB ADE

B.S., Kansas Wesleyan University, 2004

M.S., Kansas State University, 2008

AN ABSTRACT OF A DISSERTATION

submitted in partial fulfillment of the requirements for the degree

DOCTOR OF PHILOSOPHY

Department of Anatomy and Physiology
College of Veterinary Medicine

KANSAS STATE UNIVERSITY
Manhattan, Kansas

2013

Abstract

The primary aim of this dissertation was to evaluate the factors that contribute to the cardiorespiratory and vascular responses following exercise conditioning and microgravity deconditioning. The first study of this dissertation (Chapter 2) revealed that exercise training in the head down tilt posture, which places increases central blood volume compared to upright, results in cardiorespiratory adaptations in both upright and head down tilt postures which are not completely expressed with exercise training in the upright posture. These findings suggest that augmentation of the ventricular volume load during exercise training may result in adaptations that transfer across multiple body positions. In the second and third studies measurements of blood velocity and flow were performed via Doppler ultrasound. In Chapter 3 we observed that in the brachial and femoral arteries blood moves with a slightly blunted parabolic velocity profile that is very stable across a range of mean arterial pressures and downstream limb resistances. We concluded that these findings support the current calculations of shear rate based on the assumptions of laminar flow. With these assumptions confirmed, the investigation in Chapter 4 could be performed. We observed that acute exposure to a sustained antegrade shear rate, via unilateral forearm heating, increased measurements of flow-mediated dilation and the overall rate of adjustment for forearm blood flow and vascular conductance during dynamic handgrip exercise. These findings suggest that one potential stimulus for improvements in vascular function and health following exercise conditioning may be exposure to elevations in antegrade shear. Lastly in Chapter 5 we changed focus to the cardiorespiratory deconditioning following long-duration microgravity exposure. We retrospectively reviewed and analyzed previous investigations of microgravity deconditioning and demonstrated that the decrease in maximal O_2 consumption ($\dot{V}O_2$max) occurs as a function of duration of exposure and that both convective and diffusive O_2 transport pathways substantially contribute to this decline. In addition we reviewed the current literature and highlighted potential mechanisms, across several organ systems, which may contribute to this decline in $\dot{V}O_2$max. Collectively, these studies revealed the breath of plasticity for cardiorespiratory adaptations to a variety of stressors.

CARDIORESPIRATORY AND VASCULAR FUNCTION DURING STRESS

by

CARL JACOB ADE

B.S., Kansas Wesleyan University, 2004

M.S., Kansas State University, 2008

A DISSERTATION

submitted in partial fulfillment of the requirements for the degree

DOCTOR OF PHILOSOPHY

Department of Anatomy and Physiology
College of Veterinary Medicine

KANSAS STATE UNIVERSITY
Manhattan, Kansas

2013

Approved by:

Major Professor
Dr. Thomas J. Barstow

Copyright

CARL JACOB ADE

2013

.

Abstract

The primary aim of this dissertation was to evaluate the factors that contribute to the cardiorespiratory and vascular responses following exercise conditioning and microgravity deconditioning. The first study of this dissertation (Chapter 2) revealed that exercise training in the head down tilt posture, which places increases central blood volume compared to upright, results in cardiorespiratory adaptations in both upright and head down tilt postures which are not completely expressed with exercise training in the upright posture. These findings suggest that augmentation of the ventricular volume load during exercise training may result in adaptations that transfer across multiple body positions. In the second and third studies measurements of blood velocity and flow were performed via Doppler ultrasound. In Chapter 3 we observed that in the brachial and femoral arteries blood moves with a slightly blunted parabolic velocity profile that is very stable across a range of mean arterial pressures and downstream limb resistances. We concluded that these findings support the current calculations of shear rate based on the assumptions of laminar flow. With these assumptions confirmed, the investigation in Chapter 4 could be performed. We observed that acute exposure to a sustained antegrade shear rate, via unilateral forearm heating, increased measurements of flow-mediated dilation and the overall rate of adjustment for forearm blood flow and vascular conductance during dynamic handgrip exercise. These findings suggest that one potential stimulus for improvements in vascular function and health following exercise conditioning may be exposure to elevations in antegrade shear. Lastly in Chapter 5 we changed focus to the cardiorespiratory deconditioning following long-duration microgravity exposure. We retrospectively reviewed and analyzed previous investigations of microgravity deconditioning and demonstrated that the decrease in maximal O_2 consumption ($\dot{V}O_2$max) occurs as a function of duration of exposure and that both convective and diffusive O_2 transport pathways substantially contribute to this decline. In addition we reviewed the current literature and highlighted potential mechanisms, across several organ systems, which may contribute to this decline in $\dot{V}O_2$max. Collectively, these studies revealed the breath of plasticity for cardiorespiratory adaptations to a variety of stressors.

Table of Contents

List of Figures

List of Tables

Acknowledgements

Throughout my graduate career there have been many wonderful individuals who have helped guide me on my path towards this advanced degree. From the first day in the program I have felt a part of the "family" and I am privileged to have been around a group of truly great minds and people.

I especially thank Dr. Thomas J. Barstow for his outstanding mentorship. Over the past 7 years he has gone above and beyond with his patience and willingness to let me pursue my scientific interests and at times lofty dreams. His enthusiasm to take a chance on my ideas has given me the confidence to follow my passions in the years to come.

In addition to Dr. Barstow, I am thankful for the professional support and scientific guidance from my Doctoral committee members: Dr. Craig A. Harms, Dr. Tim I. Musch, Dr. David C. Poole, Dr. Brett J. Wong, Dr. Gary D. Gadbury. The additional experiences and opportunities to work in the laboratories of Dr. Harms and Dr. Wong have been instrumental in giving me a greater breadth of knowledge and research experience. Likewise, a special thanks to Dr. Musch and Dr. Poole for the time, advice and the multiple opportunities that have been pivotal in my progress as a scientist in-the-making.

I also want to thank the many former and current graduate students with whom I've had the privilege of working with including: Dr. Steven Copp, Susanna Schlup, Samuel Wilcox, Jesse Craig, Dr. Daniel Hirai, Dr. Sara Corn, Josh Smith, Ben Skutnick, Calli Dunnum, and Sarah Fieger. I would also like to give a special thanks to Ryan Broxterman who has made the last several years rewarding, productive, fun, and above all exciting.

A special gratitude and appreciation goes to my family. To my parents for instilling in me the values of honesty and hard work, that have been the cornerstone for all my achievements. Finally, my treasured wife Kala Ade for supporting me through the years of crazy hours, scatter brained moments and periodic grumpiness. Without her by my side this journey would not have come so far and I would likely be living in a box in the back of the lab.

Preface

Chapters 2-4 of this dissertation represent original research papers that have been published or are currently under review in peer-reviewed journals (citations may be found below).

Ade, CJ, Broxterman, RM, Barstow, TJ. Effects of body posture and exercise training on cardiorespiratory responses to exercise. *Resp Phys Neurobiol* 188, 39-48, 2013

Ade CJ, Broxterman RM, Wong BJ, Barstow TJ. Antegrade and Retrograde Blood Velocity Profiles in the Intact Human Cardiovascular System. *Exp Physiol* 97 (7), 849-60, 2012

Ade, CJ, Broxterman, RM, Craig J, Schlup SJ, Wilcox SL, Barstow, TJ. Influence of prior sustained antegrade shear rate on the vascular responses during dynamic forearm exercise. *Exp Physiol*. In review

A part of Chapter 2 within this dissertation contains data collected as part of a master's thesis. This part consists of the data that pertains to the aims focused on the comparison of the acute cardiorespiratory responses to incremental head down tilt exercise with those during upright exercise.

Chapter 1 - Introduction

The stress of sustained dynamic exercise requires the integration of individual physiologic systems controlling the movement of molecular oxygen from atmospheric air to muscle mitochondria. With the transition from rest to exercise O_2 transport requires: (i) the appropriate pulmonary ventilation and ventilation-to-perfusion ratio within the lung; (ii) an effective alveolar-to-pulmonary capillary diffusion capacity; (iii) blood that contains a normal hemoglobin structure and concentration; (iv) a cardiac structure and function that can effectively increase cardiac output via increases in stroke volume and heart rate; (v) a peripheral circulation capable of increasing muscle blood flow via targeted increase in vascular conductance and preferential distribution of cardiac output to active tissue without compromising arterial blood pressure; (vi) normally functioning capillary hemodynamics capable of increasing red blood cell (RBC) flux and capillary hematocrit; and (vii) adequate intramuscular structures (i.e., myoglobin and mitochondria), enzymes, and substrates for cellular respiration (181, 203, 249). Furthermore, these demands on the pulmonary, cardiovascular, and muscular systems are exercise intensity dependent, such that during maximal aerobic exercise ($\dot{V}O_2$max) all steps within the O_2 transport pathway are important determinants (241, 242).

Of the above systems that contribute to $\dot{V}O_2$max, the cardiovascular system is one that plays a critical role in coupling pulmonary gas exchange with O_2 diffusion and utilization within the active skeletal muscle. In addition, the cardiovascular system demonstrates a significant plasticity to adapt to alterations in hemodynamic and environmental stress. Two stressors that result in widespread adaptations within the cardiovascular system include exercise conditioning and exposure to microgravity. Following both stressors, significant adaptations in structural and functional components of the cardiovascular system are observed and often contribute to the paralleled changes in $\dot{V}O_2$max (17, 202). However, questions still remain surrounding the stimuli that mediate the changes in cardiorespiratory function in response to these stressors (51, 131, 203). It is therefore the primary aim of the current dissertation to evaluate the factors that

contribute to the cardiorespiratory and vascular responses following exercise conditioning and microgravity deconditioning.

Following a period of aerobic exercise conditioning, increases in maximal cardiac output and systemic O_2 transport are achieved (17). This improved cardiac function can be attributed to a larger stroke volume stemming primarily from increases in ventricular end-diastolic volume, ventricular compliance, and increased diastolic filling. One mechanism mediating these adaptations is the "chronic volume overload" or cardiac distension that occurs during dynamic exercise (17, 203). Within a given exercise session the increased cardiac filling and subsequent increased cardiac distension, observed as an increased left ventricular end-diastolic volume and stroke volume, may act as an exercise stimulus for myocardial adaptation. However, it is unknown if augmentations in ventricular filling during exercise training impact cardiorespiratory adaptations. Therefore, in chapter 2 of this dissertation we utilized an exercise training protocol in the head down tilt posture to induce changes in ventricular filling, and examined the effects of this on stroke volume and aerobic capacity. Previous investigations have demonstrated that the head down tilt posture increases central venous pressure, an index of effective ventricular filling pressure, and left ventricular end-diastolic volume compared to upright and supine postures (81, 115, 166). As such we hypothesized that (i) endurance training in the upright posture would increase $\dot{V}O_2$peak, sub-maximal stroke volume, and peak stroke volume during upright exercise, but not during head down tilt exercise, (ii) training in the head down tilt posture would increase $\dot{V}O_2$peak, sub-maximal stroke volume, and peak stroke volume in both upright and head down tilt testing postures, and (iii) that the increase in sub-maximal and peak stroke volume would be greater after head down tilt training compared to upright.

Within the peripheral circulation, adaptations to exercise conditioning positively impact vascular structure, function, and overall cardiovascular health (83, 131, 172). One key exercise stimulus mediating these vascular adaptations may be the mechanical shear stress acting on the endothelium, consequent to the increased vascular conductance and blood flow observed during dynamic exercise (164). Previous reports suggest that endothelial cells exposed to different types and magnitudes of shear stress exhibit a cascade of increased intra-cellular signaling which will

influence endothelial cell phenotype. Moreover, sustained increases in antegrade shear stress similar to that experienced during exercise, increased nitric oxide bioavailability and endothelial function, while retrograde and oscillatory shear patterns are associated with a pro-atherosclerotic state and a decrease in endothelial function (131). However, this apparent plasticity for endothelial cell phenotype via modification of the shear stress pattern is not completely defined.

Recent reports highlight the current assumptions made when assessing shear stress non-invasively via Doppler ultrasound (92, 176). One critical assumption has been that blood flow through peripheral arteries has laminar properties resulting in a parabolic velocity profile, and that the profile remains steady when the cardiovascular system is under stress. Given the potential for shear stress to modify vascular function and the possible error associated with the above assumptions, we first set out to determine the blood velocity profile in the intact human cardiovascular system when downstream vascular resistance was elevated (cold pressor test) and decreased (exercise) (Chapter 3). Following this investigation, we determined the effects of sustained antegrade shear stress, independent of muscular contractions, on the vasodilator responses to exercise (Chapter 4).

Unlike exercise conditioning, the cardiorespiratory adaptations to sustained microgravity results in a "spaceflight deconditioning" that becomes evident when gravity is restored. The characteristics of this deconditioning include decreases in total blood volume (5), cardiac function and mass (60, 177), an impaired macro- and microvascular function (146, 217, 221), and skeletal muscle atrophy (77, 234, 235). In addition, one important hallmark response of this deconditioning is a significant decrease in $\dot{V}O_2$max upon return to gravity (34, 36, 247). However, there are currently no investigations that have determined the importance of the various independent variables within the O_2 transport pathway to the decline in $\dot{V}O_2$max following sustained microgravity exposure. Given the versatility of the integrative model advocated by Wagner and associates in describing the determinants of $\dot{V}O_2$max in health and disease, we applied a similar technique to microgravity exposure (Chapter 5) (202, 239, 241, 242).

In chapter 5 we present a model for the rate of decline in $\dot{V}O_2max$ as a function of microgravity exposure. Then using Fick's Principle of Mass Conservation and Law of Diffusion for O_2 movement we calculated the convective and diffusive components of $\dot{V}O_2max$ following 60 and 360 days of microgravity exposure. In addition, we review the current literature and highlight potential mechanisms contributing to this decline in $\dot{V}O_2max$.

Chapter 2-5 of this dissertation are self-contained and are presented in standard journal article format (Introduction, Methods, Results, Discussion). Chapter 6 provides an overall summary and conclusion for the above series of investigations.

Chapter 2 - Effects of body posture and exercise training on cardiorespiratory responses to exercise

Summary

The primary aims of the present study were to evaluate cardiorespiratory responses to incremental head down tilt exercise and to determine if the cardiorespiratory adaptations obtained from endurance training in the head down tilt posture transfer to the upright posture. 22 men (25 ± 3 yrs) performed $\dot{V}O_2$peak cycle exercise tests in the upright and head down tilt postures. Of these, 11 men were endurance trained on a cycle ergometer in the upright posture for 8 wks (upright training group; UTG) or in the upright posture for 4 wks followed by 4 wks in the head down tilt posture (head down training group; HTG). During acute exercise, $\dot{V}O_2$peak was decreased in the head down tilt posture compared to upright (2.01 ± 0.51 vs. 2.32 ± 0.61 L/min respectively, $P < 0.05$). Stroke volume (SV) at 100 Watts was greater during head down tilt cycling compared to the upright (77 ± 5 vs. 71 ± 4 ml/beat, $P < 0.05$). Following training $\dot{V}O_2$peak increased in both groups during upright exercise. However, $\dot{V}O_2$peak during head down tilt cycling was only increased in the HTG. Sub-maximal and peak SV in the HTG increased in both upright and head down tilt postures. SV in the UTG increased only in the upright posture and was unchanged during head down tilt cycling. In conclusion, acute head down tilt exercise increases sub-maximal SV compared to upright exercise. Furthermore, training in the head down tilt posture induces cardiorespiratory adaptations in both upright and head down tilt postures, while the adaptations to upright exercise training are primarily observed when upright exercise was performed.

Introduction

At rest, the transition from the upright to the supine posture increases ventricular preload and stroke volume (SV) (12, 13, 180, 206, 226). This altered gravitational vector and reduced hydrostatic column increase pulmonary capillary wedge pressure, an index of ventricular filling pressure, and ventricular end-diastolic volumes (180, 226). Similar cardiovascular responses are observed during supine cycling. Poliner et al. (180) demonstrated that supine cycling at an intermediate intensity (~98-122 Watts) increased left ventricular end-diastolic volume compared to upright cycling, suggesting greater cardiac filling. These findings are supported by additional reports of an elevated SV during supine exercise compared to upright (12, 13, 66, 139, 180, 198, 199, 226).

Similar to the supine posture, the head down tilt posture has been widely used to further redistribute blood volume toward the central cavity (81, 114, 115, 166). Kakurin et al. (114) demonstrated that a head down tilt posture is associated with a greater central fluid shift compared to the supine position. As such, the head down tilt bed rest model is commonly used in place of the supine model to simulate the effects of microgravity. In addition, short duration head down tilt studies have consistently demonstrated a greater increase in central venous pressure and left ventricular end-diastolic volume compared to supine rest (81, 166). This increase in ventricular preload and chamber volume caused by the head down tilt posture, coupled with the Frank-Starling relationship, results in a greater SV compared to the supine posture (203). However, to our knowledge no study has reported the effects of exercise on SV in the head down tilt posture.

In addition to postural differences in central cardiovascular responses, comparisons between dynamic upright and supine exercise models reveal that cycling in the supine position decreases both $\dot{V}O_2$peak and time-to-exhaustion relative to upright posture (59, 65-67, 117, 122, 192, 198). Egna et al. (65) demonstrated that the decrease in exercise time-to-fatigue between upright and supine exercise is correlated with the height of the hydrostatic column. Therefore,

the decreased $\dot{V}O_2$peak observed previously during supine exercise is often attributed to a decreased gravitational assistance to muscle blood flow, which would be aggravated in head down tilt posture. However, to date, the forearm (78, 104, 254) and arm cranking (124) exercise models have been the primary methods used to examine the cardiorespiratory adjustments to exercise when the contracting muscle is placed above the heart. To our knowledge it remains unknown how dynamic large muscle mass exercise performance is affected when performed above heart-level, like that achieved with head down tilt posture (Figure 2.1).

Training adaptations of the cardiorespiratory system in response to chronic exercise include increases in $\dot{V}O_2$peak, lactate threshold (LT), and SV (112). Previous studies have demonstrated a strong postural specificity for training induced cardiorespiratory adaptations. Ray and colleagues (198, 199) trained individuals for 8 wks in either the upright or supine posture. Training consisted of a combination of high-intensity interval and endurance training. These investigators demonstrated significant increases in $\dot{V}O_2$peak in both groups. However, the increase in $\dot{V}O_2$peak displayed significant postural specificity so that greater increases in aerobic capacity were seen when subjects were tested in the specific training posture. Similarly, each group only demonstrated a training induced increase in SV when measured in their respective training posture. These data suggest a lack of transfer between upright and supine postures. However, to date, it is unknown if the increased ventricular preload and chamber volumes associated with resting head down tilt posture compared to upright and supine postures will result in cardiorespiratory training adaptations that will transfer to traditional upright exercise.

The rationale for the present study was that because effective ventricular filling is greater during resting head down tilt posture compared to supine and upright postures (81, 115, 166), cycling training in the head down tilt posture may result in greater ventricular adaptations compared to upright training and that the increased CO and SV would increase $\dot{V}O_2$peak when measured in both the upright and head down tilt postures. Therefore, the primary aims of the present study were to 1) compare the acute cardiorespiratory responses to incremental head down tilt exercise with those during upright exercise, and 2) to determine if the cardiorespiratory adaptations obtained from endurance training in the head down tilt posture transfer to the upright condition. It was hypothesized that (i) head down tilt exercise would increase sub-maximal SV,

8

but decrease $\dot{V}O_2$peak compared to upright exercise. Furthermore, it was hypothesized that (ii) endurance training in the upright posture would increase $\dot{V}O_2$peak, sub-maximal SV, and SVpeak during upright exercise, but not during head down tilt exercise, but that (iii) training in the head down title posture would increase $\dot{V}O_2$peak, sub-maximal SV, and SVpeak in both upright and head down tilt testing postures. In addition, it was hypothesized (iv) that the increase in sub-maximal and SVpeak would be greater after head down tilt training compared to upright.

Methods

Subjects

22 men (age 25 ± 3 yrs (mean ±SD); stature 177.5 ± 8.2 cm; mass 75.0 ± 17.6 kg; BMI 23.8 ± 17.6 kg x m^{-2}) completed the experiments. All subjects were free from known cardiovascular, pulmonary, or metabolic disease and were non-smokers as determined from medical history questionnaire. None were regularly participating in structured exercise activities before their involvement in the study. Verbal and written consent were obtained from all subjects following approval of the study by the Institutional Review Board for Research Involving Human Subjects at Kansas State University, which conformed to the Declaration of Helsenki.

Experimental Design

All testing was completed in an air-conditioned laboratory at a temperature of 20-25°C. Each subject performed two randomly ordered exercise protocols on different days. One testing session consisted of a graded cycling test in the upright posture, while in the other session a graded cycling test in the -6° head down tilt posture was performed (Figure 1). Upright cycle tests were performed on a electronically braked cycle ergometer (800 Ergometer, SensorMedics, USA). Head down tilt cycle tests were performed on a mechanically braked Monarck 818E cycle ergometer mounted to a custom-made apparatus that placed the subject in the appropriate exercising posture with the crank shaft ~10 cm above the level of the subject's back resulting in -6° head down tilt posture. Both cycle ergometers were calibrated to ensure accurate work load settings prior to the beginning of the study and pilot work determined that each ergometer elicited similar exercise responses as evident by a similar $\dot{V}O_2$ (800 Ergometer,1.11±0.11 vs Monarck,1.16±0.12 l min-1, P>0.05) and heart rate (800 Ergometer,125±20 vs Monarck,123±16 bpm, P>0.05) at 100 Watts. During head down tilt cycling subjects laid on a padded mat with their feet secured to the pedals. At each test the subject was positioned to allow a slight bend in the knee when the leg was fully extended and seat height was recorded to ensure consistency across testing sessions. Following 5-minutes of baseline rest, the subjects began cycling at 60 revolutions per minute at 20 Watts for additional 5-minutes. The work rate then progressively

increased 25 Watts every minute until the subject could not maintain the pedal rate for 5 consecutive revolutions, despite verbal encouragement.

Following the completion of each testing sessions, 11 of the initial 22 subjects completed two additional exercise training periods (Table 1). These subjects underwent two 4 wk periods of endurance cycling training. All sessions were performed on a mechanically braked Monarch 818E cycle calibrated prior to the study. Seat height was recorded to ensure consistency across training sessions. The first training period consisted of 4 wk of upright cycling at 70% $\dot{V}O_2$peak for 1 h/day, 3 days/wk. This initial 4 wk training period provided a comparable level of training stimuli across all groups at an attempt to normalize each subject's fitness level prior to the postural training intervention. Following the initial training period, subjects were tested again (Midtest) and randomly sub-divided into either a continued upright training group (UTG) or a head down tilt training group (HTG). This second training period consisted of 4 wk cycling at 70% posture specific $\dot{V}O_2$peak for 1 h/day,3 days/wk. Following the second training period each subject performed graded cycling tests in the upright and head down tilt postures on separate days (Posttest). Brief periods of rest were permitted during the training sessions, if necessary, and was not included in the total exercise session time. Heart rate was monitored during each training session to ensure the correct exercise intensity was achieved. The subjects were instructed to maintain their normal levels of physical activity and dietary habits throughout the training period. This study design allows for the initial training adaptations due to an increased level of physical activity to occur within the initial 4 wk training period allowing for any further adaptations following the second 4 wk (i.e., Midtest vs Posttest) period to be primarily the result of the training posture.

Experimental Measurements

Breath-by-breath metabolic and ventilatory data were continuously measured during all exercise tests (SensorMedics 229 Metabolic Cart, SensorMedics Corp.,Yorba Linda, CA) and converted to fifteen second mean. Heart rate (HR) was collected continuously with a four lead ECG interfaced to the metabolic cart. Oxygen pulse was measured as the oxygen consumption

11

per heart beat. The maximum 15 s average $\dot{V}O_2$, $\dot{V}CO_2$, HR, and $\dot{V}E$ obtained during the incremental tests were considered as peak values for a given exercise condition. The $\dot{V}O_2$ corresponding to the lactate threshold was determined as the $\dot{V}O_2$ at which $\dot{V}CO_2$ increased out of proportion with respect to $\dot{V}O_2$ and an increase in $\dot{V}E/\dot{V}O_2$ with no increase in $\dot{V}E/\dot{V}CO_2$ (8).

Pulmonary capillary blood flow was determined via an acetylene single-breath exhalation technique and used as an index of cardiac output (CO) at rest and when possible 30 seconds into a minimum of three exercise stages ranging between 50-200W. The acetylene single-breath exhalation technique has been used previously to estimate cardiac output at rest and during exercise (57, 62, 140). Since acetylene and carbon monoxide are both soluble in blood, during the constant exhalation the concentrations of acetylene and carbon monoxide decline at a rate that is proportional to pulmonary capillary blood flow (252). Subjects were instructed to take a full inhalation of a test gas mixture of 0.3% methane, 0.3% acetylene, 0.3% carbon monoxide, 21% oxygen, with the remainder nitrogen. Following maximal inhalation, subjects were told to exhale at a constant rate of 200-800 ml/s for at least 3 seconds. Each CO value was accepted if the subject performed the procedure correctly and the data output was sufficient to make the calculations. The CO: $\dot{V}O_2$ relationship was determined for each subject via linear regression and interpolated to find the CO at 100 watts and extrapolated to the CO at $\dot{V}O_2$peak. The regression equation provided a more accurate analysis of the data during exercise than a single measurement. The sub-maximal intensity of 100 watts was used to compare with the protocol previously used by Poliner et al. (1980) and Ray et al. (1990). The calculated CO was divided by the time-aligned heart rate to calculate SV. Pulmonary capillary blood flow can underestimate CO due to intrapulmonary shunts and therefore values reported in the current study should not be directly compared with values measured via echocardiography (207).

Statistical Analysis

Data are given as mean ± SD. The effects of head down tilt cycling on the cardiorespiratory adjustments to incremental exercise in the initial 22 subjects were tested by paired T-tests. The effects of training and posture on the cardiorespiratory function were tested by a two-way within-subject analysis of variance with the between factor 'training group' (UTG

versus HTG) and the repeated factor 'time' (Pretest *versus* Midtest *versus* Posttest). Significant interactions or main effects were determined with Student-Newman-Keuls Method as a post hoc analysis test. Significance was set at $p < 0.05$ for all analyses.

Results

Acute Responses

Table 2-2 summarizes the group mean peak cardiorespiratory response to acute upright and head down tilt exercise. Exercise times and peak power outputs were significantly greater in the upright than head down tilt posture. Head down tilt exercise decreased both absolute and relative $\dot{V}O_2$peak compared to upright. Peak HR was significantly decreased during head down tilt exercise compared to upright exercise. The mean $\dot{V}O_2$ at LT was significantly lower during head down tilt cycling compared to upright. However, relative to $\dot{V}O_2$peak there was no difference between the two postures. Peak respiratory exchange ratio was not significantly different between the two postures.

$\dot{V}O_2$ and HR at 100 Watts were not significantly different between the two postures. Figure 2 illustrates the individual and group mean SV responses at 100 watts. Notice that sub-maximal SV is significantly greater during head down tilt exercise compared to upright (73.9 ± 10.6 vs. 67.5 ± 8.5 ml respectively; $P < 0.001$). This increase resulted in an elevated sub-maximal CO during head down tilt exercise. In addition, sub-maximal O_2 pulse ($\dot{V}O_2$/ HR) was increased during head down tilt exercise compared to upright (8.9 ± 1.3 vs. 8.1 ± 1.3 ml O_2 x beat^{-1} respectively, $P < 0.001$).

Training Adaptations

Table 2-3 summarizes the mean cardiorespiratory responses to training. $\dot{V}O_2$peak during upright exercise increased significantly in the UTG after 8 wks compared to Pretest (Figure 2.3A). However, in the HTG Posttest-$\dot{V}O_2$peak during upright cycling was significantly increased above both Pretest and Midtest values (Figure 2-3B). Similarly, when measured during head down tilt cycling, Posttest-$\dot{V}O_2$peak only slightly, but significantly, increased in the UTG after 8 wks compared to Pretest, while it was significantly greater in the HTG compared to Pretest and Midtest values (Figure 2-3 C and D). Both groups demonstrated similar changes in maximal O_2 pulse. No significant changes occurred in RERpeak or HRpeak after training in

either group. The mean $\dot{V}O_2$ at LT measured during upright exercise was unchanged in the UTG and HTG. The LT in the UTG increased significantly during head down tilt exercise after 8 wks. When measured as a percent of $\dot{V}O_2$peak, LT was unchanged after training in both groups.

Figure 2-4 illustrates the peak SV responses to training. During upright exercise peak CO and SV significantly increased at 4 wks in the UTG but did not increase further, whereas in the HTG COpeak and SVpeak were increased after 8 wks above Pretest and Midtest values. Similarly, COpeak and SVpeak during head down tilt cycling did not change in the UTG, but significantly increased in the HTG.

Sub-maximal cardiorespiratory responses to training during upright and head down tilt exercise at 100 Watts are summarized in Table 2-4. There were no significant changes in $\dot{V}O_2$ or HR at 100 Watts after training in either group. Similar to peak responses, sub-maximal SV during upright exercise increased in both groups after 8 wks of training (Figure 2-5). However, sub-maximal SV during head down tilt cycling was significantly increased only in the HTG.

Discussion

The primary findings of the present study are that acute exercise in the head down tilt posture results in an approximately 10% greater sub-maximal stroke volume compared to upright posture, and that chronic endurance training in the head down tilt posture increases maximal cardiorespiratory performance during both head down and upright exercise. These findings are consistent with our first hypothesis. The second and third hypotheses were also well supported by the data. In addition, the increase in $\dot{V}O_2$peak, CO, and SV following training in the upright posture (UTG) was only observed during upright cycling, as it did not transfer to HDT cycling. Conversely, the effects of head down tilt training (HTG) transferred to both upright and head down tilt cycling. Training in the upright posture increased $\dot{V}O_2$peak by ~4%, with no significant change in SV during head down tilt cycling after 8 wk of training compared to the ~17% and ~12% significant increase in $\dot{V}O_2$peak and SV, respectively, achieved with 4 wk of training in the head down tilt posture. However, similar increases in $\dot{V}O_2$peak during upright cycling were observed between upright (~7%) and head down tilt (~10%) training groups. In addition, the data is inconsistent with the fourth hypothesis in that the increase in stroke volume was not greater after head down tilt training compared to upright training (Table 2-3 and 2-4). Taken together these observations indicate that 1) acute exercise in the head down tilt posture increases sub-maximal SV, but significantly decreases peak aerobic capacity, compared to upright, and that 2) cardiorespiratory adaptations to training in the head down tilt posture transfer to upright exercise.

Influence of Posture on Cardiorespiratory Performance

During head down tilt cycling $\dot{V}O_2$peak was approximately 85% of upright cycling $\dot{V}O_2$peak (Table 2.2). The decreased peak aerobic capacity presented here is consistent with previous findings comparing upright and supine exercise in that exercise in the supine posture consistently decreases $\dot{V}O_2$peak and peak power compared to upright cycling (59, 66, 105, 117, 122, 192, 198). The decrease in LT reported in the present study during head down tilt cycling is

in agreement with some (102, 105, 122) but not all studies examining supine exercise (59, 111). In addition, Egana and colleagues demonstrated that the difference between cycling times in the upright and supine postures is significantly correlated with subject height and therefore the hydrostatic column (65). These reports suggest that reducing the hydrostatic column decreases exercise performance. The precise mechanisms behind this posture- related decline in aerobic capacity may be attributed to several factors. First, muscle perfusion pressure is decreased during supine and head down tilt posture compared to upright and may well contribute to the decline in exercise performance (78, 254). Nielson et al. (1983) demonstrated that arterial pressure in the leg mirrored the change in pressure cause by alterations in the hydrostatic column (165). Therefore, since muscle perfusion pressure is a product of arterial and hydrostatic pressure, any reduction in the height of the hydrostatic column will proportionally decrease muscle perfusion and potentially exercising blood flow. Secondly, the effects of the muscle pump may be attenuated in the absence of a venous hydrostatic column, as with head down tilt posture. Laughlin and Joyner (1987, 2003) suggest that an effective muscle pump may only exist when sufficient venous pressure is present within the circulation (128, 130).

The finding that sub-maximal SV was significantly increased during head down tilt cycling compared to upright is consistent with previous reports evaluating cardiac performance during supine cycling (12, 13, 66, 139, 180, 198, 199, 226). This increased SV during head down tilt exercise may be attributed to the Frank Starling (or length-tension) relationship such that the central fluid shift and presumed increased effective filling pressure improves cardiac performance (203). Unfortunately, SV is a poor surrogate of ventricular filling pressure. However, if an ejection fraction of 83% is assumed (180, 199) then an estimate of left ventricular end diastolic volume can be made. As expected, the calculated end-diastolic volume during head down tilt in the present study is approximately 10 ml greater compared to upright (90.2 ± 12.9 vs. 80.4 ± 10.1 ml respectively), suggesting a greater cardiac volume overload during head down tilt cycling. In addition, the slope of the CO:$\dot{V}O_2$ relationship was not significantly different between upright and head down tilt postures. Others have demonstrated a similar response between upright and supine exercise (180). However, these data are in contrast to Leyk et al. (1992) who report an increased CO during supine cycling up to 160 watts compared to upright.

This study demonstrated significant improvements in $\dot{V}O_2$peak following several weeks of head down tilt exercise training. In addition, we confirmed the third hypothesis that this increase in aerobic capacity would transfer to upright cycling. As highlighted by Wagner and colleagues the determinants of $\dot{V}O_2$peak include both convective ($\dot{V}O_2 = CO \times [CaO_2 - CvO_2]$) and diffusive ($\dot{V}O_2 = D \times [\text{capillary } PO_2 - \text{mitochondrial } PO_2]$) O_2 transport (240, 242, 243). Applying these determinants to the findings of the present study reveals several potential factors by which head down tilt cycling increased both head down tilt and upright exercise performance.

Factors contributing to improved convective O_2 transport post-training include an increase in COpeak and vascular O_2 content. Ray et al. (1990) reported no change in blood or red cell volume following several weeks of supine cycling training, suggesting vascular O_2 content may not have increased following the present training program. However, an increase in CO will have a profound impact on peak $\dot{V}O_2$. In the present study, COpeak increased approximately 10% and 13% following head down tilt training when measured during upright and head down tilt postures respectively. These findings are consistent with the 10% increase in COpeak measured during upright cycling following swim training (145). Furthermore, these data support previous reports of a significant positive correlation between CO and $\dot{V}O_2$max (68).

Improvements in diffusional O_2 capacity (DO$_2$) following training can occur via changes within the muscle microcirculation. These include increased capillary blood flow ($\dot{Q}$cap), improved $\dot{Q}$cap/$\dot{V}O_2$ matching, increased capillary hematocrit, increased capillary to fiber ratio, and increased capillary length. Training interventions of similar duration and intensity have reported increases in DO$_2$ (202). However, the present study does not allow us to identify if any of these factors or the resultant DO$_2$ are increased with head down tilt cycling training.

The primary cardiovascular adaptations in this study were increases in both SV and CO. Specifically, SV increased during upright cycling in both training groups. However, during head down tilt cycling, stroke volume only increased in the HTG. These findings suggest that the effects of head down tilt cycling training on cardiovascular adaptations translate to different

exercising postures better than traditional upright training. Martin et al. (1987) demonstrated that 12 wks of swim training increased peak SV 18% and 10% during supine and upright exercise respectively (145). In contrast, Ray et al. (1990) suggested that central cardiovascular adaptations, including left ventricular end-diastolic, end-systolic, and stroke volume, are posture specific. In their study several weeks of high intensity interval and prolonged continuous cycling in the supine posture only increased sub-maximal SV measured during supine exercise, not upright. Possible differences compared to the present study may be attributed to several factors. First, the head down tilt posture consistently results in a greater central fluid shift and effective ventricular filling pressure compared to the supine posture (81, 166). This elevated ventricular preload may have resulted in greater myocardial adaptations (i.e, chamber size and/or compliance). Second, Ray et al. (1990) had subjects perform a more high-intensity interval style of training, whereas the present study utilized only a constant work rate endurance training program. As such, subjects in the present study performed approximately 20 min of additional exercise each week, thus placing them in as state of "chronic volume loading" for a greater period of time (160, 203). In addition, these diverse cardiovascular adaptations following recumbent cycling training may be dependent on slight hemodynamic differences and myocardial adaptations between supine and head down tilt exercise that have not yet been rigorously evaluated. Further investigations evaluating effective ventricular filling pressure and diastolic function are needed to determine the potential differences in training adaptations between supine and head down tilt postures. However, the results of the present study extend those of Ray et al (1990) and Martin et al. (1987) who focused on supine cycling and swimming (145, 199). The present study utilized a new recumbent model of cycling exercise different from the traditionally studied upright or supine postures. In addition, the present study provides additional insight to changes in peak SV and CO and the extension of benefits to upright exercise.

The training induced increases in SV observed in the present study are likely associated with changes in left ventricular end-diastolic volume. Previous reports suggest that left ventricular end-systolic volume and ejection fraction, a surrogate of myocardial contractility, are unchanged following upright or supine training (17, 199, 201). Therefore, we believe the primary mechanisms associated with the increases in SV in the present study are those directly impacting

diastolic volume. One such mechanism is an increase in effective ventricular filling pressures owing to an increase in blood or plasma volume which leads to an elevated SV. Blood volume was not measured in the present study, but previous reports suggest that changes in blood volume are variable with training (199). Second, training can increase ventricular compliance. Levine et al. (1991) demonstrated that endurance trained athletes have a greater increase in SV for a given change in ventricular pressure compared to untrained controls due to an increased compliance and distensibility (136). This elevated compliance allows for a greater range in ventricular volumes in which the Frank-Starling relationship can be effective. During head down tilt cycling when the ventricle is presumably exposed to a high filling pressure, a less compliant ventricle will require a large change in pressure to elevate SV. If training has little impact on compliance, little to no change in SV measured during head down tilt cycling would be observed. However, if the training stimulus did in fact increase ventricular compliance, an increase in SV would be observed both during upright and head down tilt cycling tests (136). It therefore seems likely that changes in ventricular compliance may account for the increase in SV measured during upright and head down tilt cycling for the HTG that was not observed in the UTG. Third, chronic ventricular volume overload, like that experienced during endurance training, results in myocyte longitudinal growth, also known as eccentric hypertrophy. Moore et al. (1993) measured left ventricular myocyte length following several weeks of endurance training in rats (158). They demonstrated that trained rats have significantly longer myocytes compared to sedentary controls, accomplished by adding sarcomeres in series with existing sarcomeres. This type of cardiac hypertrophy resulted in substantial increases in ventricular chamber volumes. For example, if the ventricle is assumed to be elliptical, a 5% increase in myocyte length will increase ventricular volume ~10% (157, 158). Therefore it is plausible that an increase in myocyte length of this magnitude would explain the 9-10% increase in SV measured following head down tilt training.

Relevance

The key implications of the present study are twofold. First, as previously demonstrated by Fitzpatrick et al. (1996) and Wright et al. (1999) when a contracting forearm is elevated above heart level, exercise tolerance is significantly limited (78, 254). The results of the present study

extend these findings as evident from a significantly decreased $\dot{V}O_2$peak and LT during head down tilt cycling when the legs are elevated above heart level. In addition, subjects performing head down tilt exercise repeatedly complained of a "burning" sensation of the quadriceps at sub-maximal exercise intensities suggestive of greater lactic acid accumulation. These reports are similar to those reported during supine exercise (198). Furthermore, the present study utilized whole body exercise (i.e., cycling) not a small muscle mass model like handgrip exercise (78, 254). However, despite this decrease in exercise tolerance the central cardiovascular responses were greater during sub-maximal head down tilt cycling suggesting a cardiac volume overload that is advantageous during training.

Second, endurance exercise training results in beneficial cardiac adaptations primarily due to a chronic ventricular volume overload, as evident by the increased sub-maximal SV measured during upright cycling (203). The significant increase in sub-maximal and maximal SV measured during upright and head down tilt cycling in the HTG suggests that head down tilt cycling training results in a high chronic ventricular volume overload that may be greater than experienced during traditional upright cycling. This sets the foundation for future work in populations who would benefit from a high central cardiovascular training stimulus. However, further research is needed to determine if this specific training modality will improve measures of ventricular function as assessed by Doppler echocardiography or magnetic resonance imaging, and vascular function assessed by flow-mediated dilation.

Experimental Considerations

Several experimental considerations are relevant to the interpretation of the present study. First, the sample size was limited to untrained college-aged men. This may limit extrapolation of these data to other populations (i.e., women, athletes, older individuals, and patients with heart failure). In addition, the number of trained subjects was limited to 11 men. Despite a small sample size, 4 out of 5 subjects within the HTG demonstrated substantial increases in $\dot{V}O_2$peak during both upright and head down tilt exercise (Figure 2.3B and 3D), which is suggestive of a large effect size and supports the statistical conclusions. This is in contrast to the high variability observed in the UTG across the second 4 wk training period (Figure 2.3C) during head down tilt

21

cycling. Post-hoc sample size analysis (SigmaStat 3) of the UTG cardiorespiratory adaptations during head down tilt exercise present dataset via a commercially available calculator (SigmaStat 3) revealed that a sample size of >30 would have been necessary to observe a significant increase. Therefore, despite a limited sample size the primary conclusions appear to be appropriate. Second, due to the impact sex hormones can have on cardiovascular function (154), women were not included in the present study. Third, the acetylene single-breath exhalation technique is used as an estimate of pulmonary capillary blood flow, which in healthy adults can be used as a surrogate measurement of CO. Furthermore, Dibski et al. (2005) reported that the single-breath exhalation technique is difficult to perform above the second ventilatory threshold (i.e., in the severe exercise intensity domain) and recommended measurements be performed below this threshold (57). Therefore, multiple measurements were made in the present study at several sub-maximal work rates to minimize measurement error, limit subject discomfort, and to allow for extrapolation to maximal exercise.

Conclusion

The present study demonstrated that posture affects maximal cardiorespiratory responses as evident from a lower $\dot{V}O_2peak$ but higher SV during head down tilt cycling compared to upright. Additionally, endurance exercise training in the head down tilt posture resulted in significant increases in $\dot{V}O_2peak$, SV, and CO that were observed during both upright and head down tilt cycling. Furthermore, these data indicate that upright endurance training only improves cardiorespiratory responses during upright cycling and does not transfer to the head down tilt posture. Therefore, we conclude that training in a head down tilt position can be used to increase cardiorespiratory performance and function across multiple body positions. This outcome may be due to an increased central cardiac stimulus subsequent to the central fluid shifts associated with the head down tilt posture.

Table 2.2-1. Physical Characteristics of the training subjects

	UTG (n=6)			HTG (n=5)		
Age, yr	23.8	±	1.3	28.0	±	3.7
Height, cm	181	±	9.3	180	±	8.4
Weight, kg						
Pretest	73.2	±	7.0	82.2	±	24.7
Midtest	75.6	±	10.2	75.9	±	12.0
Posttest	72.7	±	6.9	76.2	±	10.0

Values are mean± SD. UTG, upright training group; HTG, head down tilt training group

Table 2-2: Peak cardiorespiratory responses to acute upright and head down tilt exercise (n=22)

	Upright Exercise			Head Down Tilt Exercise			Difference %
WR, W	220	±	51	186	±	30*	15
VE, l/min	80.8	±	15.7	73.6	±	13.0*	9
VO_2, l/min	2.44	±	0.50	2.09	±	0.39*	15
VO_2, ml/kg/min	33.1	±	5.9	28.4	±	4.7*	15
VCO_2, l/min	2.74	±	0.47	2.39	±	0.41*	13
O_2 Pulse, ml/beat	13.6	±	3.1	12.9	±	2.8*	5
RER	1.13	±	0.06	1.15	±	0.07	2
HR, bpm	181	±	13	164	±	14*	10
LT, l/min	1.44	±	0.38	1.27	±	0.31*	11
LT, %	59.0	±	9.1	61.4	±	10.0	4

Values are mean ± SD. WR, work rate; VE, ventilation; VO_2, O_2 uptake; VCO_2, CO_2 output; RER, respiratory exchange ratio; HR, heart rate; LT, lactate threshold.

* Significantly different from Upright Exercise

Table 2-3: Peak cardiorespiratory responses during upright cycling before and after training

Variable	UTG Pretest			UTG Midtest			UTG Posttest			HTG Pretest			HTG Midtest			HTG Posttest		
WR, W	229	±	29	267	±	30^{α}	288	±	31^{α}	245	±	48	280	±	37^{α}	280	±	37^{α}
VE, l/min	81.2	±	14.1	85.2	±	15.6	94.6	±	19.7	81.5	±	13.9	86.2	±	16.9	93.8	±	15.8
VO_2, l/min	2.52	±	0.37	2.77	±	0.46	2.90	±	0.45^{α}	2.58	±	0.54	2.81	±	0.51^{α}	3.08	±	$0.53^{\alpha\beta}$
VO_2, ml/kg/min	34.6	±	5.64	37.1	±	7.23	40.0	±	6.04	32.5	±	8.08	37.5	±	8.00^{α}	40.8	±	7.93^{α}
VCO_2, l/min	2.87	±	0.35	3.11	±	0.54	3.34	±	0.63	2.76	±	0.50	3.07	±	0.52^{α}	3.27	±	0.54^{α}
O_2 Pulse, ml/beat	13.2	±	1.35	15.1	±	3.05	16.3	±	3.05^{α}	14.5	±	3.55	15.6	±	3.07	16.8	±	3.47^{α}
RER	1.14	±	.06	1.12	±	0.05	1.14	±	0.05	1.08	±	1.05	1.10	±	0.04	1.10	±	0.07
HR, bpm	191	±	9	185	±	9	180	±	16	180	±	11	181	±	6	185	±	9
LT, l/min	1.50	±	0.24	1.63	±	0.36	1.64	±	0.24	1.59	±	0.37	1.79	±	0.60	1.69	±	0.39
LT, %	59.6	±	4.6	58.9	±	8.6	57.0	±	6.8	62.8	±	12.5	63.4	±	14.8	56.3	±	11.3
CO, l/min	16.0	±	1.8	18.2	±	3.1^{α}	18.7	±	2.7^{α}	16.7	±	3.6	17.7	±	3.3	19.5	±	$3.1^{\alpha\beta}$
SV, ml	86.3	±	10.5	98.8	±	19.1^{α}	101.7	±	16.4^{α}	93.5	±	22.9	97.5	±	19.5	106.0	±	$20.4^{\alpha\beta}$

Values are mean ± SD. UTG, upright training group; HTG, head-down tilt training group; WR, work rate; VE, ventilation; VO_2, O_2 uptake; VCO_2, CO_2 output; RER, respiratory exchange ratio; HR, heart rate; LT, lactate threshold; CO, cardiac output; SV, stroke volume.

α Significantly different from Pretest
β Significantly different from Midtest
* Significantly different from UTG

25

Table 2-4: Peak cardiorespiratory responses during head down tilt cycling before and after training

Variable	UTG Pretest			UTG Midtest			UTG Posttest			HTG Pretest			HTG Midtest			HTG Posttest		
WR, W	188	±	21	204	±	29	229	±	$40^{\alpha\beta}$	195	±	27	215	±	29	245	±	$33^{\alpha\beta}$
VE, l/min	68.9	±	9.6	78.1	±	21.4	80.6	±	12.9	79.1	±	14.1	85.0	±	18.1	97.5	±	24.6^{α}
VO_2, l/min	2.06	±	0.23	2.30	±	0.49	2.43	±	0.54^{α}	2.21	±	0.41	2.40	±	0.45	2.81	±	$0.43^{\alpha\beta}$
VO_2, ml/kg/min	28.3	±	3.29	31.0	±	8.41	33.6	±	7.25^{α}	27.9	±	6.42	32.0	±	6.16	35.4	±	6.82^{α}
VCO_2, l/min	2.34	±	0.27	2.63	±	0.59	2.83	±	0.68	2.49	±	0.45	2.72	±	0.52	3.13	±	0.51^{α}
O_2 Pulse, ml/beat	12.7	±	1.83	13.8	±	2.66	14.7	±	2.81^{α}	13.6	±	3.17	14.4	±	3.08	16.7	±	$3.11^{\alpha\beta}$
RER	1.14	±	0.10	1.14	±	0.03	1.16	±	0.05	1.13	±	0.02	1.14	±	0.04	1.09	±	0.08
HR, bpm	164	±	18	166	±	11	165	±	12	164	±	10	168	±	11	169	±	12
LT, l/min	1.18	±	0.18	1.40	±	0.24	1.47	±	0.24^{α}	1.42	±	0.26	1.47	±	0.25	1.59	±	0.41
LT, %	57.9	±	9.1	61.8	±	9.1	61.4	±	10.8	64.9	±	8.7	61.4	±	3.8	56.5	±	5.7
CO, l/min	13.7	±	1.2	15.2	±	2.9	15.5	±	2.6	14.9	±	2.3	16.0	±	2.5	18.1	±	$2.8^{\alpha\beta}$
SV, ml	84.4	±	8.7	91.5	±	17.4	93.7	±	12.9	91.7	±	18.6	96.2	±	18.3	107.5	±	$20.8^{\alpha\beta}$

Values are mean ± SD. UTG, upright training group; HTG, head-down tilt training group; WR, work rate; VE, ventilation; VO_2, O_2 uptake; VCO_2, CO_2 output; RER, respiratory exchange ratio; HR, heart rate; LT, lactate threshold; CO, cardiac output; SV, stroke volume.

α Significantly different from Pretest
β Significantly different from Midtest
* Significantly different from UTG

Table 2-5: Cardiorespiratory data during upright and head down tilt cycling at 100 watts

Variable	UTG									HTG								
	Pretest			Midtest			Posttest			Pretest			Midtest			Posttest		
Upright Exercise																		
VO_2, l/min	1.19	±	0.12	1.25	±	0.08	1.21	±	0.13	1.23	±	0.09	1.26	±	0.09	1.32	±	0.08
HR, bpm	127	±	11	125	±	11	117	±	13	129	±	23	121	±	15	121	±	17
CO, l/min	8.8	±	0.6	9.3	±	0.6	9.13	±	0.6	9.0	±	0.6	9.2	±	0.7	9.9	±	$0.5^{\alpha\beta}$
SV, ml	69.5	±	4.0	75.11	±	8.7	78.6	±	8.4^{α}	71.1	±	10.2	77.0	±	10.5	82.4	±	11.2^{α}
Head Down Tilt Exercise																		
VO_2, l/min	1.18	±	0.14	1.25	±	0.09	1.22	±	0.14	1.25	±	0.11	1.18	±	0.13	1.26	±	0.11
HR, bpm	124	±	5	122	±	6	117	±	8	127	±	16	123	±	15	116	±	12
CO, l/min	8.8	±	0.3	9.3	±	0.7	8.9	±	0.5	9.5	±	0.5	9.0	±	0.7	9.5	±	0.7
SV, ml	71.0	±	3.0	76.8	±	9.2	76.9	±	5.5	75.6	±	11.4	74.2	±	12.4	82.5	±	$11.4^{\alpha\beta}$

Values are mean ± SD. UTG, upright trained group; HTG, head down tilt trained group; VO_2, O_2 uptake; HR, heart rate; CO, cardiac output; SV, stroke volume

α Significantly different from Pretest
β Significantly different from Midtest
* Significantly different from UTG

Figure 2-1. A schematic representation of the hydrostatic column and contracting muscle mass relative to the heart during upright (A) and head down tilt (B) exercise. Notice the contrasting cardiovascular environment between the two postures.
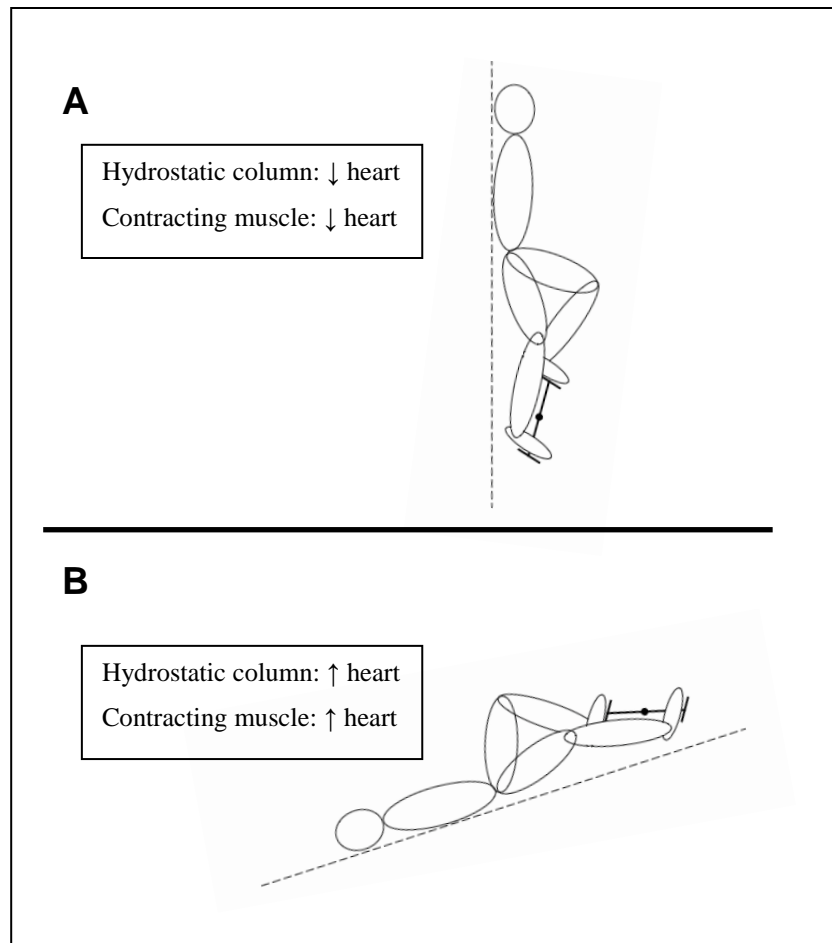
Figure 2-2. Stroke volume at 100 Watts during acute upright and head down tilt exercise. The solid line indicates the group's mean response. Dashed lines represent individual responses. Stroke volume was significantly greater during acute head down tilt cycling compared to upright. * Significant difference vs. upright, (P<0.001).
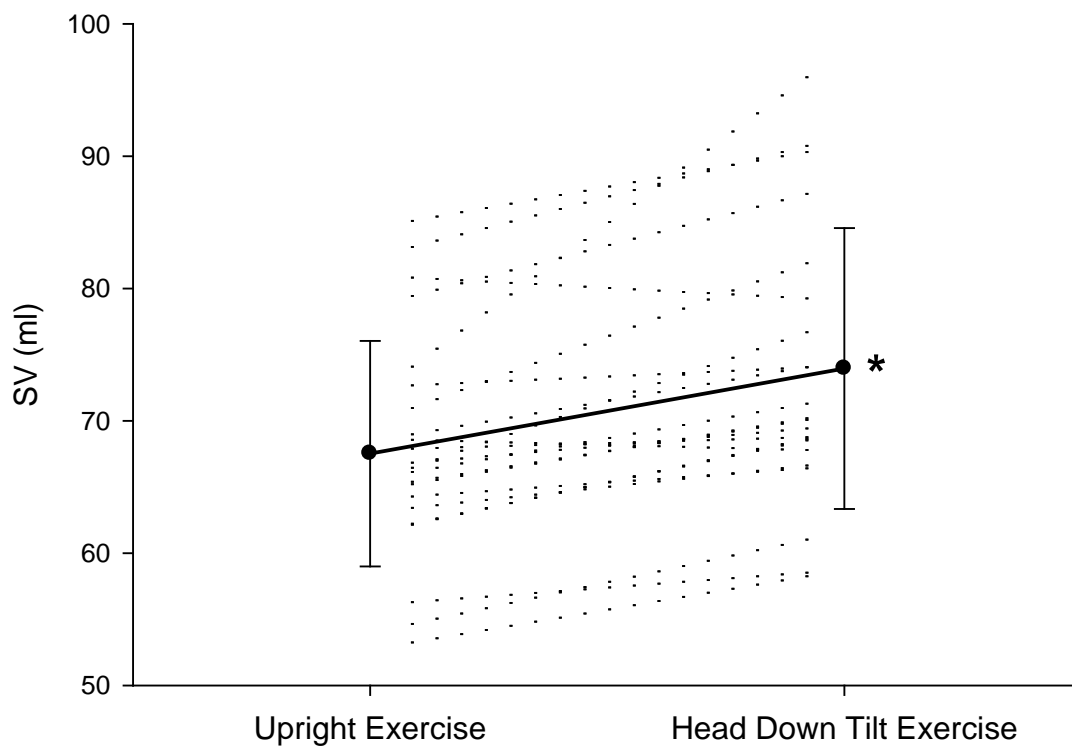
Figure 2-3. $\dot{V}O_2$peak responses before and after exercise training
in the upright trained (UTG) and head down tilt trained (HTG) groups measured in both the
upright and head down tilt postures. α Significant difference vs. Pretest, (P<0.05). β Significant
difference vs. Midtest, (P<0.05).
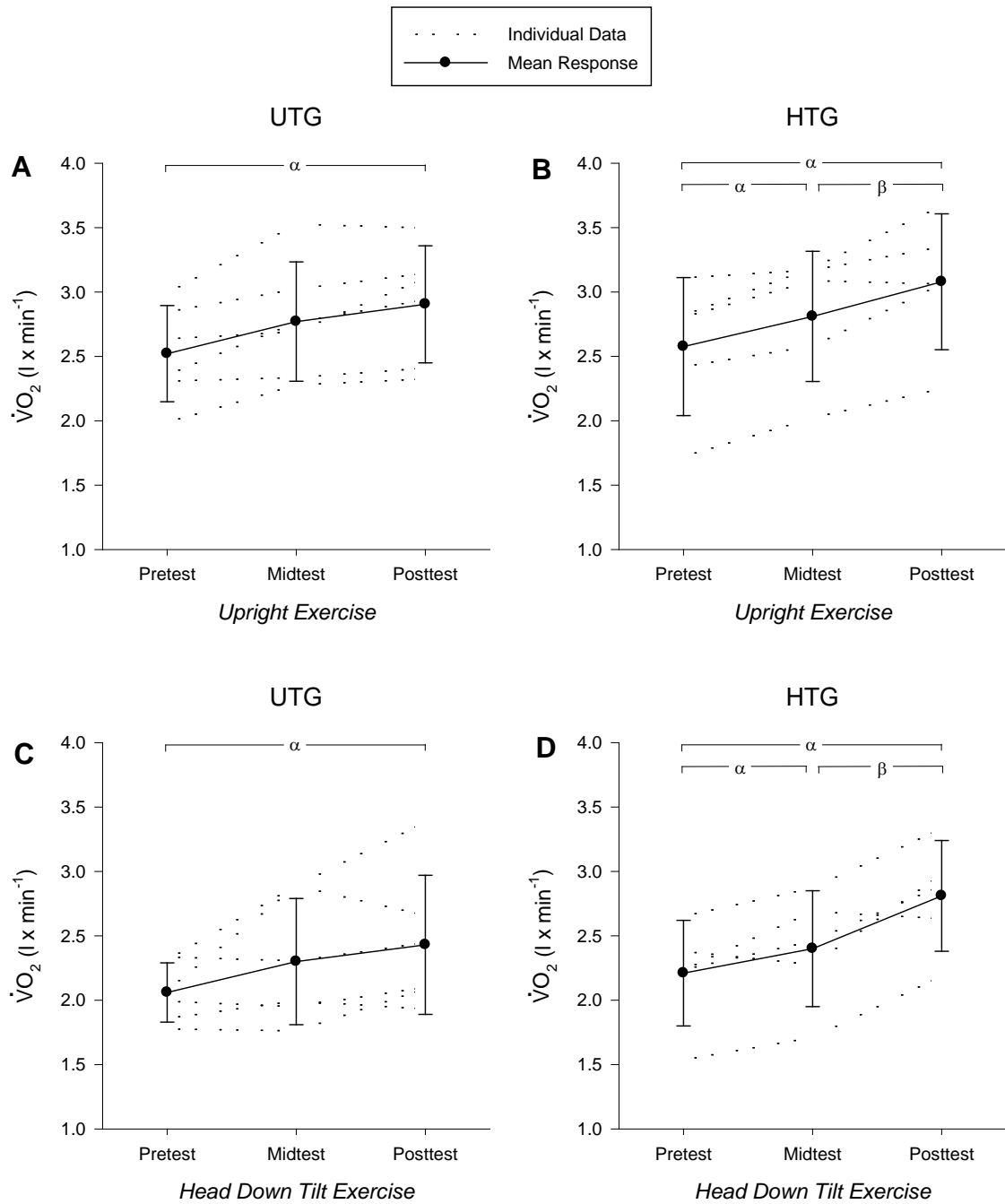
Figure 2-4. Peak SV before and after training measured in the upright and head down tilt postures.

Stroke volume is increased during both upright and head down tilt exercise in the HTG. UTG, upright training group; HTG, head down tilt training group. α Significant difference vs. Pretest, (P<0.05). β Significant difference vs. Midtest, (P<0.05).
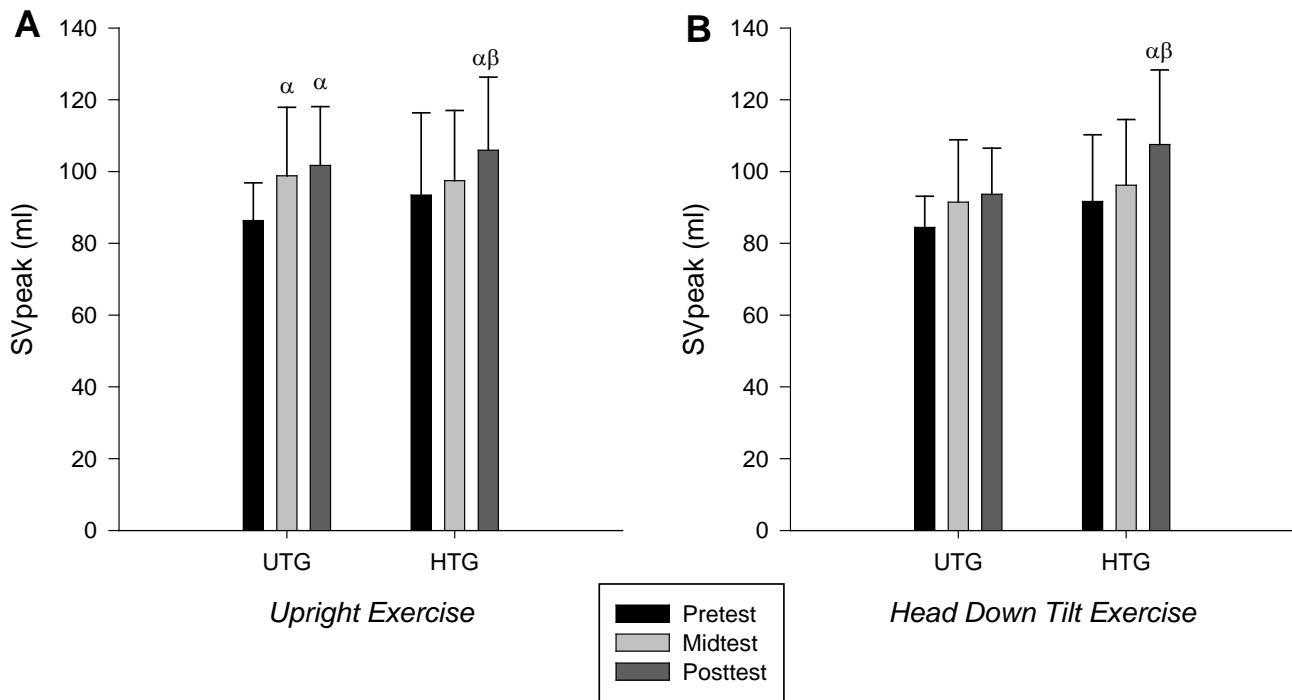
Figure 2-5. Sub-maximal (100 Watts) SV before and after training measured in the upright and head down tilt postures.

During upright exercise SV increased in both groups after training (A). However, during head down tilt exercise SV only increased in the HTG (B). UTG, upright training group; HTG, head down tilt training group. α Significant difference vs. Pretest, (P<0.05). β Significant difference vs. Midtest, (P<0.05).
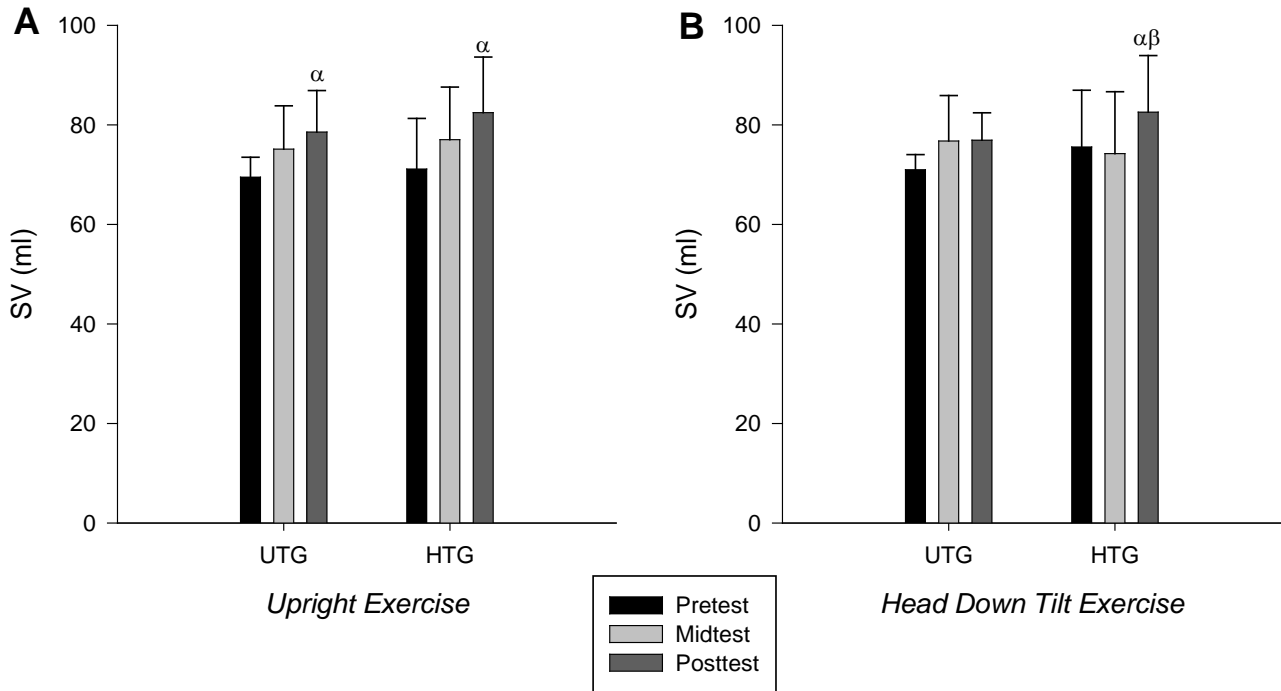
Chapter 3 - Antegrade and retrograde blood velocity profiles in the intact human cardiovascular system

Summary

Current assessments of the effects of shear patterns on vascular function assume that a parabolic velocity profile is always present. Any substantial deviation in the profile away from this may result in misinterpretation of the importance shear patterns have on vascular function. The current investigation tested the hypothesis that antegrade and retrograde blood flow would have a parabolic velocity profile at rest, during cold pressor test (CPT), and exercise. Eight healthy subjects completed a cold pressor test and a graded knee extension exercise test. Doppler ultrasound was used to determine time-average-mean velocity (V_{MEAN}) and time-averaged-peak velocity (V_{PEAK}) for both antegrade and retrograde flow in the femoral (FA) and brachial arteries (BA). The V_{MEAN}/V_{PEAK} ratio was used to interpret the shape of the blood velocity profile (parabolic, $V_{MEAN}/V_{PEAK} = 0.5$; plug-like, $V_{MEAN}/V_{PEAK} = 1.0$). At rest, BA and FA V_{MEAN}/V_{PEAK} ratios of antegrade and retrograde flow were not significantly different than 0.5. During CPT antegrade V_{MEAN}/V_{PEAK} in the BA (0.56 ± 0.02) and FA (0.58 ± 0.03) were significantly greater than 0.5. During peak exercise, the V_{MEAN}/V_{PEAK} ratio of antegrade flow in the FA (0.53 ± 0.04) was not significantly different than 0.5. In all conditions the retrograde V_{MEAN}/V_{PEAK} ratio was lower compared to antegrade. These data demonstrate that blood flow through two different conduit arteries under two different physiological stressors maintains a velocity profile that resembles a slightly blunted parabolic velocity profile.

Introduction

Vascular function is a key variable predicting the likelihood of an adverse cardiovascular event (255). Recent investigations demonstrate that shear stress contributes to endothelial function, remodeling, and the formation of atherosclerotic lesions (131, 164). Chronic increased antegrade blood flow and shear stress, such as that achieved with exercise, have been shown to improve endothelial function as determined via flow-mediated dilation (163, 193, 232). Conversely, retrograde and oscillatory shear in both animal and human models have been associated with a pro-atherosclerotic condition paralleled by a decrease in endothelial function (27, 107, 151, 229, 258). Unfortunately, as Halliwill and Minson (92) and Parker et. al. (176) have recently reported, the current assessment of shear stress relies on inherent assumptions based on Poiseuille's equation. These assumptions include:

i) The vessel is rigid and long compared to its radius;
ii) The physical properties of blood maintain a constant viscosity independent of the shear rate;
iii) The flow is laminar flow that is not pulsatile, resulting in a parabolic profile;
iv) Blood velocity at the vessel wall is zero (101, 147).

In turn, each of these factors will have a direct effect on the interaction of blood flow and the endothelium. Therefore, these assumptions must be evaluated before confident conclusions can be drawn concerning shear patterns.

In animal studies, antegrade blood flow moves with a parabolic-like profile (14, 91, 214). Unfortunately, many of these studies were performed in vessels smaller than the brachial and femoral arteries studied in humans. Recently, Osada and Radegran (170, 171) found that the blood velocity profile of humans becomes more parabolic in shape with the transition from rest to exercise, when controlling for blood pressure phases and muscle contraction. Information regarding retrograde blood flow profiles, however, remains undetermined. Furthermore, the findings of Osada and Radegan (2005, 2006) suggests that the velocity profile is not a constant variable within the cardiovascular system. Conversely, the stability of the velocity profile remains undetermined in smaller arteries or with other types of physiologic stress.

The purpose of the present investigation was to non-invasively determine the blood velocity profile during both antegrade and retrograde flow in the intact human cardiovascular system, using the relationship between mean blood velocity (V_{MEAN}) and peak blood velocity (V_{PEAK}) across the vessel lumen (142, 170, 171). Parabolic velocity is present when mean velocity is one-half the maximum velocity ($V_{MEAN}/V_{PEAK} = 0.5$). Any substantial deviation from this ratio would be considered evidence of the presence of either a plug-like profile ($V_{MEAN}/V_{PEAK} = 1.0$) or a sharpened-parabolic profile ($V_{MEAN}/V_{PEAK} \approx 0$). This investigation provides important and novel information regarding the fluid dynamics occurring within the human cardiovascular system at rest and during physiologic stress. Our approach was to determine antegrade and retrograde blood velocity profiles in the brachial and femoral arteries at rest, during a cold pressor test, and during dynamic leg exercise. It is well established that changes in vascular resistance alter blood flow characteristics thus potentially altering the shape of the velocity profile (174, 219, 229). Therefore, the goal was to determine blood velocity profiles when downstream resistance is elevated (CPT) and decreased (exercise). We hypothesized that (a) the velocity profile would not be significantly different during CPT and exercise compared to rest, (b) antegrade and retrograde flow would each demonstrate a parabolic velocity profile, and (c) the retrograde blood velocity profile would not be significantly different from that of antegrade.

Methods

Subjects

Eight subjects (6 men; 2 women; age 21 ± 2 yrs (mean $\pm$ SD); stature 178.1 ± 12.2 cm; mass 91.2 ± 38.5 kg; BMI 28.1 ± 9.8 kg x m^{-2}) completed the experiments. All subjects were non-smokers and had no history of cardiovascular, pulmonary, or metabolic disease as determined by medical history questionaire. Women were tested during the follicular phase (days 1-14) of their menstrual cycle to standardize the influence of female hormones. Verbal and written consent was obtained from all subjects following approval of the study by the Institutional Review Board for Research Involving Human Subjects at Kansas State University, and conformed to the Declaration of Helsenki.

Experimental Measurements

Basic Measurements

Heart Rate (HR) was monitored via three-lead electrocardiograph. Mean arterial pressure (MAP) was measured beat by beat via finger photoplethysmography (NexfinHD; BMEYE, Amsterdam, The Netherlands).

Ultrasound

Blood velocities in the brachial and femoral arteries were measured via Doppler Ultrasound (Vivid 3; GE Medical Systems, Milwaukee, WI) with a phased linear array transducer probe operating at an imaging frequency of 6.7 MHz. Blood velocities were measured in pulse waved mode at a Doppler frequency of 4.0 MHz. Doppler velocity measurements were performed and corrected for an angle of insonation less than 65°, which is less than that previously reported in similar studies (193, 195). The mean insonation angle used in the present study was $60.9 \pm 1.3°$ and was kept constant throughout each experiment, which provides a valid

37

measurement of blood velocity (126). For all studies the Doppler gate was set to the full width of the vessel to ensure complete insonation. The mean sampling volume in the present study for the femoral and brachial arteries was 7 and 4 mm respectively. Measurements of the common femoral artery were made 2-3 cm below the inguinal ligament to minimize turbulent flow caused by the bifurcation of the common femoral artery into the superficial and profunda branches (95, 99, 143). The mean femoral artery depth and resting diameter in the present study was 18.4 ± 3.8 mm and 6.42 ± 0.33 mm, respectively. Measurements in the brachial artery were made 2-5 cm above the antecubital fossa. The mean brachial artery depth and diameter was 9.5 ± 2.5 mm and 4.01 ± 0.49 mm, respectively. The locations of the bifurcations were not determined in the present study. However, unpublished observations indicate that when in a recumbent position (120°) the femoral artery bifurcation is ~4-6 cm distal to the inguinal ligament. Likewise, the bifurcation was not seen in the 2D image suggesting that all Doppler measurements were made >1 cm from the bifurcation. Mean blood velocity (V_{MEAN}; cm × sec^{-1}) was defined as time-averaged mean velocity over each complete cardiac cycle while peak velocity (V_{PEAK}; cm × sec^{-1}) was defined as the time-averaged blood velocity taken from the maximum outer envelope of the Doppler waveform, representing peak velocities in the vessel. Both were calculated using the manufacturer's on-screen software. The blood velocity profile index was expressed as the V_{MEAN}/V_{PEAK} ratio (142, 170, 171). All blood velocities were determined as the average of 5-6 consecutive cardiac cycles and corrected for the insonation angle using the manufacture's signal processing software (GE Medical Systems, Milwaukee, WI). During exercise, cardiac cycles with similar antegrade flow and the absence of measureable retrograde flow (so as to minimize muscle contraction artifact). Blood flow was calculated in the brachial (BABF) and femoral (FABF) arteries using the product of V_{MEAN} and vessel cross sectional area (CSA). If parabolic profiles are present within each artery, an alternative calculation of blood flow using the product of [V_{PEAK} x 0.5] and CSA will produce similar results. Vessel diameters were measured at each experimental time point via two-dimensional sonography and used to calculate vessel cross sectional area (CSA = πr^2; cm^2). Vessel diameters were not significantly different compared to baseline in the brachial artery during CPT and the femoral artery during exercise. Femoral artery diameter significantly decreased during CPT compared to baseline (6.2 ± 0.4 and 6.3 ± 0.5, respectively vs. 6.5 ± 0.3, P<0.05).

38

V_{MEAN}, V_{PEAK}, and the V_{MEAN}/V_{PEAK} ratio were determined for both antegrade and retrograde phases of the cardiac cycle. The antegrade phase began when mean blood velocity increased above the minimum velocity of the previous cardiac cycle by visual inspection and ended when the average velocity returned to zero (Figure 3-1). In some instances a smaller second antegrade flow was present later in diastole. This second antegrade phase was not included in the calculation of antegrade velocities, but was included in the calculations of blood flow and velocity measurements across the entire cardiac cycle. The retrograde phase was defined from the end of the antegrade phase to the point when the average velocity returned to zero. All Doppler signals were stored on a computer and offline analysis was completed using the manufacture's signal processing software (GE Medical Systems, Milwaukee, WI).

Experimental Procedures

All testing was completed in an air-conditioned laboratory at a temperature of 20-25°C. Subjects performed two randomly ordered testing protocols on different days. One testing session consisted of two series of cold pressor tests (CPT) and the other session was composed of graded knee extension exercise.

Protocol 1: Cold Pressor Test

Subjects performed two randomly ordered cold pressor tests with 20 minutes recovery between each test. One test was performed while evaluating the brachial artery and one while evaluating the femoral artery. The cold pressor test consisted of a 2-minute baseline, 2-minutes with the right hand submerged in ice water (~3°C), and 2-minute recovery. The cold pressor response in the brachial artery was evaluated with the subject in the supine position. Measurement of the cold pressor response in the femoral artery was performed with the subject in a seated position to mimic the position and hydrostatic influences experienced during knee extension exercise.

Protocol 2: Graded Exercise

Subjects performed incremental exercise on a custom-built knee extension ergometer (143). Exercise was performed in a seated position with the thigh parallel to the ground and the lower leg initially perpendicular to the ground. Following 2-minutes of baseline, subjects began kicking at 40 contractions per minute. The work rate progressively increased every minute until the subject could not maintain the contraction rate for at least 5 contractions despite verbal encouragement. Work was generated by compressing air in a pneumatic cylinder as the lower leg was extended. Full extension of the lower limb was limited to a fixed linear displacement (d) of 10.9 cm, which represents ~20° knee extension.

Data Analysis

HR and MAP were determined by averaging the signals over the last 30 seconds of each interventional test stage. Limb vascular conductance (ml^{-1} x min^{-1} x mmHg) was calculated as the ratio of blood flow to MAP, while limb vascular resistance (mmHg x ml^{-1} x min^{-1}) was calculated as the ratio of MAP to blood flow. A one-way within-subject repeated measures ANOVA with post hoc Tukey test to adjust for multiple comparisions was used to independently determine the effects of cold pressor and exercise on MAP, HR, vascular conductance, vascular resistance, V_{MEAN}, and V_{PEAK}. A two-way ANOVA (time x direction) (time x calculation method) with post hoc Tukey test was used to determine the difference between antegrade and retrograde V_{MEAN}/V_{PEAK} and blood flow calculation methods, respectively. A single sample t-test was used to compare the V_{MEAN}/V_{PEAK} ratio to 0.5. Linear correlation analysis was used to assess the relationship between V_{MEAN} and V_{PEAK} across individuals. Significant differences between regression slopes were tested using a Student's *t* test. All data is expressed as mean ± standard deviaton. Statistical significance was declared when $P < 0.05$.

Results

Figure 3-1 illustrates the Doppler waveform profile in a representative subject during CPT (Panel A) and knee extension exercise (Panel B). Retrograde flow (below baseline) in this individual was present during CPT, but not during exercise.

Cold Pressor Test: Brachial Artery

Table 3-1 summarizes the group mean blood velocity response of the brachial artery to CPT. MAP significantly increased and limb vascular conductance was decreased at *1-minute* CPT and *2-minute* CPT compared to baseline. BABF calculated using $V_{PEAK}/2$ ($BABF_{VPEAK/2}$) was significantly decreased at all time points compared to BABF calculated using V_{MEAN} ($BABF_{VMEAN}$). Figure 3-2A illustrates the significant linear regression between $BABF_{VMEAN}$ and $BABF_{VPEAK/2}$ across individuals during CPT.

The mean ratio of V_{MEAN}/V_{PEAK} across the entire cardiac cycle during both minutes of CPT and recovery were not significantly different compared to baseline (Table 3-1), but were significantly greater than 0.5. The baseline antegrade mean ratio of V_{MEAN}/V_{PEAK} was not significantly different than 0.5, indicating a parabolic shape. The antegrade ratios during both minutes of CPT and recovery were not significantly different compared to baseline (Figure 3-3A). However, *1-minute* CPT and recovery antegrade ratios were significantly greater than 0.5. The baseline retrograde mean V_{MEAN}/V_{PEAK} was not significantly different than 0.5. Further, the retrograde V_{MEAN}/V_{PEAK} ratio during CPT and recovery was not significantly different than baseline, but was significantly decreased compared to antegrade at each time point.

Figure 3-4A illustrates the linear regression between V_{MEAN} and V_{PEAK} across individuals in the brachial artery during CPT, while table 3-2 includes the regression parameters for each testing condition. The regression slopes did not significantly change with time for either antegrade or retrograde velocities. However at baseline, *1-minute* CPT, and recovery the retrograde regression slope was significantly lower than that for antegrade.

41

Cold Pressor Test: Femoral Artery

Table 3-3 summarize the mean blood velocity response of the femoral artery to CPT. CPT elicited increases in MAP at *1-minute* CPT and *2-minute* CPT compared to baseline. Limb vascular conductance was significantly decreased at *1-minute* CPT compared to baseline, but not at *2-minute* CPT. FABF at *1-minute* CPT was decreased compared to baseline, but not at *2-minute* CPT or and recovery. FABF calculated using $V_{PEAK}/2$ ($FABF_{VPEAK/2}$) was significantly decreased at all-time points compared to FABF calculated using V_{MEAN} ($FABF_{VMEAN}$). Figure 3-2B illustrates the significant linear regression between $FABF_{VMEAN}$ and $FABF_{VPEAK/2}$ across individuals during CPT and knee extension exercise.

The mean ratio of V_{MEAN}/V_{PEAK} across the entire cardiac cycle during both minutes of CPT and recovery was not significantly different compared to baseline (Table 3-3). The baseline antegrade and retrograde V_{MEAN}/V_{PEAK} was not significantly different than the 0.5 parabolic profile value, but antegrade V_{MEAN}/V_{PEAK} during CPT and recovery was significantly greater than 0.5. The ratio during CPT and recovery was not significantly different from baseline in either the antegrade or retrograde direction (Figure 3-3B). The retrograde V_{MEAN}/V_{PEAK} for baseline, CPT, and recovery was significantly lower than the corresponding antegrade V_{MEAN}/V_{PEAK} ratios.

Figure 3-4B illustrates the linear regression between V_{MEAN} and V_{PEAK} across individuals in the femoral artery during CPT. The regression slopes did not significantly change with time for either antegrade or retrograde velocities (Table 3-2). Furthermore, in contrast to that seen for the brachial artery, the retrograde regression slope was not significantly different from that for antegrade.

Dynamic Leg Exercise: Femoral Artery

Table 3-4 summarizes the group mean blood velocity in the femoral artery during knee extension exercise. Exercise increased MAP, limb vascular conductance, $FABF_{VMEAN}$, and

$FABF_{VPEAK}$, and decreased limb vascular resistance compared to baseline. The mean ratio of V_{MEAN}/V_{PEAK} across the entire cardiac cycle during knee extension exercise was not significantly different compared to baseline. The baseline and exercise antegrade V_{MEAN}/V_{PEAK} was not significantly different than 0.5. Retrograde flow was only present at baseline and V_{MEAN}/V_{PEAK} was not different than 0.5. Antegrade V_{MEAN}/V_{PEAK} ratio was unchanged across exercise intensities compare to baseline.

Figure 3-4C illustrates the linear regression between V_{MEAN} and V_{PEAK} across individuals in the femoral artery during knee extension exercise, while table 3-2 includes the regression parameters for each testing condition. The antegrade regression slope at 50%-peak power was significantly higher compared to baseline, but not at peak power. The baseline retrograde regression slope was not significantly different compared to antegrade.

Discussion

The primary finding of the present study is that the brachial and femoral arterial blood velocity profiles are remarkably stable despite changes in MAP and downstream limb resistance/conductance when using the V_{MEAN}/V_{PEAK} ratio as an index of the distribution of intra-luminal blood velocities. This finding is consistent with our first hypothesis. However, the data is inconsistent with the second hypothesis that blood flow has a true parabolic profile during cold pressor and exercise stress. At rest and during exercise, the V_{MEAN}/V_{PEAK} ratio is not significantly different from that of a perfect parabolic profile (0.5), but during CPT the antegrade ratio becomes significantly greater than 0.5, suggesting the presence of a slightly blunted parabolic shape. Likewise, in contrast to our third hypothesis the retrograde profile was slightly but significantly different than antegrade, but was always parabolic. Taken together these observations indicate 1) a consistent velocity profile despite the pulsatile nature of blood flow, 2) that the antegrade and cardiac cycle velocity profile have a slightly blunted parabolic shape, and 3) that differences exist between antegrade and retrograde profiles.

The interaction of blood flow and endothelial cells contributes to vascular control within the arterial circulation, in large part through the resulting shear stress, which is defined as the stress parallel to the vessel wall created by the friction between flowing blood and the endothelium. Changes in blood flow and shear patterns influence the pro-vasodilatory function of the endothelial (131, 164). Recent work by Tinken et al. suggests that the greater the magnitude of antegrade flow and shear within the physiologic range the better the pro-vasodilatory function compared to low flow and shear (232). In contrast, oscillatory shear increases the release of superoxide (151), the expression of endothelian-1 (258), adhesion molecules (27), and reactive oxygen species-producing enzymes (107), while suppressing endothelial NO synthase expression (107). Likewise, Thijssen et al. demonstrated that retrograde shear stress decreases the pro-vasodilatory function of the endothelial (229). Furthermore, recent work by Padilla et al. (173, 174) suggests that increases in sympathetic nervous activity and age-related decrements in NO synthesis may increase the magnitude of retrograde shear. The present study demonstrates a stable retrograde velocity profile when downstream vascular resistance is

acutely increased during CPT, suggesting that changes in the calculated shear stimulus are not the result of variations in the velocity profile.

Calculations of shear rate using Poiseuille's equation are based on four major assumptions outlined in the introduction. When this calculation is applied to the cardiovascular system, three potential sources of error exist. First, the vasculature is composed of a compliant network of branches, not long rigid tubes with fixed diameters. Vessel distensibility can decrease shear by ~30% compared to rigid vessels (178). Second, blood may not always exhibit Newtonian fluid properties. However, in vessels with an internal diameter greater than 0.5mm, like those of the current study, blood behaves as a Newtonian fluid (147). Third, the velocity profile may not always be a true parabola. As demonstrated in the current study, the V_{MEAN}/V_{PEAK} ratio at rest and during exercise was not significantly different than 0.5, consistent with a parabolic profile. In support of parabolic-like profiles within the arterial system, multiple in-vitro studies evaluating blood movement in glass tubes report the presence of parabolic-like flow (80, 200). Further, Hale et al. (1955) reported in the femoral artery of the dog that during antegrade flow the velocity profile approached that of a parabola, but that reversal of flow (retrograde) created a profile in which the lamine near the vessel edge moved at a greater rate than its center (91), i.e. not parabolic in form. This is in contrast with the present study in which retrograde flow was interpreted as maintaining a parabolic-like profile based on the V_{MEAN}/V_{PEAK} ratio. The difference may in part be due our inability to distinguish where within the lumen of the vessel the peak velocity is occurring.

Similar reports on antegrade flow have been made in venous microvessels of the rat at rest. Using fluorescently labeled red blood cells, Bishop et al. (14) observed a nearly parabolic velocity distribution across a wide range of blood velocities with a V_{MEAN}/V_{PEAK} ratio not significantly different than 0.5. The previous findings of Hale et al. (91) and Bishop et al. (14) in combination with the present study provide support for the conclusions that parabolic-like flow is a routine occurrence within the intact circulation.

The data in the present study during exercise is related to that reported in previous investigations utilizing the reciprocal index (V_{MAX}/V_{MEAN}) to determine the velocity profile.

Using Doppler ultrasound, Osada and Radegran (170, 171) determined that at rest in the femoral artery the velocity profile ranged from a V_{MAX}/V_{MEAN} ratio of ~1.3 to ~1.75, which corresponds to V_{MEAN}/V_{PEAK} ratio of 0.76 and 0.57 respectively, suggesting a profile that is less parabolic and more blunted than that reported in the present study. Likewise during knee extension exercise the velocity profile ranged from a V_{MAX}/V_{MEAN} ratio of ~1.6 to ~1.9, which corresponds to V_{MEAN}/V_{PEAK} ratio of 0.63 and 0.52 respectively. Possible difference may be attributed to how the blood velocities were measured and when the velocity ratio was calculated. First, the Doppler ultrasound beam width and insonation angles can affect blood velocity measurements. Difference in the ultrasound set-up between the present study and those of Osada and Radegran may account for the observed differences. Second, Osada and Radegran evaluated the velocity profile during the systolic and diastolic pressure phases, and report at rest a significantly more plug-like profile ($V_{MEAN}/V_{PEAK} \approx 0.76$) during the systolic phase compared to the diastolic phase ($V_{MEAN}/V_{PEAK} \approx 0.57$). Assuming the diastolic phase represents 2/3 of the cardiac cycle the calculated average resting V_{MEAN}/V_{PEAK} ratio across the entire cardiac cycle is ≈ 0.63, which is greater than a ratio of 0.58 and 0.53 observed in the resting femoral artery of the present study. These differences suggest that the velocity profile may be dependent on within-subject factors that have not yet been evaluated. Further investigations evaluating arterial compliance, blood viscosity, and vessel configuration (i.e. tortuous vs. straight) are needed to determine what factors impact the velocity profile.

While the ratios between studies are different they suggest that the femoral artery velocity profile is a blunted parabolic shape. Furthermore, the results of the present study extend those of Osada and Radegran who focused on the effects of blood pressure phases and muscle contraction on femoral artery velocity profiles during submaximal exercise. The present study provides additional insight with exercise and CPT in multiple arteries. Likewise, the present study focuses on antegrade, retrograde, and the entire cardiac cycle, which is commonly used for measurements of shear rate and blood flow.

Calculation of blood flow traditionally is the product of mean blood velocity and vessel cross sectional area. In addition if a parabolic velocity profile is present, blood flow, in theory, can be calculated as the product of peak blood velocity, the V_{MEAN}/V_{PEAK} ratio for a parabola

(0.5), and vessel cross sectional area. However, the findings of the current study and those of Osada and Radegran suggest that the assumption of a V_{MEAN}/V_{PEAK} ratio of 0.5 is incorrect. Across the entire cardiac cycle the V_{MEAN}/V_{PEAK} ratio is 6 to 12% greater than 0.5, which results in a ~ 4-20% error in the calculation of blood flow when assuming a perfect parabolic profile.

Relevance

The key implications of the present study are two fold. First, as previously noted by Halliwill and Minson (92) and Parker et. al (176), calculations of shear rate contain inherent assumptions, as discussed above. The results of the present study support one of these assumptions that the velocity profile is remarkably stable. Furthermore, while the V_{MEAN}/V_{PEAK} ratio of ~ 0.6 across the entire cardiac cycle suggests a blunted parabolic shape it is much closer to the perfect parabolic ratio of 0.5 than the plug-profile ratio of 1.0. Therefore, the present data support the use of mean flow to estimate shear in healthy populations, especially in the evaluation of endothelial function via flow-mediated dilation, which requires estimation of the shear stimulus (176).

Second, the aforementioned work by Thijssen (229) and Padilla (173, 174) suggest the need for more research regarding the consequences of retrograde shear. The stability of the retrograde velocity profile in the present study suggests that the calculation of retrograde shear is an acceptable approximation. This sets a foundation for future work in aged and diseased populations in which retrograde flow is more prevalent and potentially pathogenic (45, 173, 256).
Further research is needed to determine whether V_{MEAN}/V_{PEAK} differences from 0.5 indicated physiological significant differences in actual shear stress to the endothelium

Limitations

Several limitations are relevant to the interpretation of the present findings. First, the sample size used was small and consisted of young healthy men and women and this may limit the extrapolation of these data to other populations. However, the correlation coefficients across

a broad range of blood velocities provide evidence that the findings of the present study are robust and would not have been improved with a larger sample size. Second it is well established that the cyclic effects of sex hormones in women can impact vascular function (154). In an attempt to mitigate these effects all women were tested during the follicular phase of their menstrual cycle. Third, the velocity profile was evaluated using ratios of blood velocities, not direct observations, such as with cinematography. Since cinematography is unpractical in humans, the use of the V_{MEAN}/V_{PEAK} ratio provides insight to what is happening within the vessel. Unfortunately, the sample volume of a pulsed Doppler ultrasound does not permit evaluation of individual lamiae across the vessel lumen, limiting the ability of this technique to distinguish the specific instantaneous velocity profile. Likewise, differences in Doppler ultrasound beam width, insonation angle, and spectral broadening may limit the accuracy of blood velocity measurements. An ultrasound beam width that is smaller than the vessel diameter (i.e. doesn't complete insonate the vessel cross section) results in overestimation of mean blood velocities (100). Furthermore, Evans et al. suggests that in the presence of a parabolic profile, the mean velocity could be overestimated by 30-33% when the beam width is less than a quarter of the vessel diameter (70). In the context of the present study, an overestimation of V_{MEAN} would result in a higher V_{MEAN}/V_{PEAK} ratio. Therefore, the slight differences between brachial and femoral V_{MEAN}/V_{PEAK} ratios observed in the present study and the differences between V_{MEAN}/V_{PEAK} ratios reported in the present study compared to those of Osada and Radegran (2005, 2006) may be partially explained by incomplete vessel insonation caused by a narrow ultrasound beam width. Nonetheless, the similarity between the results of the present study and the cinematographic observations of earlier work in the intact dog femoral artery provide evidence that the assumption of parabolic-like flow within the human limb conduit arteries is justified.

Conclusion

The present study demonstrates that the blood velocity profile remains constant during CPT and dynamic exercise and that the antegrade profile has a slightly blunted parabolic shape, while the retrograde profile closely resembles a true parabolic shape. In addition, the profile in both directions is extremely resistant to change when limb vascular resistance/conductance and

48

mean arterial pressure is manipulated. We conclude that these results provide support of the current practice of calculating shear rate based on the assumption of laminar flow, but that those calculations may only provide an approximation of shear rate, not an exact measure. The presence of a blunted parabolic profile will induce error into any shear rate calculation. However, based on the findings of the current study that error will remain constant during CPT and dynamic exercise.

Table 3-1: Systemic and Brachial Artery Hemodynamic Responses to Cold Pressor, n=7

Variable	Baseline	CPT - 1:00 min	CPT - 2:00 min	Recovery
MAP, mmHg	83.5 ± 5.6	92.7 ± 8.4**	95.9 ± 7.3***	84.2 ± 5.4
HR, beats x min^{-1}	60 ± 8	61 ± 8	62 ± 9	62 ± 8
Vascular Conductance, ml x min^{-1} x mmHg^{-1}	0.82 ± 0.42	0.56 ± 0.21*	0.59 ± 0.32*	1.17 ± 0.74
Vascular Resistance, mmHg x ml^{-1} x min^{-1}	1.48 ± 0.61	2.05 ± 0.76	2.06 ± 0.80	1.25 ± 0.81
BABF$_{VMEAN}$, ml x min^{-1}	67.8 ± 34.7	52.4 ± 20.3	57.5 ± 34.0	98.0 ± 61.1
BABF$_{VPEAK/2}$, ml x min^{-1}	57.0 ± 32.8$^{\alpha\alpha\alpha}$	43.0 ± 15.4$^{\alpha\alpha\alpha}$	50.1 ± 30.7$^{\alpha\alpha\alpha}$	86.5 ± 55.6$^{\alpha\alpha\alpha}$
Cardiac Cycle				
V$_{PEAK}$, cm x sec^{-1}	13.4 ± 6.6	10.4 ± 2.5	12.4 ± 6.3	17.2 ± 11.1
V$_{MEAN}$, cm x sec-1	7.95 ± 3.45	6.18 ± 1.70	7.14 ± 3.47	9.79 ± 6.09
V$_{MEAN}$/V$_{PEAK}$	0.61 ± 0.06	0.59 ± 0.03‡	0.58 ± 0.02‡	0.58 ± 0.02‡
Antegrade				
V$_{PEAK}$, cm x sec^{-1}	57.5 ± 9.3	50.7 ± 8.3	48.7 ± 5.5**	58.6 ± 9.1
V$_{MEAN}$, cm x sec-1	31.2 ± 5.3	28.2 ± 4.2	26.3 ± 4.3*	32.4 ± 6.2
V$_{MEAN}$/V$_{PEAK}$	0.54 ± 0.02	0.56 ± 0.02‡	0.54 ± 0.03	0.55 ± 0.02‡
Retrograde				
V$_{PEAK}$, cm x sec^{-1}	16.7 ± 2.7	14.2 ± 3.8	14.6 ± 3.7	15.6 ± 4.2
V$_{MEAN}$, cm x sec-1	8.08 ± 0.94	6.72 ± 1.75**	6.94 ± 1.38*	7.47 ± 1.54
V$_{MEAN}$/V$_{PEAK}$	0.49 ± 0.05^{+++}	0.47 ± 0.03^{+++}	0.48 ± 0.04^{++}	0.48 ± 0.05^{+++}

Values are means ± SD. MAP, mean arterial pressure; HR, heart rate; FABF$_{VMEAN}$, femoral artery blood flow calculated as V$_{MEAN}$ x CSA; FABF$_{VPEAK/2}$, femoral artery blood flow calculated as (V$_{PEAK}$/2) x CSA; V$_{PEAK}$, average peak blood velocity; V$_{MEAN}$, average mean blood velocity

Significantly different from Baseline *(P<0.05), **(P<0.01), ***(P<0.001)

Significantly different from Antegrade V$_{MEAN}$/V$_{PEAK}$ ratio $^{+}$(P<0.05), $^{++}$(P<0.01), $^{+++}$(P<0.001)

‡ Significantly different from 0.5 (P<0.05)

Significantly different from BABF$_{VMEAN}$ $^{\alpha}$(P<0.05)), $^{\alpha\alpha}$(P<0.01), $^{\alpha\alpha\alpha}$(P<0.001)

Table 3-2: Linear regression analysis of blood velocities.

	Cold Pressor Test				Knee Extension Exercise		
	Baseline	CPT, minute 1	CPT, minute 2	Recovery	Baseline	50% Peak	Peak Power
Brachial Artery							
Antegrade							
y-intercept, M	-0.61	-4.20	-6.69	-6.56	-	-	-
Slope, b	0.55	0.64	0.67	0.66	-	-	-
R	0.98	0.99	0.94	0.99	-	-	-
Retrograde							
y-intercept, M	2.88	0.52	1.67	2.26	-	-	-
Slope, b	0.31^{+}	0.43^{+}	0.36^{+}	0.34^{+}	-	-	-
R	0.91	0.98	0.96	0.92	-	-	-
Femoral Artery							
Antegrade							
y-intercept, M	0.65	3.12	4.72	3.05	3.43	-9.08	-3.90
Slope, b	0.56	0.52	0.49	0.52	0.49	0.73*	0.59
R	0.93	0.95	0.95	0.93	0.92	0.98	0.96
Retrograde							
y-intercept, M	-0.98	-1.29	-1.59	-1.33	1.10	-	-
Slope, b	0.54	0.57	0.59	0.57	0.41	-	-
R	0.94	0.93	0.96	0.96	0.93	-	-

Linear model: $V_{MEAN} = M(V_{PEAK}) + b$; CPT, cold pressor test.

[+] Significantly different from Antegrade Slope ($P<0.05$)

* Significantly different from Baseline ($P<0.05$)

Table 3-3: Systemic and Femoral Artery Hemodynamic Responses to Cold Pressor, n=8

Variable	Baseline			CPT - 1:00 min			CPT - 2:00 min			Recovery		
MAP, mmHg	89.6	±	13.5	95.9	±	15.6*	98.2	±	12.6**	87.6	±	10.8
HR, beats x min^{-1}	71	±	12	72	±	11	73	±	13	70	±	12
Vascular Conductance, ml x min^{-1} x mmHg^{-1}	1.76	±	0.87	1.20	±	0.38*	1.45	±	0.75	1.77	±	0.88
Vascular Resistance, mmHg x ml^{-1} x min^{-1}	0.69	±	0.31	0.93	±	0.33**	0.88	±	0.45*	0.69	±	0.33
FABF$_{VMEAN}$, ml x min^{-1}	150	±	57.0	111	±	28.5*	138	±	66.1	149	±	60.5
FABF$_{VPEAK/2}$, ml x min^{-1}	128	±	45.3$^{\alpha\alpha\alpha}$	90	±	25.1*$^{\alpha\alpha\alpha}$	113	±	56.7$^{\alpha\alpha\alpha}$	124	±	53.6$^{\alpha\alpha\alpha}$
Cardiac Cycle												
V$_{PEAK}$, cm x sec^{-1}	12.9	±	4.9	10.0	±	3.2*	12.2	±	6.6	13.4	±	6.0
V$_{MEAN}$, cm x sec-1	7.55	±	3.06	6.14	±	1.78	7.43	±	3.65	8.04	±	3.36
V$_{MEAN}$/V$_{PEAK}$	0.58	±	0.07	0.62	±	0.05‡	0.61	±	0.04‡	0.61	±	0.04‡
Antegrade												
V$_{PEAK}$, cm x sec^{-1}	44.2	±	7.6	44.2	±	7.5	44.1	±	7.7	45.2	±	7.8
V$_{MEAN}$, cm x sec-1	25.4	±	4.6	25.9	±	4.1	26.2	±	3.9	26.3	±	4.3
V$_{MEAN}$/V$_{PEAK}$	0.57	±	0.04	0.58	±	0.03‡	0.60	±	0.03‡	0.58	±	0.03‡
Retrograde												
V$_{PEAK}$, cm x sec^{-1}	20.6	±	5	20.2	±	4.4	18.0	±	4.3	18.2	±	4.9
V$_{MEAN}$, cm x sec-1	10.2	±	2.9	10.2	±	2.7	9.0	±	2.7	8.9	±	2.9
V$_{MEAN}$/V$_{PEAK}$	0.48	±	0.04^{+++}	0.50	±	0.05^{+++}	0.50	±	0.05^{+++}	0.49	±	0.05^{+++}

Values are means ± SD. MAP, mean arterial pressure; HR, heart rate; FABF$_{VMEAN}$, femoral artery blood flow calculated as V$_{MEAN}$ x CSA; FABF$_{VPEAK/2}$, femoral artery blood flow calculated as (V$_{PEAK}$/2) x CSA; V$_{PEAK}$, average peak blood velocity; V$_{MEAN}$, average mean blood velocity

Significantly different from Baseline *($P<0.05$), **($P<0.01$), ***($P<0.001$)

Significantly different from Antegrade V$_{MEAN}$/V$_{PEAK}$ ratio $^{+}$($P<0.05$), $^{++}$($P<0.01$), $^{+++}$($P<0.001$)

‡ Significantly different from 0.5 ($P<0.05$)

Significantly different from BABF$_{VMEAN}$ $^{\alpha}$($P<0.05$)), $^{\alpha\alpha}$($P<0.01$), $^{\alpha\alpha\alpha}$($P<0.001$)

Table 3-4: Systemic and Femoral Artery Hemodynamic Responses to Knee Extension Exercise, n=8

Variable	Baseline			50% Peak Power			Peak Power		
MAP, mmHg	92.1	±	7.1	122	±	10.6***	129	±	16.6***
HR, beats x min^{-1}	77	±	13	108	±	20***	138	±	15***
Vascular Conductance, ml x min^{-1} x mmHg^{-1}	1.78	±	0.99	4.42	±	1.25*	5.98	±	1.90*
Vascular Resistance, mmHg x ml^{-1} x min^{-1}	0.73	±	0.36	0.24	±	0.07**	0.18	±	0.05**
FABF$_{VMEAN}$, ml x min^{-1}	164	±	90	544	±	181***	768	±	248***
FABF$_{VPEAK/2}$, ml x min^{-1}	153	±	77	502	±	137**	739	±	213***
Cardiac Cycle									
V$_{PEAK}$, cm x sec^{-1}	15.7	±	7.1	49.7	±	10.4*	69.5	±	14.5*
V$_{MEAN}$, cm x sec-1	8.4	±	4.2	26.9	±	7.3*	35.9	±	8.2*
V$_{MEAN}$/V$_{PEAK}$	0.53	±	0.03	0.54	±	0.05	0.52	±	0.04
Antegrade									
V$_{PEAK}$, cm x sec^{-1}	43.0	±	10.5	50.0	±	10.0	69.4	±	13.8***
V$_{MEAN}$, cm x sec-1	24.3	±	5.5	27.3	±	7.5	36.8	±	8.5**
V$_{MEAN}$/V$_{PEAK}$	0.57	±	0.05	0.54	±	0.06	0.53	±	0.04
Retrograde									
V$_{PEAK}$, cm x sec^{-1}	15.2	±	4.29						
V$_{MEAN}$, cm x sec-1	7.31	±	1.88						
V$_{MEAN}$/V$_{PEAK}$	0.49	±	0.04^{+++}						

Values are means ± SD. MAP, mean arterial pressure; HR, heart rate; FABF$_{VMEAN}$, femoral artery blood flow calculated as V$_{MEAN}$ x CSA; FABF$_{VPEAK/2}$, femoral artery blood flow calculated as (V$_{PEAK}$/2) x CSA; V$_{PEAK}$, average peak blood velocity; V$_{MEAN}$, average mean blood velocity

Significantly different from Baseline *(P<0.05), **(P<0.01), ***(P<0.001)

Significantly different from Antegrade V$_{MEAN}$/V$_{PEAK}$ ratio [+](P<0.05), [++](P<0.01), [+++](P<0.001)

[‡] Significantly different from 0.5 (P<0.05)

Significantly different from BABF$_{VMEAN}$ [α](P<0.05)), [αα](P<0.01), [ααα](P<0.001)

Figure 3-1. Representative Doppler waveforms during (A) Cold Pressor Test and (B) knee extension exercise.

Note that antegrade blood velocities occur above baseline and were evaluated between the initial increase in blood velocity with systole and the start of retrograde blood velocity when the Doppler waveform transitioned below baseline.
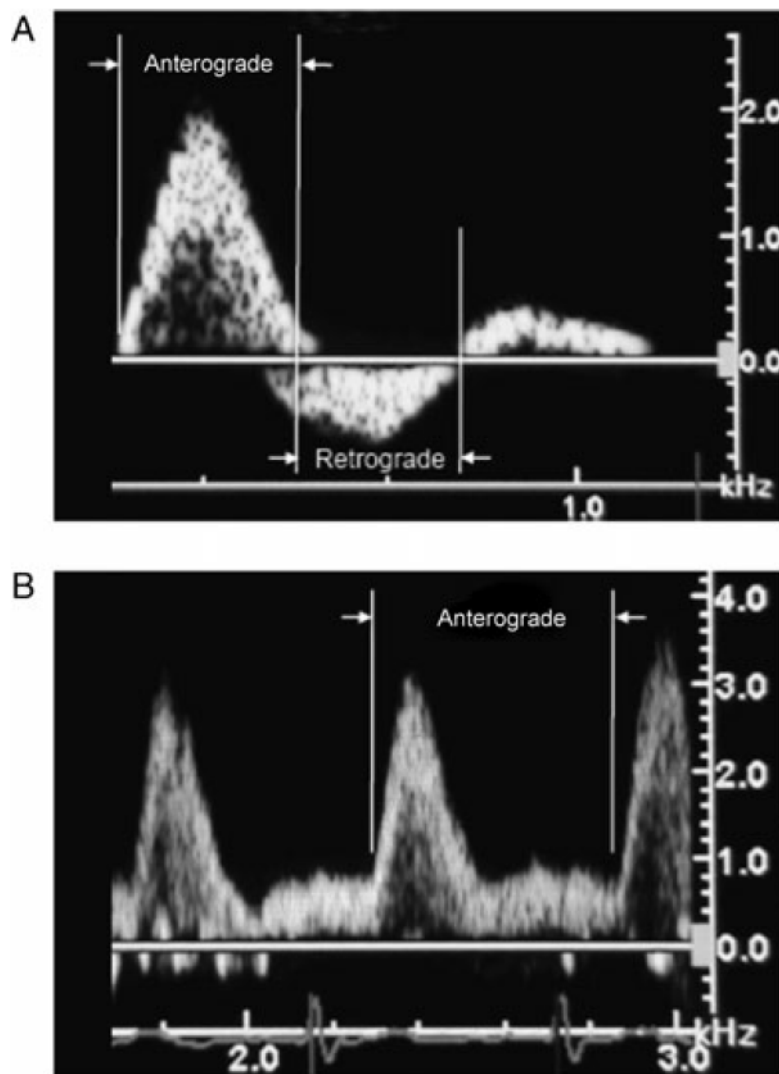
Figure 3-2. Blood flow calculated using $V_{PEAK}/2$ x CSA as a function of blood flow calculated using V_{MEAN} x CSA in the (A) brachial and (B) femoral arteries.

Solid symbols represent flow during CPT, open symbols represent flow during dynamic exercise. The solid line indicates the line of identity. The dashed line indicates the significant (P<0.001) linear regression between the two methods of calculating blood flow.
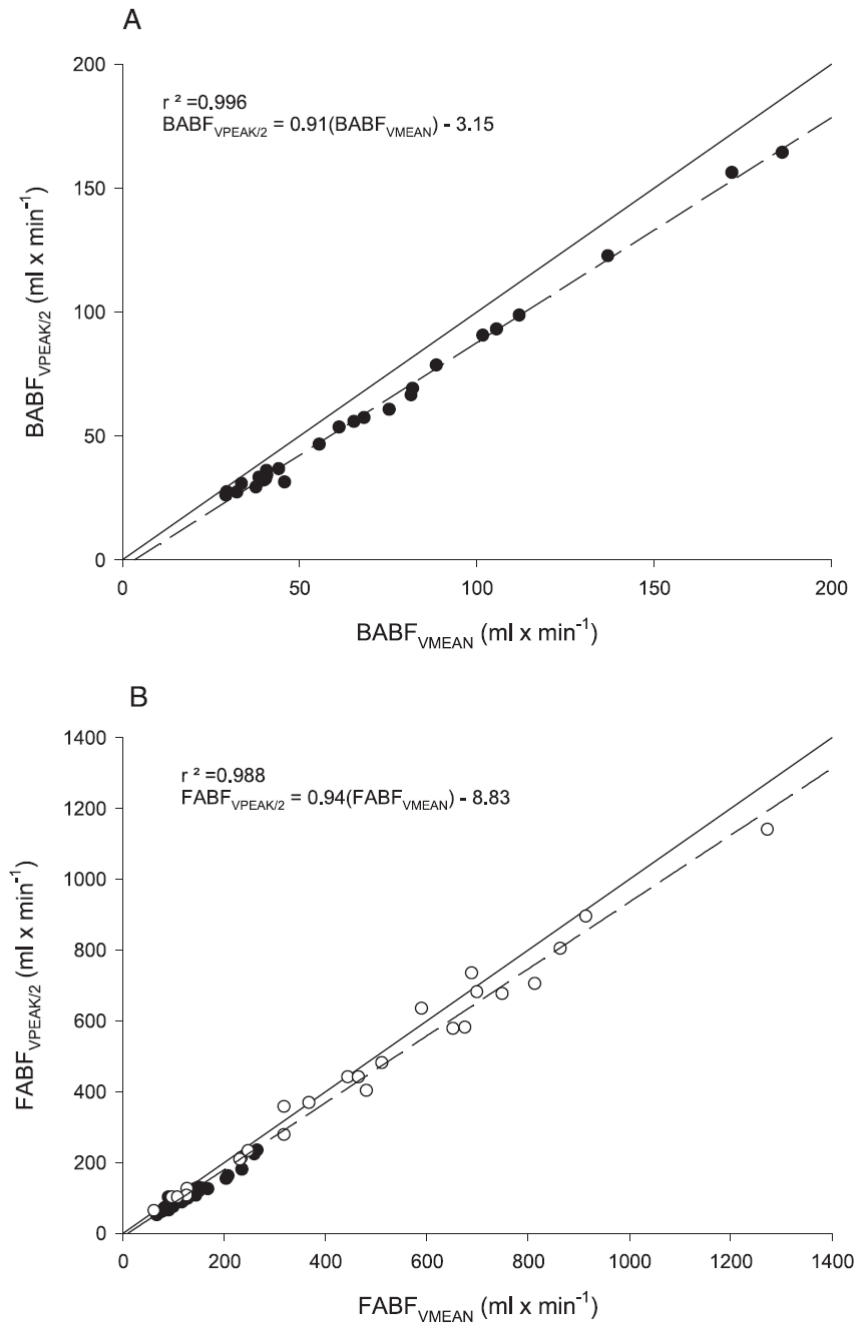
Figure 3-3. Group $\pm$ SD changes in antegrade and retrograde V_{MEAN}/V_{PEAK} ratio during cold pressor test in the (A) brachial artery and (B) femoral artery.

The cold pressor test did not impact the brachial or femoral V_{MEAN}/V_{PEAK} ratio. Antegrade flow had a significantly higher V_{MEAN}/V_{PEAK} ratio compared to retrograde under all conditions. [+] Significant difference vs. antegrade, [‡] significant difference vs. 0.5.
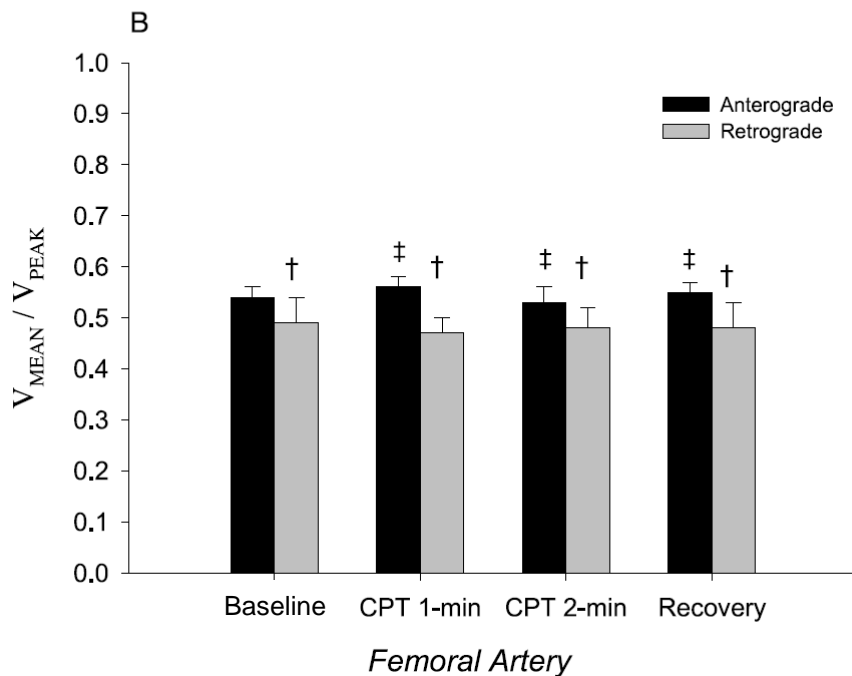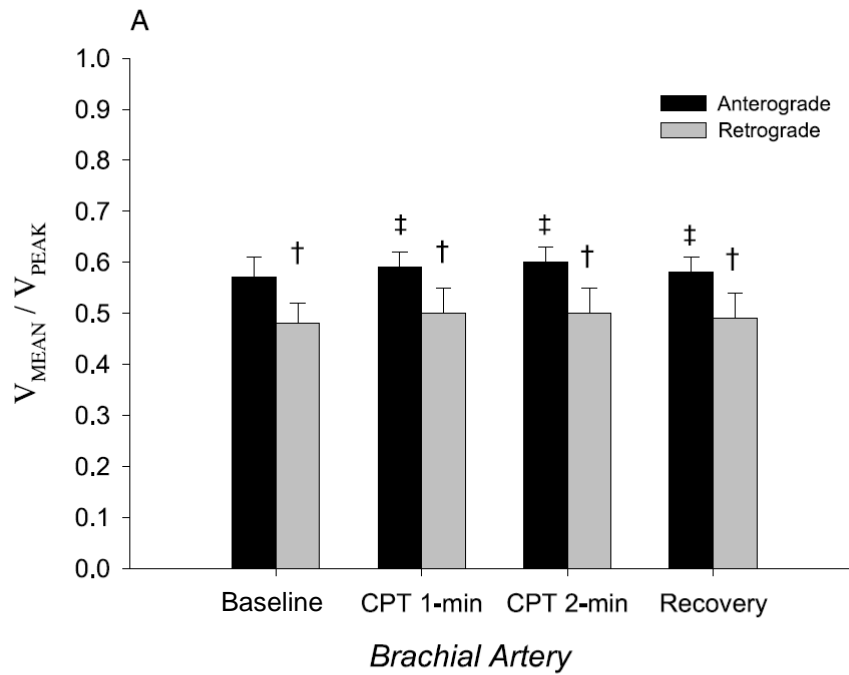
Figure 3-4. V_{MEAN} as a function of V_{PEAK} in subjects determined over 3-5 cardiac cycles in the brachial artery during (A) CPT and in the femoral artery during (B) CPT and (C) knee extension exercise.

The solid line indicates the line of identity (V_{MEAN}/V_{PEAK} =1; plug-like profile) and the dotted line indicates the line representing a parabolic profile (V_{MEAN}/V_{PEAK} = 0.5). Retrograde velocities have been inverted to positive values.
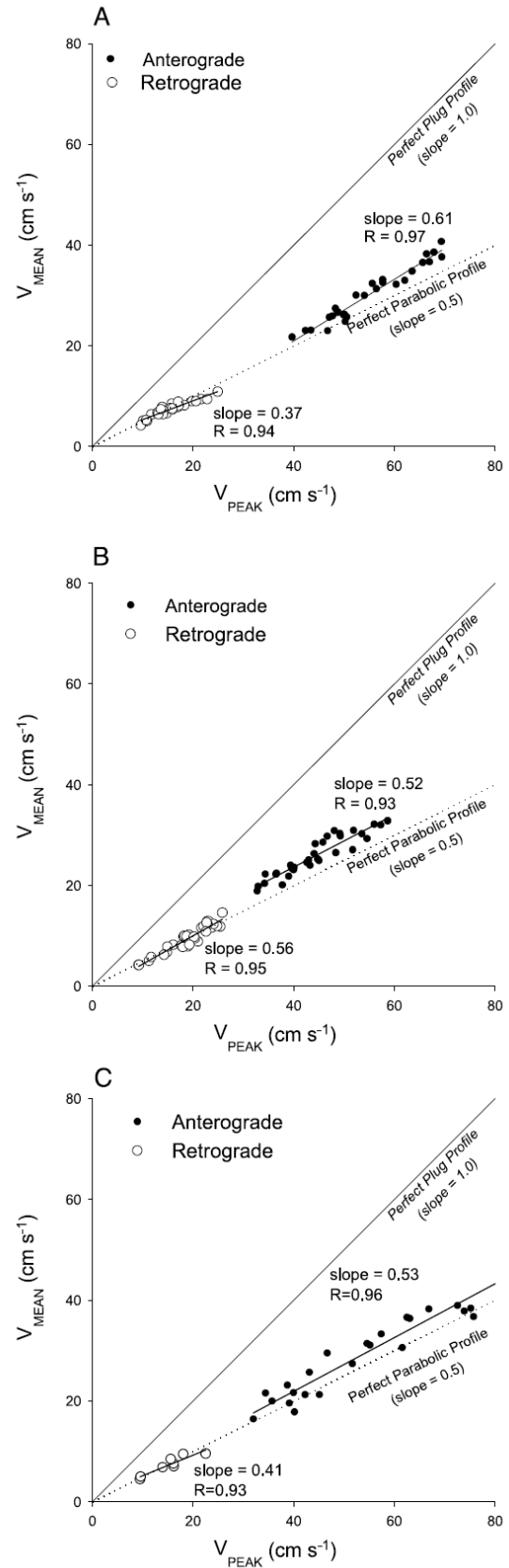
Chapter 4 - Influence of prior sustained antegrade shear rate on the vascular responses during dynamic forearm exercise

Summary

Previous investigations have demonstrated that elevations in antegrade shear stress are associated with an antiatherosclerotic condition and a pro-vasodilatory state. However, the effects of prior exposure to sustained elevations in antegrade shear on the on-transient kinetics of vascular adjustments to exercise remain unknown. Therefore, the purpose of the present study was to determine the effects of antegrade shear on forearm vascular conductance (FVC) and blood flow (FBF) during dynamic forearm exercise. Eight men (25 ± 3 yr; mean $\pm$ SD) completed a flow-mediated dilation (FMD) test and a constant-load exercise test corresponding to 40% peak power output, were performed prior to and following a 30 min intervention consisting of forearm heating, which has previously been shown to increase antegrade shear rate in the brachial artery. During exercise, FBF (Doppler ultrasound), muscle deoxygenation (deoxy-[Hb+Mb]) determined via near-infrared spectroscopy, and mean arterial pressure (MAP) were measured and averaged into 3 sec bins; FVC was calculated as FVC = FBF/MAP$\times$100. FBF, FVC, and deoxy-[Hb+Mb] data were fit with a monoexponential model. During the heating intervention, antegrade shear rate increased 150%. FMD was increased 43% following heating. The rate of adjustment in FVC and FBF to exercise was faster post-heating (21.4 ± 2.60 and 29.7 ± 7.5 s, respectively) compared to pre-heating (38.2 ± 15.3 and 42.2 ± 13.3, respectively; $P<0.05$). Heating resulted in slowed kinetics and reduced steady-state for deoxy-[Hb+Mb] following heating. These results demonstrate that vascular and endothelial functions at rest and during dynamic exercise are positively influenced by acute elevations in antegrade shear rate patterns.

Introduction

Chronic aerobic exercise decreases the risk for all-cause cardiovascular disease, while simultaneously increasing aerobic exercise capacity and quality of life (15, 175). However, only a fraction of the decreased cardiovascular risk can be explained by modifications of traditional risk factors (i.e., body mass index, lipids, hypertension, diabetes, etc.) (85, 113, 159, 231). One contributing component to the overall improvement in cardiovascular health may be the vascular adaptations or 'vascular conditioning' associated with exercise training, which include positive structural and functional changes coupled with an anti-atherosclerotic state (83, 131, 172). However, the signal generated by a given exercise bout as a modifier of vascular function is not completely defined (51, 131).

One key exercise stimulus mediating vascular adaptation may be the mechanical shear stress acting on the endothelium, consequent to the increased vascular conductance and blood flow observed at exercise onset (164). Evidence from isolated cell culture studies suggests that endothelial cells exposed to an increased shear stress exhibit a cascade of increased intra-cellular signaling which could contribute to the increased vascular function associated with exercise training (131). Furthermore, endothelial cells respond to shear stress in a time-dependent manner such that there is a near-immediate response followed by a slower transient response that varies with the duration of the shear stimuli (7). The immediate response to an increased shear stress is observed within seconds and includes the release of the vasoactive substance nitric oxide (168). In the intact human cardiovascular system, this immediate response is evident during reactive flow-induced or flow-mediated dilation (FMD), in which increased flow and shear rate following 5 min limb occlusion results in conduit artery vasodilation, primarily facilitated via endothelial-dependent NO release (123, 204). Therefore, the FMD test has become a reproducible clinical test to evaluate endothelial function (194, 227). Similar to the immediate response, a sustained increase in shear stress lasting several minutes to hours, similar to that experienced during endurance exercise, results in various intracellular adaptations. Following 3hr of exposure to unidirectional shear stress, cultured endothelial cells demonstrate an increased eNOS gene transcription and eNOS mRNA expression (197, 237). Similarly, 2hrs of increased shear stress in

60

isolated perfused coronary arterioles increases eNOS and super oxide dismutase (SOD-1) expression, both of which will contribute to an increased NO bioavailability (253). In addition, Green and colleagues have characterized the impact of different experimental shear patterns within the intact human cardiovascular system on endothelial function via the FMD test (228, 229, 232, 233). Tinken et al. (232) demonstrated that when mean shear rate is acutely increased for 30 min via a single bout of exercise or forearm heating, FMD is significantly increased. These data suggest that acute elevations in shear rate within the intact artery result in an enhanced endothelial function. Cumulatively these studies provide evidence that shear stress is a key signal during an exercise bout for endothelial and subsequent vascular adaptation.

During exercise the on-transient temporal mismatch between oxygen delivery ($\dot{Q}O_2$) and oxygen consumption ($\dot{V}O_2$) is observed in aged (9, 49) and diseased (58) conditions. This matching of $\dot{Q}O_2$ to $\dot{V}O_2$ is dependent on the increase in muscle blood flow which is achieved in part via the targeted vasodilation of microvascular and feed arteries within the active limb. The dynamics of this response is in part mediated by local mechanisms, which include both metabolic and endothelium-mediated control (31, 54, 129). Nitric oxide (NO) released from the vascular endothelium or the locally contracting muscles, has been highlighted as a key vasoactive substance contributing to the coordinated increase in muscle blood flow during exercise (41, 42, 129). Recently, Casey et al. (26) demonstrated that the vasodilator response to dynamic forearm exercise is attenuated following arterial infusion of a NO synthase (NOS) inhibitor. These authors concluded that NO-mediated dilation significantly contributes to increase in limb vascular conductance during the exercise on-transient. Therefore, the increased vasodilator response and improved matching of $\dot{Q}O_2$ to $\dot{V}O_2$ following exercise training may be an effect of an increased shear stress and NO availability experienced during each exercise bout within a training regimen (84, 163). However, it remains unknown if an acute increase in shear stress, like that achieved during a single bout of exercise, improves vascular function during exercise.

The primary aim of the present study was therefore to determine if prior increased shear stress in a conduit artery, independent of muscular contractions, increases vascular function as

determined via FMD and the on-transient vasodilator response to moderate forearm exercise. It was hypothesized that prior exposure to a single bout of antegrade shear via forearm heating, which has previously been shown to elicit a similar shear rate pattern as dynamic exercise (163, 232), would (i) increase the FMD response to post-occlusion (i.e., reactive hyperemia), (ii) increase the vasodilator and subsequent blood flow responses to dynamic forearm exercise, and (iii) improve the matching of $\dot{V}O_2$ to $\dot{Q}O_2$ as determined via near infrared spectroscopy during forearm exercise.

.

Methods

Subjects

Eight men (25 ± 3 yrs (mean ± SD); stature 178.8 ± 6.4 cm; mass 92.0 ± 18.0 kg; BMI 28.9 ± 6.0 kg x m^{-2}) completed the experiments. All subjects were free from known cardiovascular, pulmonary, or metabolic disease and were non-smokers as determined via health history questionnaire. Verbal and written consent were obtained from all subjects following approval of the study by the Institutional Review Board for Research Involving Human Subjects at Kansas State University, which conformed to the Declaration of Helsinki.

Study design and protocol

All testing sessions were performed at the same time of day for a given subject in a temperature controlled laboratory following an overnight fast and after refraining from exercise, alcohol, and caffeine for at least 12 hrs. Subjects completed three visits, each separated by a minimum of 48 hrs. The first visit consisted of graded dynamic forearm exercise test to determine peak power output. At the second and third visits, a FMD test and a constant-load exercise test were randomly performed on separate days before and after a 30 min antegrade shear rate intervention. The intervention consisted of heating of the forearm designed to increase mean and antegrade shear rate and decrease retrograde shear.

Incremental Exercise. To determine peak power output, subjects performed an incremental dynamic forearm exercise test on a custom built forearm ergometer. Exercise was performed in a supine position, with the right arm extended laterally (~80°) at heart level. Following 1 min of baseline, subjects began forearm contractions at 20 contractions min^{-1}. Contractions consisted of squeezing a handgrip device, which compressed an adjustable pneumatic cylinder 4 cm, at a duty cycle of 1:2 s work-rest cycle with concentric contraction contributing to ~100% of the work phase. The work rate progressively increased 0.5 Watts every 30 sec until the subject could not maintain the correct contraction rate for at least 3 contractions

despite verbal encouragement. Peak power output (PPO) was defined as the highest power output at which a minimum of 15 s of the test stage was completed.

FMD. Conduit artery endothelial function was assessed by FMD in the brachial artery of the right arm according to the guidelines suggested by Thijssen et al. (2011) before and 10 min after the 30 min heating intervention (Figure 4-1A) (227). During a 15 min supine rest period, subjects were instrumented for continuous measurement of beat-by-beat HR and MAP via finger photoplethysmography (Nexfin HD; BMEYE, Amsterdam, The Netherlands). A rapid inflation/deflation pneumatic cuff (Hokanson) was positioned on the right arm proximal to the olecranon process. Measurements of brachial artery shear rate (SR = 4 x V_{mean}/diameter) were made using a linear array transducer probe proximal to the pneumatic cuff operating at an imaging frequency of 6.7 MHz and an insonation angle less than 60 degrees (Vivid 3; GE Medical Systems, Milwaukee, WI). V_{mean} was calculated as half the peak blood velocity to account for incomplete sampling of Doppler shifts across the full width of the artery (3, 227). Shear rate was used as an estimate of shear stress without accounting for blood viscosity. After a clear image of the brachial artery was obtained, measurements of both blood velocity and artery diameter were recorded for a baseline period of 1 min. Following baseline, the pneumatic cuff was inflated to (>280 mmHg) for 5 min. Blood velocity and diameter measurements were resumed 15 s prior to cuff deflation and continued for 2 min post-occlusion. Since the Vivid 3 ultrasound system does not support duplex imaging, blood velocities and artery diameters were measured at alternating 5 s intervals throughout the FMD protocol.

Constant-load Exercise. Subsequent to the incremental test, subjects completed a square-wave transition within the moderate intensity domain before and 10 min after the forearm heating intervention (Figure 4-1B). Initially subjects rested in the supine position for 15 min. In each exercise trial, baseline data was collected for 1 min, followed by a step increase in work rate to 40% PPO for 6 min. During the course of each exercise trial beat by beat heart rate (HR) and mean arterial pressure (MAP) were continuously measured as previously described. Brachial artery blood velocity and diameter were measured with a linear phased array transducer probe and averaged into 3 sec bins and corrected for an angle of insonation less than 60 degrees. Forearm blood flow (FBF, ml x min^{-1}) was calculated using the product of mean blood velocity

64

(V_{mean}, cm x sec^{-1}) and brachial artery cross-sectional area (cm^2). V_{mean} was calculated as half the peak blood velocity. Vessel diameters were measured every 60 seconds via two-dimensional sonography and used to calculate cross-sectional area (CSA = π x radius^2). Forearm vascular conductance (FVC, ml x min^{-1} (100 mmHg)$^{-1}$) was calculated as the ratio of FBF to MAP x 100.

Skeletal muscle hemoglobin + myoglobin deoxygenation (deoxy-[Hb+Mb]) of the right flexor digitorum superficialis was evaluated by near-infrared spectroscopy (NIRS) (OxiplexTS; ISS, Champaign, IL). Briefly, the NIRS probe consisted of eight light emitting diodes operating at two wavelengths (690 and 830 nm) and a single detector fiber bundle (source detector separation of 2.0-3.5 cm). The near-infrared probe was placed longitudinally along the belly of the flexor digitorum superficialis (~15 cm proximal to the wrist). Muscle location was verified via surface electromyography and manual palpations. The data were stored at >25Hz and averaged into 3 sec bins off-line. No movement of the probe occurred during exercise. Near-infrared spectroscopy has previously been used to evaluate the redox state of microvascular hemoglobin and intracellular myoglobin. Specifically, the concentration of these deoxygenated heme molecules is an estimate of microvascular fractional O_2 extraction that describes the balance between $\dot{V}O_2$ and $\dot{Q}O_2$ (49, 71, 121, 125).

Antegrade shear rate intervention. Acute alteration of the shear rate pattern in the brachial artery of the right arm was performed in the supine position via unilateral forearm heating in a similar method as Tinken et al. (232). Briefly, the forearm was wrapped with a digitally controlled heating pad designed to increase forearm skin temperature to ~40°C. Since the target heating stimulus was not instantaneous a 10 min warming period was used followed by a 30 min intervention period in which skin temp was clamped at between 38-40°C. Following the 30 min intervention the forearm was cooled back to resting skin temperatures (~32°C) over a 10-15 min period. Testing did not continue until this return to baseline had been achieved. Skin temperature was continuously monitored via skin thermocouples (Thermes USB; Physitemp Instruments, Clifton NJ) placed on the anterior portions of the forearm. Measurements of mean, antegrade, and retrograde shear rate were calculated using mean, antegrade and retrograde blood velocities, respectively. The oscillatory shear index (OSI) was used to characterize the magnitude of the shear rate oscillations throughout a cardiac cycle (174). The OSI is calculated as follows:

OSI = |retrograde shear| / (|antegrade shear|+|retrograde shear|) such that OSI values of zero correspond to a unidirectional shear rate while values of 0.5 are indicative of oscillations with a mean shear rate of zero.

Data Analysis

The on-transient kinetics for FBF, FVC, and [HHb] during constant-load forearm exercise were analyzed using non-linear regression with a least squares technique (Sigma Plot 10). The responses were fitted as follows:

$$Y(t) = Y(baseline) + Amp \,[1-e^{-(t-TD)/\tau}]$$

Where $Y(t)$ is the dependent variable at any time (t), Y(baseline) is the resting baseline prior to exercise onset, Amp represents the amplitude of the response, TD the time delay, and τ is the duration of time for the dependent variable to change 63% of the steady-state amplitude. The initial rate of increase for FVC (k_r,FVC = FVC/ τ(FVC)) and [HHb] ((k_r, [HHb] = [HHb]/ τ([HHb])) were calculated from the modeled parameters.

FMD responses are reported as the absolute (mm) and relative (%) increase in brachial artery diameter above baseline. The relevant shear stimulus generating the FMD response following cuff deflation was determined as the area under the shear rate curve (AUC$_{SR}$), calculated for data up to peak diameter for each individual using the trapezoid rule, as per the guidelines established by Thijssen et al (227).

Statistical Analysis

Data are presented as mean±SD. One-tailed paired t-tests were used to test for differences in the FMD response and the model parameters of FBF, FVC, and [HHb] during constant-load exercise before and after the shear rate intervention. A one-tailed test is appropriate in this instance for testing directional hypotheses (141). A two-tailed paired t-test was used to determine

statistical significance for all other dependent variables in which no a priori directional

hypothesis was given. Statistical significance was declared when P<0.05.

Results

Figure 4-2 illustrates the shear rate patterns prior to and during the 30 min heating intervention on both the FMD and exercise test days. Forearm heating significantly increased mean and antegrade shear rate and decreased retrograde shear rate. In addition, heating significantly decreased the OSI index by ~87% compared to pre-heating on both the FMD (0.23 ± 0.08 vs. 0.02 ± 0.04, $P<0.05$) and exercise test days (0.22 ± 0.08 vs. 0.04 ± 0.06, $P<0.05$). There was no significant difference in the shear pattern between days.

FMD Response

Table 4-1 summarizes the group mean baseline characteristics and FMD response. There was no significant difference in the shear rate stimuli as determined by AUC_{SR} between FMD tests. The antegrade shear rate intervention, via forearm heating, did not significantly alter baseline MAP, HR, brachial artery diameter. However, 30 min of sustained heating significantly increased both absolute and relative FMD (Figure 4-3).

Exercise Response

Baseline and on-transient responses during forearm exercise are summarized in Table 4-2. The 30 min heating intervention did not alter baseline or steady-state MAP, HR, or FVC. However, there was a significant increase in steady-state FBF and decrease in deoxy-[Hb+Mb] compared to pre-heating. After heating, FBF kinetics were faster compared to pre-heating (Figure 4-4A). This increase in blood flow kinetics at exercise onset was achieved in part by a faster vasodilator response following heating (Figure 4-4B). Figure 4-5 illustrates the mean fit of the measured FBF response prior to and following the heating intervention. Notice that τFVC was significantly faster following heating (Figure 4-4B). In addition, the initial rate of increase in FVC (k_r,FVC) was significantly speeded. Baseline and steady-state deoxy-[Hb+Mb] were decreased following heating. The 30 min heating intervention significantly increased τdeoxy-[Hb+Mb] (Figure 4-4C) indicating that the temporal matching of $\dot{V}O_2$ to $\dot{Q}O_2$ was improved.

Discussion

The present study is the first to examine the vascular responses to constant-load exercise following an acute elevation in shear rate, independent of muscle contractions within the human circulation. The primary findings of the present study were that 1) acute forearm heating increased brachial artery mean and antegrade shear rate, but decreased retrograde shear rate and the OSI; 2) following the heating intervention, brachial artery FMD increased compared to pre-heating; 3) the overall rate of adjustment for FBF and FVC during exercise (measured as τFBF and τFVC) was significantly faster following the 30 min forearm heating intervention; and 4) the matching of $\dot{Q}O_2$ to $\dot{V}O_2$ was improved following the intervention as evident from an increased

FBF, a longer τdeoxy-[Hb+Mb] and lower steady-state deoxy-[Hb+Mb] compared to pre-intervention. These results indicate that vascular and endothelial function are positively influenced by acute antegrade shear rate patterns, lending supporting evidence that shear rate is one signal for alterations in vascular function.

Shear stress is the mechanical interaction between blood flow and the endothelial cells lining the arterial wall. It contributes in part to the release of vasoactive substances, the regulation of endothelial gene expression, and over time the structural remodeling of the artery wall (7, 164). These endothelium-mediated responses are dependent on the direction, magnitude, pulsatility, and duration of the mechanical shear stimulus such that they will promote either a proatherosclerotic or antiatherosclerotic endothelial phenotype (131). The capacity for endothelial cells to detect and respond to changes in shear stress can be described by four broadly defined steps (46). First, shear stress along the endothelium causes mild physical cellular deformation; second, this extracellular stress and deformation is transmitted intracellularly. These initial steps rely on mechanotransducers, which detect changes in flow magnitude and direction, and initiate intracellular signals. Currently no one specific component has been determined, but several have been proposed, including flow-sensitive ion channels, integrins, glycocalyx, primary cilia, and G-protein-coupled receptors (90, 110). The third and fourth steps consist of the conversion of the intracellular mechanical stimuli to an altered chemical activity followed by the activation of specific biochemical pathways within the endothelium.

Experimental evidence from cell culture studies indicate that disturbed or oscillatory flow patterns promote atherosclerosis, while sustained increases in unidirectional laminar flow and shear stress creates a pro-vasodilatory and antiatherosclerotic state (131, 164). Briefly, oscillatory shear is linked with an increased release and expression of superoxide, endothelin-1, adhesion molecules, and reactive oxygen species-producing enzymes, while also suppressing NO production (27, 107, 151, 258). Conversely, elevations in antegrade shear stress, like that experienced during exercise, produce a contrasting response. Kuchan et al. (127) demonstrated that exposure of cultured endothelial cells to laminar fluid flow stimulates an increase in NO release. Within 30 sec of exposure, NO levels increased above baseline and continued to progressively increase over the next several hours in a shear-dependent manner. These data suggest that sustained increases in shear stress ranging from minutes to hours results in a parallel increase in NO availability. In addition, similar studies report that as little as 2-4 hrs of exposure to an amplified shear stress increase NOS levels, NOS mRNA expression, SOD mRNA expression, and increase capacity for NO production and release (197, 237, 253). Also, chronic high blood flow and shear stress produced by arteriovenous fistulas in rat and canine models results in increased NOS mRNA expression, NOS protein levels, and endothelium-dependent relaxation (108, 153, 162).

Unlike cell culture models, the intact cardiovascular system at rest exhibits a phasic flow pattern in peripheral conduit arteries such that during systole a large antegrade flow is followed by a period of retrograde flow of varying degrees that is dependent on resting vascular tone (3, 148). During exercise, the increase in blood flow and vascular conductance result in an increase in both the magnitude and duration of antegrade flow to meet the metabolic demands of the contracting muscle (31, 129, 131, 211). This elevation in flow increases the parallel acting shear stress, between blood flow and the endothelium similar to that seen in cell culture studies. However, since the hemodynamic environment experienced by endothelial cell cultures is different from the intact cardiovascular system, it is critical to evaluate the effects of in vivo increases in shear stress. Therefore, more directly related to the vascular adaptations following a single bout of exercise, Haram et al. (93) evaluated endothelial adaptation following acute exercise in rats. They demonstrated that a single 60 min bout of exercise increased endothelium-

dependent dilation that persists up to 48hrs. Likewise, Tinken et al. (232) evaluated endothelial function via brachial artery FMD following 30 min of either handgrip exercise or forearm heating. Both interventions significantly increased mean and antegrade shear rate which resulted in an increased FMD. The results of the present study extend the work of Tinken et al. (232) who focused only on resting endothelial function. By utilizing a 30 min heating protocol to increase antegrade shear rate, the present study was able to isolate the increase in antegrade shear rate independently of muscular contractions. To our knowledge this is the first study to independently confirm these previous findings of Tinken et al. (232) and to more importantly evaluate the effects of shear rate on the blood flow and vasodilator responses to dynamic exercise.

The active hyperemia that occurs during muscular exercise results in a 10- to 100-fold increase in muscle blood flow (211). The magnitude and time course of increases in blood flow is dependent on the integrated actions of metabolic control, the muscle-pump, myogenic vasodilation, and flow-induced endothelium-mediated vasodilation (31, 54, 211). Following the first contraction, muscle blood flow rapidly increases resulting in an elevated shear rate acting on the endothelium. This increase in shear rate increases the production of NO, via eNOS from L-arginine, which diffuses to the vascular smooth muscle resulting in vasodilation via cGMP and PKG pathways (129). This flow-induced vasodilation contributes in part to the increase in vascular conductance and muscle blood flow observed during exercise. The contribution of endothelial derived NO on blood flow during exercise has been evaluated in studies involving both animal and human models following pharmaceutical blockage of NO production. Hester et al. (98) demonstrated that inhibition of NO production attenuated the vasodilator response to 1 min of electrical stimulations in first and second-order arterioles of the hamster cremaster muscle. These authors provided key evidence that the transient onset of vasodilation during exercise is in part mediated by NO production. Recent work by Casey et al. (26) further evaluated the contribution of NO on the on-transient increase in vascular conductance during forearm exercise in humans. Following NOS inhibition the rate of vasodilation was decreased and the time to reach a steady-state was increased compared to control conditions. While the contributions of neuronal NO cannot be disregarded (41, 42), it is likely that a fraction of the on-kinetics of the vascular conductance adjustments from rest to exercise steady-state is in part mediated by the endothelium. In the present study, prior exposure to an increase in shear rate

acting on the endothelium resulted in significantly faster on-transient FVC and FBF responses during exercise. The ability to modulate the vasodilator kinetics during exercise via acute increases in shear rate, in combination with the work of Casey et al. (26) provides strong evidence that the endothelium substantially contributes to the rate of adjustments in exercise hyperemia in humans.

Unique to the present study was the evaluation of the dynamic balance between $\dot{V}O_2$ and $\dot{Q}O_2$ via near-infrared spectroscopy derived measurements of skeletal muscle deoxy-[Hb+Mb]. Briefly, the deoxy-[Hb+Mb] signal provides a representation of local O_2 extraction within the small arterioles, venules, and capillaries (19, 49, 71, 125). Recently, Koga et al. (121) demonstrated that the time course of muscle deoxygenation via NIRS is similar to direct measurements of the microvascular partial pressure of oxygen (PmvO$_2$) during muscular contraction, thus providing strong evidence that the τdeoxy-[Hb+Mb] is an appropriate index of local O_2 extraction kinetics during exercise. Therefore, during exercise a compromised muscle blood flow and O_2 delivery relative to $\dot{V}O_2$ results in an increased deoxy-[Hb+Mb] concentration consequent to a decreased O_2 driving pressure and increased O_2 extraction. Conversely, the present study demonstrated a slowed kinetics and reduced steady-state for deoxy-[Hb+Mb] following acute shear rate modification, via forearm heating, which suggests an improved O_2 delivery at the level of the microcirculation.

The mechanism for the decreased deoxy-[Hb+Mb] and apparent improved matching of $\dot{V}O_2$ to $\dot{Q}O_2$ in skeletal muscle observed in the present study may be resultant to an increased NO availability (72). Ferreira et al. (2006) evaluated the PmvO$_2$ kinetics in the rat spinotrapezius muscle following NOS inhibition. These authors demonstrated that NO availability has a profound impact on the matching of $\dot{Q}O_2$ to $\dot{V}O_2$ (72). In relation to the present study, prior exposure to an increased shear rate may have up-regulated the NO pathway similar to that observed in cell culture resulting in an increased NO production and overall bioavailability (127). Therefore, the slower deoxy-[Hb+Mb] kinetics (τdeoxy-[Hb+Mb]) reported in the present study suggest that exposure to 30 min of a sustained increase in antegrade shear rate, via forearm

heating, resulted in an increased muscle microvascular blood flow and improved matching of $\dot{V}O_2$ to $\dot{Q}O_2$ during moderate forearm exercise.

Experimental Considerations

Several methodological considerations are relevant to the interpretation of the present results. First, measurements of FBF and FVC taken in the brachial artery were used to evaluate the vascular responses across the entire limb. It is well documented that the vasodilator control mechanisms are different throughout the arterial tree and across the tissues they perfuse (129). In addition, previous reports from our laboratory have demonstrated differences in conduit artery blood flow kinetics compared to estimated capillary blood flow kinetics during moderate intensity knee extension exercise (95). Therefore, the present study only provides a broad measurement of limb conductance and flow.

Second, despite continuous measurements of blood velocity, the initial rapid hyperemic response that occurs within ~1-5 sec of exercise was not evaluated. At exercise onset the blood velocity obtained during the first contraction often disrupted the Doppler signal. Therefore, the first contraction was removed from the kinetic analysis.

Third, the present study did not attempt to evaluate the contribution of individual vasoactive substances (i.e., NO, adenosine, prostaglandins) via pharmaceutical blockade. While this limits identification of specific mechanisms contributing to the enhanced vasodilator responses observed following the shear rate intervention, it does not diminish the primary findings of the present study. However, previous work has demonstrated a strong NO-dependent mechanism for FMD (123, 196, 204) and the on-transient increase in vascular conductance during exercise (26, 72). Therefore, these previous studies in combination with the findings of the present study suggest that NO availability is a potential mediator for shear rate induced vascular adaptation.

The fourth experimental consideration pertains to the use of NIRS as a measurement of $\dot{Q}O_2$ to $\dot{V}O_2$ matching. The assumptions and limitations relevant to this measurement technique have

been previously been discussed in detail (49, 73, 125) and will only be highlighted here. Briefly, the NIRS-derived deoxy-[Hb+Mb] is reflective of changes in hemoglobin oxygenation within the small arterioles, venules, and capillaries and intracellular myoglobin due to similar absorption properties of the NIRS light wavelengths, thus preventing distinction between the two (47). However, the deoxy-[Hb+Mb] signal has previously been used to evaluate microvascular O_2 exchange and its kinetic response to exercise is not appreciably different from direct $PmvO_2$ measurements (121). In addition, the influence of skin blood flow and volume on the NIRS signal cannot be ignored (48), but has been shown to contribute minimally to the NIRS signal (144). In the present study forearm heating was used to generate an increase in skin temperature and blood flow resulting in an increased brachial artery blood flow and antegrade shear rate. However, skin temperature was controlled for by inclusion of a 10-15 min post-heating period when skin temp and presumably skin blood flow were returned to pre-heating values. In addition, an increase in blood volume under the NIRS probe has a minor impact on the deoxy-[Hb+Mb] signal (125). Therefore, we believe the deoxy-[Hb+Mb] response observed in the present study is the result of altered vascular function within the skeletal muscle microcirculation.

Summary and conclusions

The vast improvements in cardiovascular health and vascular function following aerobic exercise training is well documented (15, 113, 159, 175, 231); however, the underlying mechanisms stimulated within a given exercise bout are not completely defined (51, 131). This study investigated the effects of an acute increase in shear rate independent of muscular contractions via unilateral forearm heating on vascular function at rest and during exercise. The present study identified that prior exposure to a high antegrade shear rate increases FMD and the speed of the on-transient increase in FBF and FVC during moderate intensity exercise. These results suggest that one potential stimulus for improvements in vascular health and function is exposure to elevations in antegrade shear.

Table 4-1. FMD Responses

	Pre			Post		
Baseline						
MAP (mmHg)	90.3	±	4.62	94.0	±	7.57
HR (bpm)	68	±	10	65	±	9
D (mm)	4.60	±	0.60	4.50	±	0.50
Flow-mediated dilation						
FMD (mm)	0.28	±	0.09	0.40	±	0.12*
FMD (%)	6.20	±	2.54	9.05	±	3.11*
SR_{AUC} (s 10^4)	22.7	±	5.67	24.3	±	6.76

Values are mean ± SD. MAP, mean arterial pressure; HR, heart rate; D, diameter; FMD, flow-mediated dilation; SR_{AUC}, area under the shear rate curve.

* Significantly different from Pre, $P < 0.05$.

Table 4-2. Exercise Responses

	Pre			Post		
Baseline						
MAP (mmHg)	90.3	±	8.58	94.9	±	7.13
HR (bpm)	68	±	8	67	±	8
FBF (ml min^{-1})	73.6	±	23.9	87.1	±	28.3
FVC (ml min^{-1} (100 mmHg)$^{-1}$)	81.5	±	24.3	92.6	±	32.9
deoxy-[Hb+Mb] (mM)	20.6	±	2.77	17.2	±	4.41*
Steady-state						
MAP (mmHg)	100	±	10.9	106	±	9.61
HR (bpm)	75	±	8	75	±	8
FBF (ml min^{-1})	286	±	67.1	314	±	71.1*
FVC (ml min^{-1} (100 mmHg)$^{-1}$)	289	±	71	295	±	55
deoxy-[Hb+Mb](mM)	35.6	±	9.95	30.39	±	10.3*
Parameter Estimates						
ΔFBF (ml min^{-1})	212	±	50.9	227	±	61.5
τ $_{FBF}$, (s)	42.2	±	13.3	29.7	±	7.52*
k_r, FBF (ml min^{-1} s^{-1})	5.44	±	1.94	8.01	±	2.95*
ΔFVC (ml min^{-1} (100 mmHg)$^{-1}$)	208	±	53.4	203	±	41.3
τ $_{FVC}$, (s)	38.2	±	15.3	21.4	±	2.9*
k_r, FVC (ml min^{-1} (100 mmHg)$^{-1}$) s^{-1})	6.48	±	3.59	9.65	±	2.39*
Δ[HHb] (mM)	15.0	±	9.50	13.2	±	8.07*
τ $_{[HHb]}$, (s)	21.2	±	14.1	33.8	±	19.7*
k_r, deoxy-[Hb+Mb] (mM s^{-1})	1.04	±	0.95	0.70	±	0.88*

Values are mean ± SD. MAP, mean arterial pressure; FBF, forearm blood flow; FVC, forearm vascular conductance; deoxy-[Hb+Mb], deoxy hemoglobin + myoglobin; τ, time constant of the response; k_r initial rate of increase.

* Significantly different from Pre, P<0.05.

Figure 4-1. Schematic representation of the experimental protocol for the flow-mediated dilation
(FMD) (A) and constant-load exercise test (B). See test for full explanation.

A

| FMD | Forearm Heating | Forearm Skin Temp clamped between 38-40°C | Forearm Cooled to Baseline temp | FMD |

0   10   20   50   60   70

B

| Exercise | Forearm Heating | Forearm Skin Temp clamped between 38-40°C | Forearm Cooled to Baseline temp | Exercise |

0   15   25   55   65   80

time (min) →
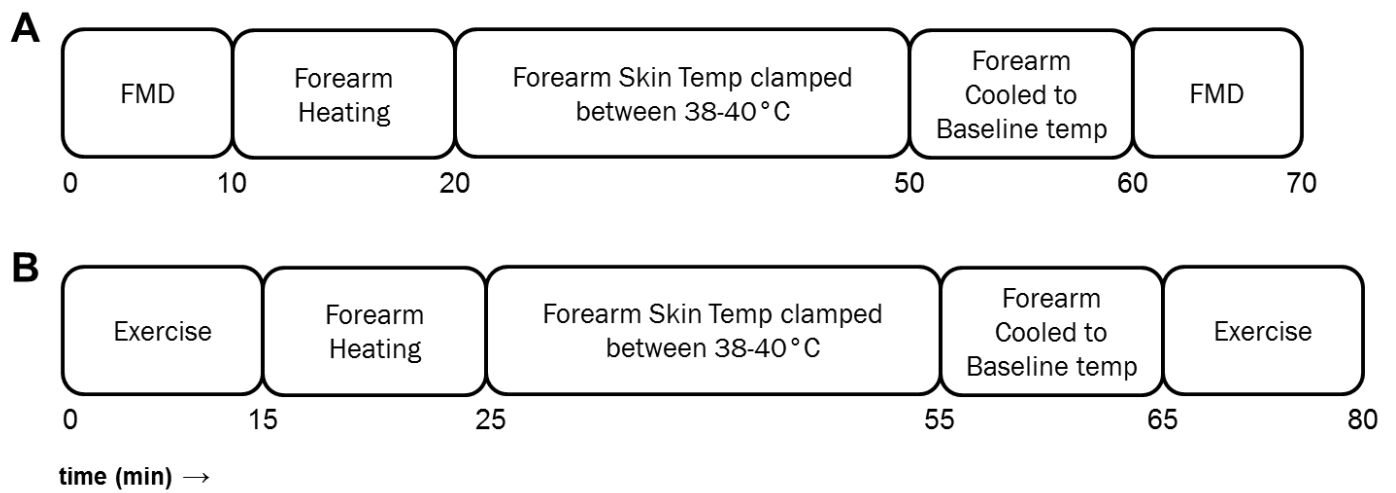
Figure 4-2. Mean, antegrade, retrograde shear rates in the brachial artery prior to and following the unilateral limb heating intervention on the (A) flow-mediated dilation and (B) constant-load exercise test days.

Limb heating significantly (P<0.05) increased mean and antegrade shear rate, while decreasing retrograde shear in both conditions. * significant difference vs. pre-heating, P<0.05.
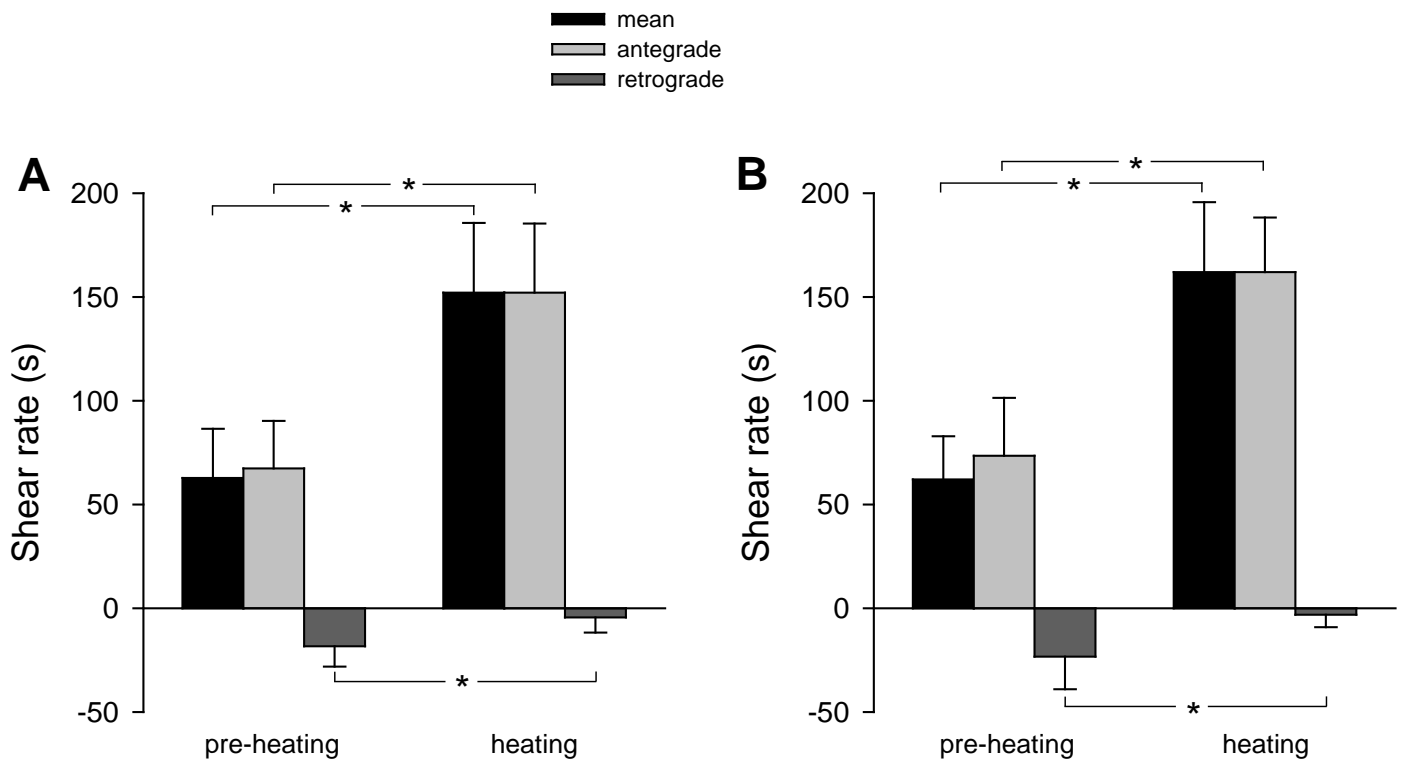
Figure 4-3. Effects of exposure to 30 min of a sustained increase in antegrade shear rate on flow-mediated dilation.

* significant difference vs. pre-heating, P<0.05.
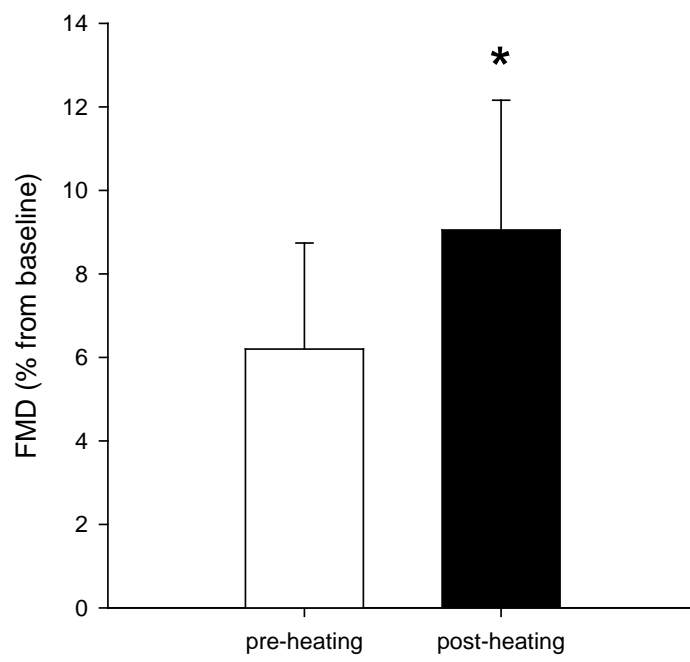
Figure 4-4. Effects of exposure to 30 min of a sustained increase in antegrade shear rate on the dynamic response (as τ) of (A) forearm blood flow (FBF), (B), forearm vascular conductance (FVC), and (C) skeletal muscle deoxygenation (deoxy-[Hb+Mb]) to moderate intensity forearm exercise.

* significant difference vs. pre-heating, P<0.05.
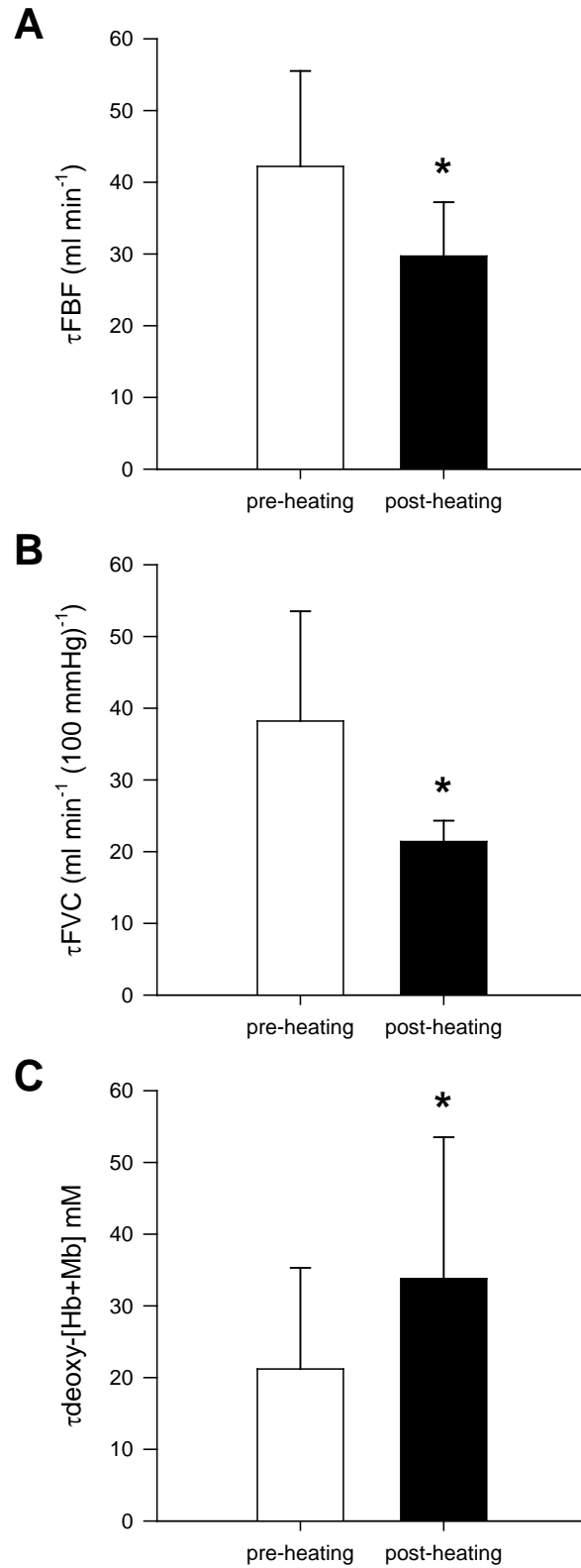
Figure 4-5. Schematic illustration of the mean fit for measured on-transient forearm vascular conductance (FVC) response during moderate intensity forearm exercise.

Note the faster FVC response following the heating intervention (dashed line) compared to pre-heating (solid line).

Chapter 5 - Convective and diffusive O_2 transport: foundations for the decreased maximal O_2 consumptions after sustained microgravity

Summary

Sustained exposure to microgravity, via spaceflight or head down bed rest (HDBR), decreases maximal O_2 consumption ($\dot{V}O_2$max) at a rate which is dependent on the duration of exposure. This brief review focuses on (1) the time-course for $\dot{V}O_2$max decline following microgravity, (2) the com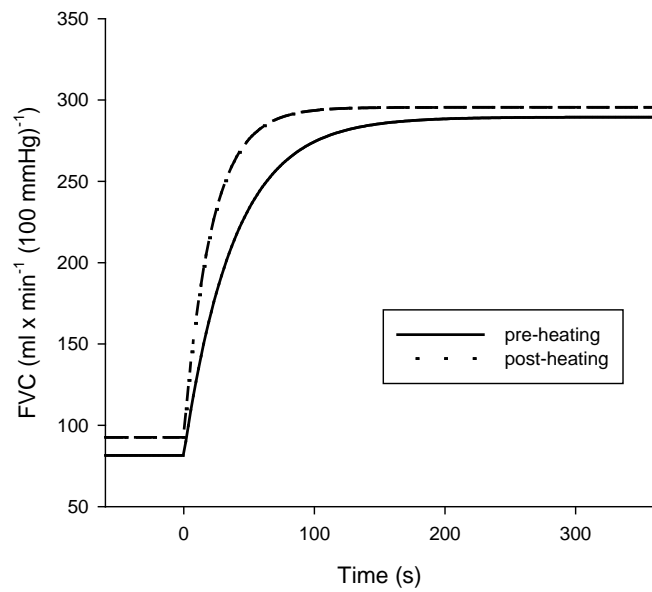ponents within the O_2 transport pathway that determine $\dot{V}O_2$max in a post-flight astronaut, and (3) the characterization of the potential mechanisms contributing to the compromised post-microgravity $\dot{V}O_2$max. Experimental evidence and retrospective analysis reveals that exposure to microgravity lasting greater than 60 days decreases $\dot{V}O_2$max by as much as 36% consequent to decreases in both convective and diffusive O_2 transport. Mechanistically, this attenuation of the O_2 transport pathway may be the combined result of a spaceflight deconditioning across multiple organ systems. Following microgravity, significant decreases in total blood volume, red blood cell mass, cardiac function and mass, vascular function, and skeletal muscle mass occur and become evident during exercise upon re-exposure to the head-to-foot gravitational forces of upright posture on Earth. The potential contribution of each individual system's adaptation to microgravity is presented and appropriately applied to the O_2 transport pathway in a post-flight long-duration astronaut. Gaps in knowledge unanswered by current scientific investigations and targets for therapeutic countermeasures are also highlighted.

Introduction

Since the 108 minute spaceflight of Yuri Gagarian in April of 1961 the scientific and medical communities have understood that the human body can adapt to life in a reduced gravitational environment (i.e., microgravity). However, when head-to-foot gravitational forces are restored, like that achieved with return to Earth (1-g) or a future planetary landing (i.e., Mars $3/8^{th}$-g), the physiologic adaptations that occurred in-flight now result in a severe "spaceflight deconditioning" that is evident across multiple organ systems (Figure 5-1). Therefore, the often overlooked consequence of spaceflight is not just the ability to survive in space, but also the capacity to endure the physiologic challenges created upon landing. As such it is common that astronauts regularly experience post-flight orthostatic intolerance, decreased sensorimotor function, and reduced muscular strength and cardiorespiratory endurance (18, 22, 234, 236).

Many post-flight disorders are the result of in-flight adaptations that seem to be dependent on the decreased level of physical activity and removal of the head-to-foot gravitational force. With exposure to microgravity the reduced gravitational and hydrostatic pressure gradients redistribute intravascular fluid volume and pressure from the legs and lower body towards the thoracic cavity and head (203, 247). The adaptations that follow collectively result in a decrease in plasma volume followed closely by a decrease in red blood cell mass (5). In addition, microgravity adversely impacts the central cardiovascular system. Post-microgravity measurements of ventricular volumes are decreased due in part to the decreased ventricular filling pressure and blood volume (36, 96). Significant cardiac atrophy is also observed following microgravity exposure that occurs as a function of duration (60, 177). However, these findings only highlight the adaptations to microgravity within the cardiovascular system. Relative to the cardiac health, scientific investigations evaluating the peripheral circulation are less numerous, but an adverse influence on vascular structure and function is also demonstrated (146, 217, 221). The pulmonary system is also impacted by the removal of gravity (187, 250). However, post-microgravity measurements of arterial saturation (SaO_2) and arterial partial pressure of oxygen (PaO_2) suggest that the effects on pulmonary gas exchange are minimal (24, 186, 188). Within the contracting muscles, particularly of the lower limbs and postural muscles,

microgravity results in a decreased mass, cross sectional area, and overall contractile strength that is only partially mitigated with exercise countermeasures (77, 234, 235).

While the response of individual biological systems to spaceflight is important to understand, it is the integrative function of the pulmonary, cardiovascular, and muscular systems following long-duration space missions that will provide critical information regarding astronaut health and exercise tolerance upon return to gravity. Maximal O_2 consumption ($\dot{V}O_2$max) is one key parameter of integrated cardiorespiratory function that is widely used to evaluate the severity of disease, the progression of aging, and the decline in astronaut health and performance (244). Thus, a detailed evaluation of the contribution of the independent physiologic variables within each organ system (i.e., lungs, heart, circulation, and oxidative enzymes) in determining $\dot{V}O_2$max post-flight provides the opportunity to investigate the mechanisms by which the body responds to the spaceflight environment. It is therefore the objective of this review to i) evaluate the decline in $\dot{V}O_2$max following long-duration space missions, ii) calculate the determinants of $\dot{V}O_2$max post-flight by retrospectively modeling the adaptations within the O_2 transport pathway and iii) consider the potential mechanisms responsible for the reduced O_2 transport capacity following long-duration spaceflight missions.

Comments on the study of spaceflight

Microgravity is defined as any substantial reduction in the gravitational force along the head-to-foot axis. During low-orbit spaceflight (Skylab, Shuttle, International Space Station, etc.) the force of Earth's gravity still persists, but is matched by the centripetal acceleration of the spacecraft and crew circling the Earth such that the resultant force is decreased creating a microgravity environment. Beyond low-Earth orbit (i.e., deep-space mission or interplanetary transit) will provide a "true" decrease in gravity, as astronauts are taken beyond the reach of Earth's gravity. While both types of spaceflight are ideal for the study of gravitational physiology, the limited research opportunities due to high cost, low sample sizes, and equipment availability make these models difficult. Therefore, the head-down tilt bed rest (HDBR) model is often used to simulate the effects of microgravity. HDBR confines the research subject to inactivity in a bed that is adjusted between 0° to -10° angle. This body posture alters the head-to-foot gravitational force to a similar extent as that experienced by in-flight astronauts (114, 115). Therefore, HDBR provides an opportunity to study the effects of microgravity exposure in a larger number of subjects across a range of simulated mission lengths in a more controlled environment.

Exercise performance and long-duration microgravity

A key hallmark of microgravity deconditioning is a significant decrease in $\dot{V}O_2$max upon return to gravity (Table 5-1). As previously highlighted, $\dot{V}O_2$max is a physiologic parameter reflecting integrated cardiorespiratory function. $\dot{V}O_2$max is also used as a predictor of athletic and work performance, and can provide insights to an astronaut's ability to successfully perform physically demanding extravehicular activities (EVA) (2, 43, 44). While, to date, aerobic capacity has not limited EVA performance, observations of unexpected tachycardia have been reported during strenuous EVA tasks (179). In addition, simulation studies indicate that EVAs in the 3/8-g of Mars may require a $\dot{V}O_2 > 30$ ml $\times$ kg^{-1} $\times$ min^{-1} which following microgravity deconditioning will require a greater fraction of $\dot{V}O_2$max that may result in exhaustion (167).

A marked reduction in $\dot{V}O_2$max is evident following short duration microgravity exposure. Convertino and colleagues have consistently demonstrated a 4-15% reduction in $\dot{V}O_2$max following 10 days of microgravity (35, 37, 38, 40, 106, 251). Furthermore, multiple investigations have also revealed additional reductions in $\dot{V}O_2$max when the duration of microgravity is extended to 20-30 days (24, 28, 39, 40, 137, 152, 216, 222-225, 236, 246). To this effect it is commonly believed that the reduction in $\dot{V}O_2$max occurs as a function of mission duration. A previous review has highlighted this relationship with a cross-sectional comparison of the change in $\dot{V}O_2$max following HDBR lasting between 7 to 30 days (34). Within this time period $\dot{V}O_2$max decreases approximately 1% for each day of microgravity exposure. However, while informative, this model of $\dot{V}O_2$max deconditioning may not be appropriate for estimating the decline following long duration space missions lasting > 30 days. To this effect, Cappelli et al. (24) evaluated the time course in the reduction of $\dot{V}O_2$ following 14, 42, and 90 days HDBR. Their results demonstrate for the first time that the rate of decline beyond 42 days is less than the

previously estimated 1% per day suggesting that $\dot{V}O_2$max may not decrease in a linear function as previously reported. Therefore, a retrospective analysis of 37 (5 spaceflight; 32 HDBR) (Table 5-1) independent investigations of the percent reduction in $\dot{V}O_2$max (%Δ$\dot{V}O_2$max) following space flight or HDBR were plotted as a function of duration (Figure 5-2). The %Δ$\dot{V}O_2$max data were then fit by linear, piecewise two-linear segment, and exponential decay models.

linear:

$$\%\Delta\dot{V}O_2\text{max (x)} = y0+(a\times x) \tag{1}$$

(where x represents duration of exposure, $y0$ represents the y-intercept (i.e., pre-flight $\dot{V}O_2$max) and a the slope of the response)

piecewise two-linear segment:

$$\%\Delta\dot{V}O_2\text{max (x)} = \text{region1(x)} = (y1*(BP-x) + y2*(x-x1))/(BP-x1); \tag{2}$$

region2(x) = (y2*(x2-x) + y3*(x-BP))/(x2-BP)

f = if(t <= BP, region1(x), region2(x))

(where x represents duration of exposure; x1 and x2 represent the minimum and maximum x-values of duration respectively; y1 and y3 represent the predicted %Δ$\dot{V}O_2$max at x1 and x2 respectively; BP represents the break point between the two regions; and y2 represents the predicted %Δ$\dot{V}O_2$max at BP (i.e., y2 = %ΔVO2max where regions intersect)). This effectively yields two linear Equations for durations above and below the BP.

exponential decay:

$$\%\Delta\dot{V}O_2\text{max (x)} = y0-A*(1-e^{-(x)/\tau}) \tag{3}$$

(where x represents duration of exposure, A represents the amplitude, and τ the time constant of the exponential response). To determine which model provided the best fit the three response curves (linear, piecewise, and exponential) were compared using Δ Akaike Information Criteria (ΔAIC):

$$\Delta AIC = N \ln [SS_{model1}/SS_{model2}] + 2(K_{model1} - K_{model2}) \qquad [4]$$

Where N is the number of data points, SS_{model1} and SS_{model2} are the residual sum of squares from the models being compared, and K is the number of parameters in the fitted model +1. When the retrospective cross-sectional data in Figure 5-2 was fit with the three models the ΔAIC indicates that an exponential decay best describes the decrease in $\dot{V}O_2max$ as a function of the duration of microgravity exposure. This analysis demonstrates that the decrease in $\dot{V}O_2max$ has a time constant of ~41 days and appears to reach a steady-state within ~160 days. Using this model the post-flight $\dot{V}O_2max$ in an average NASA Shuttle crew astronaut (26-50 yrs., 84 kg, pre-flight $\dot{V}O_2max$ 3,700 ml $\times$ min^{-1} (1)) following 60 and 360 day space missions will be approximately 2,700 ml $\times$ min^{-1} and 2,370 ml $\times$ min^{-1} respectively. The mechanisms contributing to the decline in $\dot{V}O_2max$ are complex and the importance of each independent variable within the O_2 transport pathway may also be dependent on duration. We, therefore, might hypothesize that the decline in $\dot{V}O_2max$ may be more dependent upon adaptations to the central cardiovascular mechanisms following short duration missions and peripheral (i.e., macro- and microcirculatory) mechanisms contribute more during long duration missions (34, 36, 74, 75).

Wagner and associates (202, 239, 241, 242) has advanced the theory that $\dot{V}O_2max$ is not limited by one specific independent variable, but determined by the integration of all steps of all the steps along the O_2 transport pathway. Within this pathway the movement of oxygen from air to the muscle mitochondria relies on two components of O_2 transfer: convective O_2 transport within the circulation to the active skeletal muscle capillary bed and diffusive O_2 transport which describes capillary-to-mitochondria O_2 diffusion (Figure 5-3A). Convective O_2 transport can be mathematically described with Fick's Principle of Mass Conservation:

$$\dot{V}O_2 = \dot{Q} \times (CaO_2 - CvO_2) \qquad [5]$$

where $\dot{Q}$ represents cardiac output, CaO_2 and CvO_2 represent arterial and venous O_2 contents

respectively. Equation 5 can be expanded to reveal the components of blood O_2 content, which

include hemoglobin concentration ([Hb]), arterial and venous saturation (SaO_2 and SvO_2

respectively), and diffused O_2 (removed for clarity).

$$\dot{V}O_2 = \dot{Q} \times ((1.34 \times [Hb] \times SaO_2) - ((1.34 \times [Hb] \times SvO_2)) \qquad [6]$$

The diffusion of O_2 from within the capillary circulation into the muscle mitochondria

can be described with Fick's Law of Diffusion:

$$\dot{V}O_2 = DO_2m \times (PcapO_2 - PmitO_2) \qquad [7]$$

Where DO_2m represents muscle O_2 diffusing capacity, $PcapO_2$ and $PmitO_2$ represent capillary

and mitochondria PO_2 respectively. Since during maximal exercise $PmitO_2$ is approximately 1-3

Torr it can be set to zero. In addition, $PcapO_2$ can be approximated by a constant k and muscle

venous PO_2 (PvO_2) yielding the following simplification of Equation 7.

$$\dot{V}O_2 = DO_2m \times k \times PvO_2 \qquad [8]$$

Figure 5-3B illustrates the relationship between Equation 6 and Equation 8 in

determining $\dot{V}O_2max$, with $\dot{V}O_2$ on the ordinate and PvO_2 on the abscissa, for the average pre-

flight astronaut. Using the known relationship between SaO_2 and PvO_2 via the O_2 dissociation

curve, Equation 6 is plotted as a curved line for a given $\dot{Q}max$, [Hb], and SaO_2 as a function of

PvO_2. Equation 8 is represented by the straight line from the origin and in which the slope is

equal to DO_2m. Notice that the only point satisfying the laws of mass conservation is the point

where both convective and diffusive Equations equal the same $\dot{V}O_2max$. The beauty of this

integrated relationship is that if $\dot{V}O_2max$ and the measureable variables within Equation 6 are

known then changes in DO_2m can be calculated. With this information conclusions can be drawn as to the importance of each independent variable in determining $\dot{V}O_2max$.

To facilitate the integrative modeling of convective and diffusive O_2 transport at $\dot{V}O_2max$ the changes in the measureable variables of $\dot{V}O_2max$, $\dot{Q}max$, [Hb], and SaO_2 are required. As previously mentioned, 60 and 360 days of spaceflight will reduce an average NASA astronaut's $\dot{V}O_2max$ from 3700 ml min^{-1} to 2,700 ml min^{-1} and 2,370 ml min^{-1} respectively (i.e., $\geq 30\%$) (Figure 5-2). Pre-flight $\dot{Q}max$ was calculated with the assumption of a constant linear $\dot{Q}$: $\dot{V}O_2$ relationship. The changes in $\dot{Q}max$ post-microgravity from Capelli et al. (24), Levine et al. (137), Shibata et al. (216), and Saltin et al. (210) were fit with an exponential decay curve and $\dot{Q}max$ was subsequently calculated for durations of 60 and 360 days for our reference astronaut (Table 5-2). Pre-flight [Hb] was set to 16 g dl^{-1}, which is a normal [Hb] in healthy subjects (249). Similar to $\dot{V}O_2max$ and $\dot{Q}max$, the change in [Hb] with microgravity exposure was modeled from the recent HDBR data of Capelli et al. (24). With estimates of [Hb] pre- and post-microgravity, SaO_2 assumed to be 98% at $\dot{V}O_2max$ (24), an O_2 carrying capacity of 1.34 ml $O_2 \times$ g $\times$ Hb^{-1}, CaO_2 was calculated as $CaO_2=1.34$ x [Hb] x SaO_2 (Table 2). CvO_2 was then calculated by rearranging Equation 6 ($CvO_2 = CaO_2-(\dot{V}O_2/\dot{Q})$) which allowed SvO_2 to be calculated ($SvO_2 = CvO_2/[Hb]$ x 1.34)). PvO_2 corresponding to $\dot{V}O_2max$ was calculated using a modification of Hill's Equation based on the human blood O_2 dissociation curve (215). DO_2m was calculated as $\dot{V}O_2max$ /PvO_2.

Post-microgravity determinants of $\dot{V}O_2max$

The calculations for pre- and post-microgravity exposure in the reference astronaut are summarized in Table 5-2. Figure 5-4 illustrates the integrated relationship between $\dot{Q}O_2$ and DO_2m where the curved lines represent the $\dot{Q}O_2$, as determined by $\dot{Q}max$, [Hb], SaO_2, and PvO_2, the straight lines from the origin represents DO_2m, following 60 (figure 5-4A) and 360 (figure 5-4B) day space missions. As seen in Figure 5-4A, 60 days of microgravity exposure result in an approximately 30% decrease in convective O_2 transport, owing to a decreased $\dot{Q}max$ and [Hb]. The relatively unchanged DO_2m post-60 days microgravity suggests that at this time point, O_2 delivery is the primary mediator for the ~37% decrease in $\dot{V}O_2max$. This finding supports the previous reports of a significant correlation between the change in plasma volume and $\dot{V}O_2max$ for short-duration microgravity exposure (36). Up to this duration it is likely that the decreased plasma volume and subsequent decreased $\dot{Q}max$ and [Hb] combine to limit convective O_2 delivery. The central and hemotologic mechanisms contributing to the decreased $\dot{Q}O_2$ are extensive and will be discussed in detail below (*see Potential Mechanisms: Cardiac and Blood Volume Control*).

It is critical to remember that the fractional O_2 extraction (arterial-venous O_2 difference) is dependent on both $\dot{Q}O_2$ and DO_2. The mild decrease in arterial-venous O_2 difference (16.1 to 14.1 ml $\times$ dl^{-1}) calculated post-60 days microgravity, is determined by a reduction in CaO_2 and subsequent $\dot{Q}O_2$, not an elevation in CvO_2 which would be present if O_2 extraction was compromised. In reality, CvO_2 and PvO_2 decrease as a consequence of an increase in the ratio of DO_2m to QO_2. As highlighted by Roca et al. (202) an increase in this ratio will increase O_2 extraction, but in the case of the post-60 day spaceflight astronaut this is offset by a greater decrease in CaO_2 resulting in a slight decrease in the arterial-venous O_2 difference.

Unlike 60 days of exposure, the additional 14% decrease in $\dot{V}O_2$max following 360 days

microgravity are likely the result of peripheral mechanisms that decrease muscle O_2 diffusing

capacity (DO_2m) by approximately 44% (Figure 4B). Since, the decrease in $\dot{Q}O_2$ observed

following 360 days is similar to that at 60 days, these findings suggest that the mechanisms for

the decreased convective O_2 transport occur within the first 60 days of exposure and reach a new

set-point that persists for up to 360 days. Ferretti and colleagues (75) performed a similar

analysis using a multifactorial model of $\dot{V}O_2$max limitation and suggested a similar peripheral

mechanism for the decreased $\dot{V}O_2$max following extended durations of microgravity exposure.

Therefore, the calculations of the present review clearly demonstrate that following long-

duration microgravity exposure additional factors beyond $\dot{Q}$max and blood volume, particularly

those within the periphery, contribute to the progressive decrease in $\dot{V}O_2$max. The precise

mechanisms for the 44% decrease in DO_2m following 360 days spaceflight may involve

impaired microcirculatory hemodynamics and are discussed below (see Potential Mechanisms:

Microcirculatory hemodynamics and O_2 diffusion). With respect to fractional O_2 extraction

following 360 days microgravity exposure there is a relatively greater decrease in DO_2m than

$\dot{Q}O_2$ which decreases the DO_2m/$\dot{Q}O_2$ ratio. Decreases in this ratio will increase CvO_2 and PvO_2

which is observed as a decrease in the arterial-venous O_2 difference.

Following microgravity, it has traditionally been theorized that the primary determinant

of $\dot{V}O_2$max post-flight was convective O_2 delivery. This conclusion has consistently been

supported by the large decrease in central cardiac performance and O_2 delivery owing to a

decreased cardiac output (20, 24, 76, 96, 106, 137) and reduced blood volume (37-39, 87, 109,

216, 222, 224, 251). In addition, minor changes in maximal arterial-venous O_2 difference post-

microgravity led to the presumption that peripheral factors are not responsible for the decrease in

$\dot{V}O_2$max. However, these conclusions are based on short duration studies and the contribution of

peripheral circulation may become more important with long duration space missions or when

central performance is not limited (i.e., post-flight volume loading). For instance, the presence of

93

a reduced DO_2m becomes evident when plasma volume expansion post-flight fails to restore $\dot{V}O_2max$ to pre-flight levels (216).

Similar decreases in $\dot{V}O_2max$ and $\dot{Q}max$ with minor changes in a-v O_2 difference have been reported in diseased populations (183). Like post-flight astronauts, patients with congestive heart failure (CHF) often have an unchanged or greater fractional O_2 extraction at maximal exercise, which led to the misconception of an unimpaired DO_2m (183). As recently highlighted by Poole et al. (183) in CHF the reduction in convective O_2 delivery and DO_2m occur to a similar extent so that at maximal exercise fractional O_2 extraction appears normal despite a severely compromised diffusivity of O_2.

Therefore, the present calculations for 60 and 360 day spaceflights strongly advocate for the need to tailor microgravity countermeasures based on mission duration. Shorter-duration missions should target convective ($\dot{Q}O_2$) O_2 transport, while longer-duration missions should have the objective to maintain both convective and diffusive (DO_2m) O_2 transport and the specific mechanisms associated with their maladaptation.

Potential mechanisms

Pulmonary. It is well established that lung mechanics are influenced by gravity, as previously reviewed (187, 250). Briefly, the 1-g environment of Earth results in several functional consequences which include differences in regional lung volumes, pulmonary blood flow, and the ventilation-to-perfusion ratio ($V_A/\dot{Q}$) (248). It is therefore no surprise that in the absence of gravity many of these gravitational dependent variables are altered relative to 1-g. When in microgravity the distribution of ventilation and pulmonary blood flow becomes more evenly distributed and improves $V_A/\dot{Q}$ matching, but some heterogeneity still persists (238). The improved distribution of pulmonary blood flow and an increase pulmonary capillary blood volume in microgravity also contributes to an improved pulmonary CO-diffusing capacity (DLCO) that rapidly returns to pre-flight levels upon landing (191, 238). However, DLCO during long-duration microgravity (> 120 days) may be decreased (155, 190). During both short- and long-duration spaceflight the change in lung volumes are more consistent. Sawin et al. (213) reported a decrease in vital capacity during 84 days aboard the Skylab flight that returned to normal upon landing. These findings are similar to those of short-duration spaceflight missions (69)

Most important to the present review of O_2 transport is the level of SaO_2 post-microgravity. The unchanged pulmonary diffusing capacity and gas exchange (188, 189) coupled with the long-duration HDBR study that demonstrated an unaltered SaO_2 following as much as 90 days exposure (24) suggests that arterial saturation is unaffected by microgravity. Therefore, any changes in pulmonary structure and/or function during microgravity exposure have a minimal effect on pulmonary convective and diffusive O_2 transport.

Blood volume control. Similar to the lung, intravascular fluid distribution is significantly influenced by gravity. When standing in a 1-g environment, 70-75% of the total blood volume is below the level of the heart (203). As such, the intravascular pressures at the feet approaches 200 mmHg compared to the approximately 70 mmHg measured at the level of the head. During exposure to microgravity a redistribution of the intravascular fluid volume occurs very rapidly,

resulting in a more uniform pressure generated by the heart throughout the body so that pressure in the lower limbs decreases and pressure in the head and upper extremities increases (94, 247) (Figure 5-5). This redistribution occurs within hours and following a few days results in a significant decrease in plasma and blood volume (37-39, 87, 109, 216, 222, 224, 251) followed by a decrease in red blood cell mass (24, 29, 32, 39, 40, 133). In the past, the precise mechanisms mediating these changes have been difficult to study during spaceflight and researchers therefore relied heavily on HDBR models. Unfortunately, within the last decade it has become apparent that despite a similar hematologic adaptation to microgravity the mechanisms between spaceflight and HDBR are different enough to warrant some discussion (169, 245).

The redistribution of blood volume following exposure to microgravity via HDBR increases central venous pressure (CVP), which distends the cardiac chambers (16, 166) and stimulates a neurohumorally mediated decrease in blood and plasma volumes via the Henry-Gauer reflex resulting in an increased diuresis and natriuresis (6, 82, 169). For decades this theory of fluid volume control prevailed as the primary mechanism for the microgravity induced hypovolemia.

Unlike HDBR, an increased diuresis and natiuresis have never been observed during spaceflight (63, 64). When the head-to-foot gravitational force is removed in-flight, there is a similar shift in blood volume and pressure away from the lower body upward towards the head, but no increase in CVP (21). Since the microvascular structure in the upper body is adapted for lower pressures, this very rapid increase in volume and intravascular pressure results in an increase in transcapillary filtration (94, 132, 247). Leach et al. (132) demonstrated that the movement of plasma proteins to the extravascular space is one primary mechanism for the spaceflight reduction in plasma volume. Similar increases in fluid filtration capacity have also been measured following 120 days HDBR, but are often masked by the increased diuresis (30). Therefore, the current evidence supports a rapid and sustained decrease in plasma volume during microgravity and that the mechanisms mediating the response appear to be somewhat dissimilar between HDBR and spaceflight.

In addition to the decreased plasma volume consequent to microgravity exposure, many investigations also report a reduction in total red blood cell mass and [Hb] (24, 29, 32, 39, 40, 133). The rapid and early decreased plasma volume in-flight causes an acute increase in [Hb] and hematocrit that over the following days is reduced by means of decreased erythropoietin levels and increased destruction of red blood cells (4, 5, 88, 89). Alfrey et al. (4, 5) demonstrated with the use of radiolabeled autologous red blood cells that during short duration spaceflight (9-14 days) red blood cell mass is decreased via the favored destruction of newly produced red blood cells. In addition, it seems that over time this reduced total red blood cell mass achieves a new set-point that is appropriate for the new lower circulating plasma volume.

While these adaptations may be appropriate for the microgravity environment, the post-flight consequences are severe in regards to orthostatic challenges and convective O_2 transport. Upon exposure to a strong gravitational environment, like Earth or Mars, the blood volume shifts back towards the lower limbs (203). This post-flight redistribution in blood volume away from the thoracic cavity coupled with the reduced circulating blood volume contributes to the decreased cardiac performance observed upon return to gravity (24, 137, 216). In addition, the initial post-microgravity blood volume will be perceived by the body as low resulting in a rapid increase in plasma volume beginning within hours. While this increase will assist with arterial pressure regulation and begin to aid cardiac performance, it will negatively impact O_2 carrying capacity via the reduction in hemoglobin concentration (Equation 6). Both the body's natural rate of volume correction and any medical interventions (i.e., intravenous saline infusion) will therefore alter the post-flight [Hb].

Cardiac. Since the Gemini and Apollo programs it has been clear that central cardiovascular function is affected by microgravity exposure (156, 205). In addition, a decreased exercise stroke volume was reported following several Skylab missions lasting between 28-84 days (23). These measurements were some of the first to demonstrate that the microgravity environment negatively impacts the cardiovascular system. Additional experimental data from both spaceflight and HDBR demonstrate a decreased resting, sub-maximal, maximal left ventricular end-diastolic volume, stroke volume and cardiac output during upright posture following microgravity (20, 25, 60, 61, 76, 96, 106, 137, 138, 177, 216, 218, 220). Furthermore,

several investigations suggest one primary mechanism for the post-microgravity decrease in ventricular volume is a significant decrease in circulating blood volume. Shibata et al. (216) demonstrate that resting cardiac volumes are preserved following 18 days HDBR when intravenous dextran infusions were given to restore cardiac filling pressure to baseline. In addition, Bringard et al. (20) reported a preserved maximal SV and $\dot{Q}$max following 35 days HDBR when subjects were tested in the supine position, presumably when the effects of a reduced blood volume are minimized (i.e. high effective filling pressure). These findings suggest that the reduced $\dot{Q}$max at 60 days reported in the present review is primarily due to a decreased circulating blood volume that limits ventricular preload during maximal exercise.

While changes in blood volume may be one key mechanism for the observed cardiac deconditioning post-microgravity, several additional factors have been implicated during short- and long-durations of exposure. Levine and colleagues (25, 60, 138, 177) have consistently demonstrated a decreased cardiac mass that is observed within the first two weeks of microgravity exposure. Furthermore, these authors report that this eccentric cardiac atrophy occurs at a rate of approximately 1% per week of microgravity exposure that occurs for up to 12 weeks (60). When this rate is applied to simulated 60 and 360 day missions it becomes evident that a reduction in cardiac mass will likely be a key determinant of the reduced $\dot{Q}$max and ultimately convective O_2 delivery. In addition to a reduction in cardiac volumes and mass, several investigations have reported an impaired diastolic suction and leftward shift of the left ventricular pressure-volume curve (25, 61, 96, 138), both of which will limit ventricular filling. It is critical to note that despite a decreased diastolic function, no measureable reduction in myocardial contractility has been observed following microgravity exposure (25, 61).

Peripheral circulation: Hemodynamic forces within the peripheral vasculature are key signals mediating adaptations in endothelial cell phenotype (131). For example, the increased shear stress associated with exercise training acts as a stimulus for positive adaptations in endothelial function (172, 233). Conversely, chronic exposure to low blood flow, oscillatory shear stress, and/or a reduced transmural pressure decreases vascular structure and function (131, 164, 230). The current scientific investigations of vascular adaptations to microgravity utilize

both animal and human models. Delp and colleagues (10, 33, 50, 52, 53, 146, 149, 150, 221) have extensively studied the microvascular responses to microgravity in the rat. Using a hindlimb unloading protocol (HU), the effects of microgravity can be studied in rats in a similar manner as HDBR in humans. Using this model, investigators report that the initial minutes of microgravity decrease muscle blood flow compared to baseline standing and that this reduction persists to at least 15 days HU (149), which is consistent with human spaceflight (245). However, post-microgravity sub-maximal bulk hindlimb blood flow is not significantly different compared to pre-microgravity exposure (149, 150). While the bulk flow is unaffected, the distribution of the available flow throughout the body and within the exercising limb is adversely impacted. During post-microgravity exercise, blood flow to the splenic region and kidneys remained increased compared to pre-HU (149). Likewise, blood flow is preferentially increased to muscles containing greater proportions of glycolytic fibers and decreased in those containing a high oxidative fiber composition (52, 149). This is contrary to normal 1-g exercise when blood flow is redistributed away from the splenic circulation and kidneys towards skeletal muscle (203). To this effect, at maximal exercise intensities approximately 95% of $\dot{Q}$max is

preferentially directed to the active skeletal muscle circulation to meet the high metabolic demand (129). Therefore, the appropriate and coordinated distribution of $\dot{Q}$max via adjustments in region specific vascular conductance is critical for adequate convective O_2 delivery during maximal aerobic exercise and may be significantly impaired following long-duration microgravity (52, 146, 149).

Similar to the reduced muscle blood flow observed in rats during HU, a decreased calf blood flow is reported in humans exposed to short-duration spaceflight (245). One fundamental consequence of these reductions in blood flow during microgravity includes a paralleled decrease in endothelial shear stress. As reviewed by Laughlin et al. (131), endothelial health is dependent on the magnitude and direction of the mechanical shear stress it experiences. Endothelial cells chronically exposed to a low shear stress are generally in a more proathrosclerotic state. Therefore, the alterations in the head-to-foot blood volume and pressure gradient coupled with the decreased level of physical activity in the lower limbs experienced during microgravity are likely factors responsible the maladaptation in vascular structure and function (131, 164, 230).

Mechanistically, the impaired distribution of cardiac output following microgravity appears to be the result of an impaired vasodilator and vasoconstrictor response (10, 52, 53, 103, 146, 217, 221, 257). Following 2 wks HU, arterioles from rat skeletal muscles composed of primarily type IIb fibers have a decreased response and sensitivity to the vasoconstrictor agonist KCl (221). Conversely, the vasoconstrictor responses of arterioles from the soleus, which is primarily oxidative in nature, were not different from controls (52). Recent findings from Stabley et al. (221) demonstrate a reduced vasoconstrictor response in rats following 15 days of spaceflight that is mediated by a deficit in intracellular calcium release via ryanodine receptors within the vascular smooth muscle. In addition, data from human HDBR experiments confirm the reports in animal models of microgravity (217, 257). Shoemaker et al. (217) demonstrated that the human forearm's vasoconstrictor response to a cold pressor test during a reactive hyperemia blood flow maneuver was decreased following 14 days of bed rest. These findings were the first to suggest the presence of an impaired vasoconstrictor function in humans and provide a potential mechanism for the known decreased exercise and orthostatic tolerance associated with spaceflight.

In conjunction with the attenuated vasoconstrictor response, Shoemaker et al. (217) also demonstrated a reduced vasodilator response to reactive hyperemia following acute limb occlusion and similar findings have been reported in short-duration HU in rats (53). Following unloading, the arteriole's medial layer cross-sectional area and acetylcholine-induced dilation are decreased, indicating significant structural and functional remodeling within the peripheral microcirculation (53). In addition, the severity of these maladaptations is fiber type dependent (53). While it is evident that both oxidative and glycolytic fibers are negatively impacted following microgravity exposure, the reduction in vasodilator responses is greater in the more oxidative fibers (146). Furthermore, the reduced vasodilation of arterioles to adenosine is indicative of a diminished peripheral vascular response to a metabolically-mediated increase in vascular conductance (146). In summary, it is evident that the attenuated vascular function and impaired redistribution of $\dot{Q}$max are potential mechanisms contributing to the decreased convective O_2 delivery during maximal aerobic exercise following microgravity exposure.

Microcirculatory hemodynamics and O_2 diffusion. As illustrated in figure 5-4B, during upright maximal aerobic exercise following 360 days of microgravity exposure, the diffusive capacity for O_2 to move from the capillary into the muscle mitochondria is decreased. This is divergent from many short-duration studies in which the arterial-venous O_2 difference is unaffected (34, 36, 96, 106, 137, 210). However, as proposed by Convertino (34, 36) and Ferretti et al. (74, 75) and discussed above, the peripheral limitations to O_2 movement and utilization may have a greater impact on $\dot{V}O_2$max as the duration of space missions increase.

The diffusing capacity for oxygen is determined in part by surface area and the distance of diffusion. While the distance is important, it is the RBC-to-capillary surface area that is often a more critical determinant of DO_2m, such that there is a strong association between capillary hemodynamics and DO_2m (for review see Poole et al. (181, 182, 184)). At rest, most skeletal muscle capillaries support RBC flow but have a significantly reduced capillary hematocrit to around 15% (55, 118-120). During exercise these already flowing capillaries undergo an increased RBC flux and velocity that elevates capillary hematocrit toward systemic levels (119). This increased hematocrit across the length of a capillary is referred to as longitudinal capillary recruitment and increases the overall area for diffusion (182-184). While these events within the capillary occur perfectly in the healthy circulation, in aging and diseases like congestive heart failure there is an impaired capillary RBC flux during exercise (183). In these populations, a significant number of capillaries do not support flow during exercise. As a consequence, the available surface area for O_2 diffusion is decreased resulting in a decreased DO_2m.

Microgravity's influence on capillary structure appears to be limited. Generally, skeletal muscle capillary density and capillary-to-fiber ratio are unaffected by microgravity (11, 56, 74, 97, 161, 208). These findings suggest that the decrease in the absolute number of capillaries is similar to the decrease in muscle fiber cross sectional area, resulting in an unchanged density (74). However, Ferretti et al. (74) also report a ~22% decrease in total capillary length following 42 days of HDBR that they advocate is a consequence of muscle fiber atrophy. While this decrease in length may contribute to a reduced DO_2m, the regularly reported static capillary-to-fiber ratio suggests that the available surface area for O_2 diffusion per muscle fiber is unchanged. However, the number of capillaries only sets the upper limit for available diffusion surface area;

it is the number and velocity of RBCs within a given capillary that ultimately determine the RBC-to-capillary diffusion area. Unfortunately, no study to date has evaluated the change in capillary hematocrit or the degree of longitudinal capillary recruitment following microgravity. One might speculate that healthy astronauts exposed to long-durations of microgravity may experience similar adaptations in microcirculatory hemodynamics to that of an aged or heart failure circulation.

The calculated decrease in DO_2m following 360 days microgravity in this review is supported in part by measurements of tissue deoxygenation during exercise via near-infrared spectroscopy (NIRS). Following 35 days HDBR, subjects had a significantly decreased peak deoxygenated [hemoglobin + myoglobin] signal in the vastus lateralis during incremental exercise (185, 212). The authors interpreted these findings as evidence for an impaired capacity for O_2 extraction. This is somewhat contrary to the minor decrease in DO_2m following 60 days microgravity in Figure 5-4A. However, it is important to highlight that the NIRS signal only provides a window into the movement of oxygen, not a direct measure of O_2 extraction. In practice, this signal is determined by the matching of O_2 delivery-to-O_2 utilization, DO_2m, and the state of intracellular oxidative metabolism (212). In addition, as previously mentioned, the distribution of blood is altered between muscle fiber types post-microgravity and therefore must be considered when interpreting NIRS data.

Similarly, the influence of microgravity on mitochondrial oxidative enzyme activity should be highlighted. Following 17 days of spaceflight, Trappe et al. (235) report an unaltered citrate synthase activity within the human gastrocnemius. However, investigations of longer durations indicate that oxidative enzyme activity is significantly influenced by microgravity (11, 97). Therefore, the duration of microgravity exposure may likely dictate if adaptations in intracellular oxidative metabolism occur and ultimately impact exercise performance. At this time it is unclear if these adaptations in oxidative enzyme are great enough to significantly impact $\dot{V}O_2max$ in the post-flight astronaut. Additional research in this area is needed to address this gap in knowledge.

Remaining unanswered questions and conclusions

The modeling and review of the determinants of $\dot{V}O_2max$ following long-duration microgravity exposure provides a unique opportunity to highlight the current gaps in knowledge. The first key question relates to the control of blood flow and its distribution during exercise. Specifically, what are the precise mechanisms for the reduced microvascular function currently observed in the rat HU model? Likewise, are the observations made in peripheral conduit arteries (i.e., flow-mediated dilation or reactive hyperemia) an accurate measure of what is occurring downstream within the skeletal muscle arterioles? The second group of unanswered questions focuses on the determinants of DO_2m. Does the microcirculatory hemodynamic response to exercise change following spaceflight? Is there a decreased longitudinal capillary recruitment in astronauts similar to heart failure patients that explain the decreased DO_2m? To that point, it is critical to remember that the modeled decrease in DO_2m made in the present review is only an initial estimation. The appropriate measurements must be performed in astronauts to accurately determine the changes in convective and diffusive O_2 transport.

CONCLUSIONS

Sustained microgravity exposure results in a time dependent decrease in $\dot{V}O_2max$. Without the inclusion of countermeasures this decrease occurs at a rate such that a 37% decrease in $\dot{V}O_2max$ is expected following a 360-day space mission. This decline in aerobic capacity is initially mediated by a decrease in convective O_2 transport that is followed by a decrease in diffusive O_2 transport. To date, many of the independent components within the O_2 transport pathway have been evaluated. However, substantial gaps in knowledge still remain, particularly within the peripheral circulation. Finally, such a dramatic decline in aerobic capacity will have a substantial impact on space mission performance and safety. Astronauts, their flight surgeons, and the scientific community must continue to facilitate the study of gravitational physiology, with particular focus on the countermeasures that impact the various steps within the O_2 transport pathway.

Table 5-1. % Change in Maximal Oxygen Uptake Post-Microgravity
Exposure without Countermeasure Procedures

Reference	Model	Duration	%Δ
Friman G et al. (79)	BR	7	-5.76
Convertino VA et al. (40)	BR	8	-9.71
Katkovskiy BS et al. (116)	SF	8.7	-13.00
Katkovskiy BS et al. (116)	SF	9.4	-10.07
Convertino VA et al. (35)	BR	10	-15.12
Convertino VA et al. (38)	BR	10	-7.02
Williams DA et al. (251)	BR	10	-15.49
Hung J et al. (106)	BR	10	-15.00
Convertino VA et al. (37)	BR	10	-8.03
Convertino VA et al. (37)	SF	10	-7.45
Convertino VA et al. (37)	SF	10	-4.26
Convertino VA et al. (37)	BR	10	-10.19
Levine BD et al. (137)	SF	11.5	-22.46
Capelli C et al. (24)	BR	14	-13.21
Stremel RW et al. (224)	BR	14	-12.27
Convertino VA et al. (40)	BR	14	-9.09
Convertino VA et al. (39)	BR	15	-13.99
Watenpaugh DE et al. (246)	BR	15	-13.54
Chase GA et al. (28)	BR	15	-1.95
Trappe T et al. (236)	SF	17	-10.31
Trappe T et al. (236)	BR	17	-6.79
Shibata S et al. (216)	BR	18	-20.08
Saltin B et al. (209)	BR	20	-27.27
Stenger MB et al. (222)	BR	21	-12.50
Meehan JP et al. (152)	BR	28	-16.49
Stevens PM et al. (223)	BR	28	-20.90
Taylor HL et al. (225)	BR	28	-17.40
Greenleaf JE et al. (86)	BR	30	-20.49
Lee SM et al. (134)	BR	30	-16.36
Chase GA et al. (28)	BR	30	-10.95
Lee SM et al. (134)	BR	30	-16.00
Lee SM et al. (135)	BR	30	-23.00
Bringard A et al. (20)	BR	35	-38.54
Porcelli S et al. (185)	BR	35	-18.00
Capelli C et al. (24)	BR	42	-16.61
Katkovskiy BS et al. (116)	BR	60	-26.07
Capelli C et al. (24)	BR	90	-32.38

BR, bed rest; SF, spaceflight

Table 5-2. Estimated changes in O_2 transport for an average reference astronaut following microgravity exposure

Variable	Pre-Flight	60 days	360 days
$\dot{V}O_2$max, $l \times min^{-1}$	3.70	2.7	2.37
$\dot{Q}$max, $l \times min^{-1}$	23.0	17.2	17.2
CaO_2, $ml \times dl^{-1}$	21.3	19.7	19.6
CvO_2, $ml \times dl^{-1}$	5.2	4.0	5.8
PvO_2, Torr	16.0	14.1	18.4
a-vO_2 diff, $ml \times dl^{-1}$	16.1	15.7	13.8
SaO_2, %	98.0	98.0	98.0
[Hb], $g \times dl^{-1}$	16.0	14.8	14.7
$\dot{Q}O_2$, $\%\Delta_{pre-flight}$	-	-30.7%	-31.2%
DO_2m, $\%\Delta_{pre-flight}$	-	-17.0%	-44.2%

$\dot{V}O_2$max, maximal oxygen uptake; $\dot{Q}$max, maximal cardiac output;

CaO_2, arterial O_2 content; CvO_2, venous O_2 content; PvO_2, venous PO_2; a-v O_2 diff, arterial-venous oxygen difference; SaO_2, arterial saturation; [Hb], hemoglobin concentration; $\dot{Q}O_2$, convective O_2

delivery; DO_2m, O_2 diffusing capacity

Figure 5-1. Schematic illustration of the adaptations to long-duration spaceflight missions. Removal of gravitational forces and a decreased level of physical activity result in fluid redistribution, changed cardiac loading, and unloading of the musculoskeletal system. Upon return to gravity, spaceflight deconditioning becomes evident across multiple organ systems that may all contribute to a decreased post-flight cardiorespiratory function.

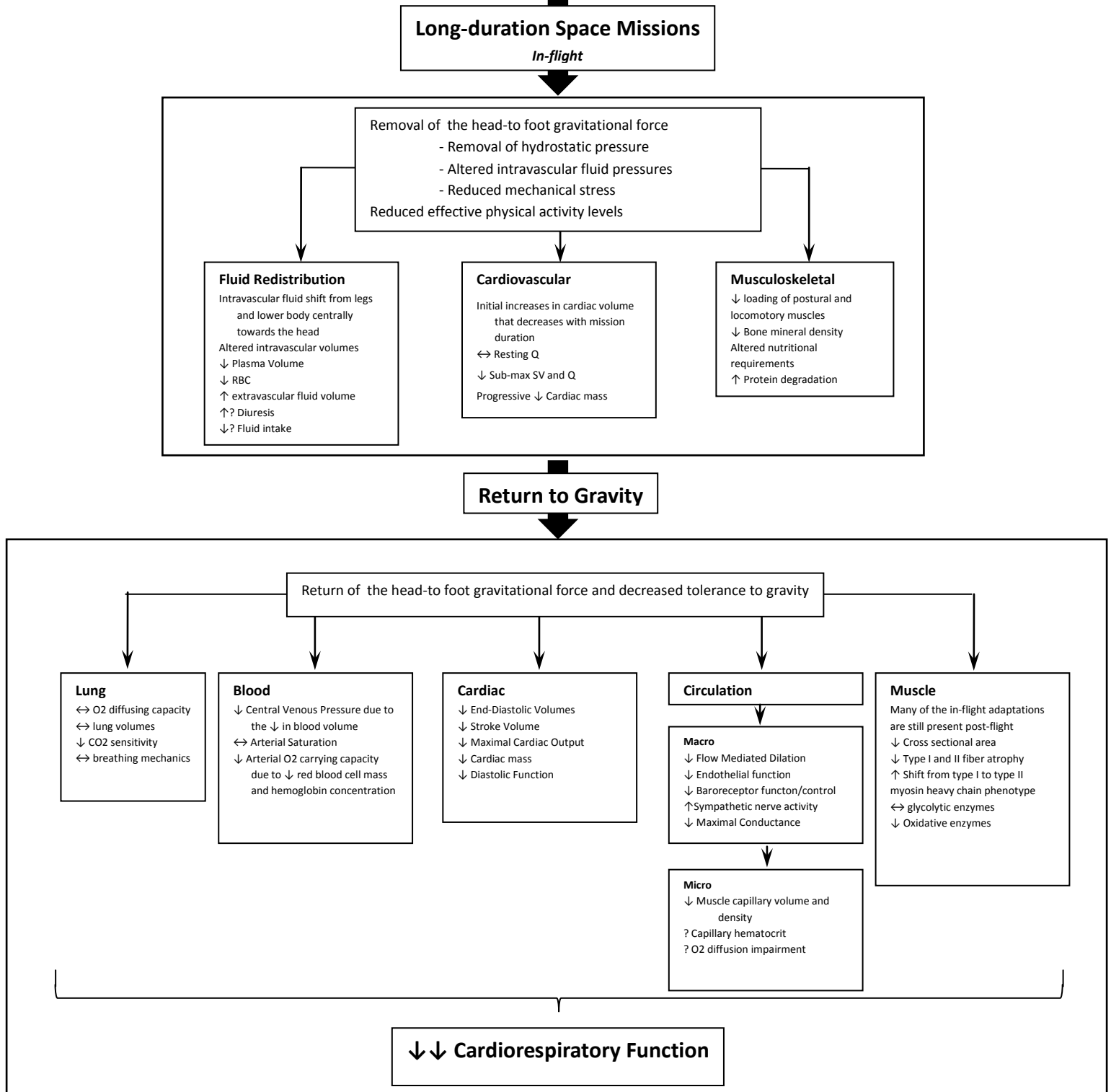Figure 5-2. Analysis of the percent change in $\dot{V}O_2$max as a function of microgravity duration.

Closed symbols refer to data obtained from published HDBR studies. *Open symbols* refer to data obtained from published spaceflight experiments.
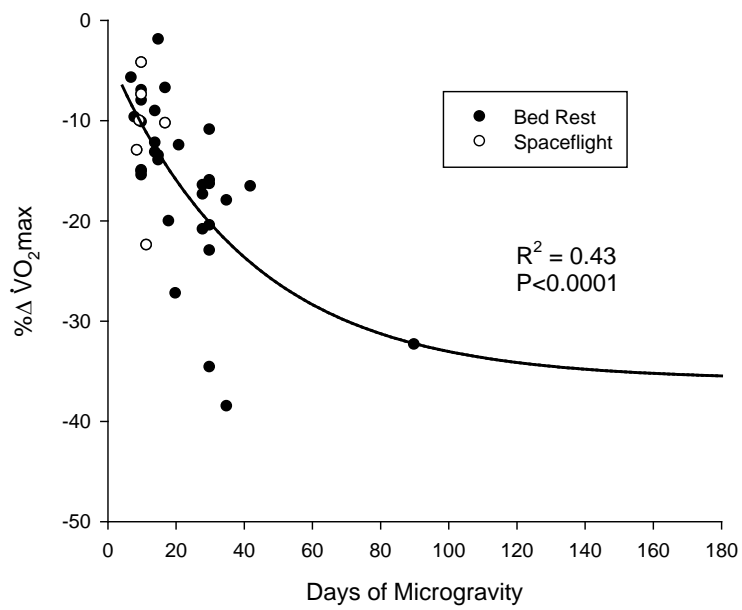
Figure 5-3. (Panel A) Diagram of oxygen transport in skeletal muscle. Convective O_2 transport occurs from the arteriole, across the capillary bed, to the venule.

Diffusion of oxygen is dependent on the RBC-to-capillary surface area and distance between RBC and muscle mitochondria. (Panel B) Graphical representation of the convective and diffusive components that determine $\dot{V}O_2$max in a pre-flight astronaut. Note that both components of the O_2 transport pathway intersect to yield $\dot{V}O_2$max.
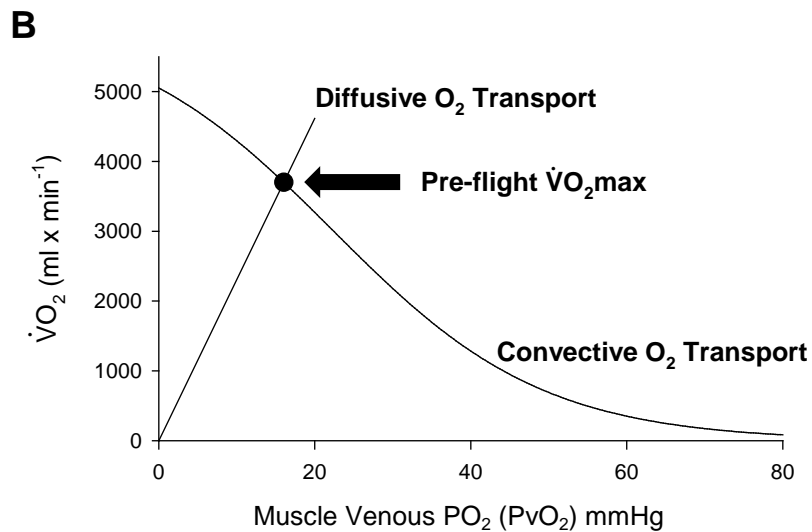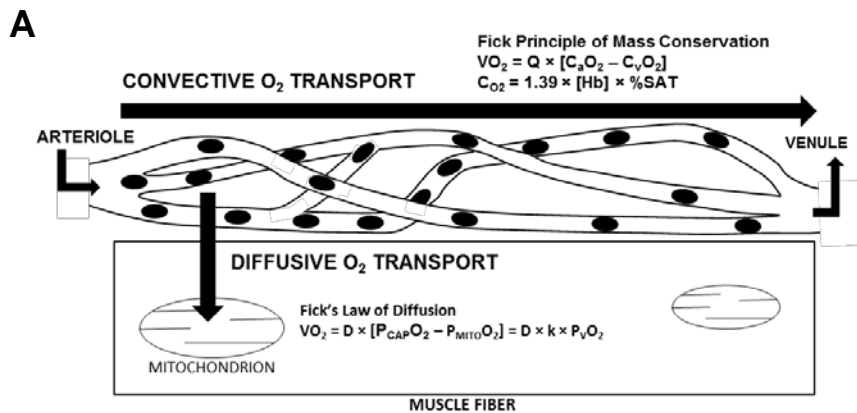
Figure 5-4. Illustration of the influence of long-duration spaceflight on the determinants of $\dot{V}O_2$max (dashed lines).

(Panel A) Following 60 days microgravity $\dot{V}O_2$max is primarily reduced by an impaired convective O_2 transport (curved lines). (Panel B) After 360 days of microgravity $\dot{V}O_2$max is determined by both impaired convective and diffusive (straight line) O_2 transport.

A

B
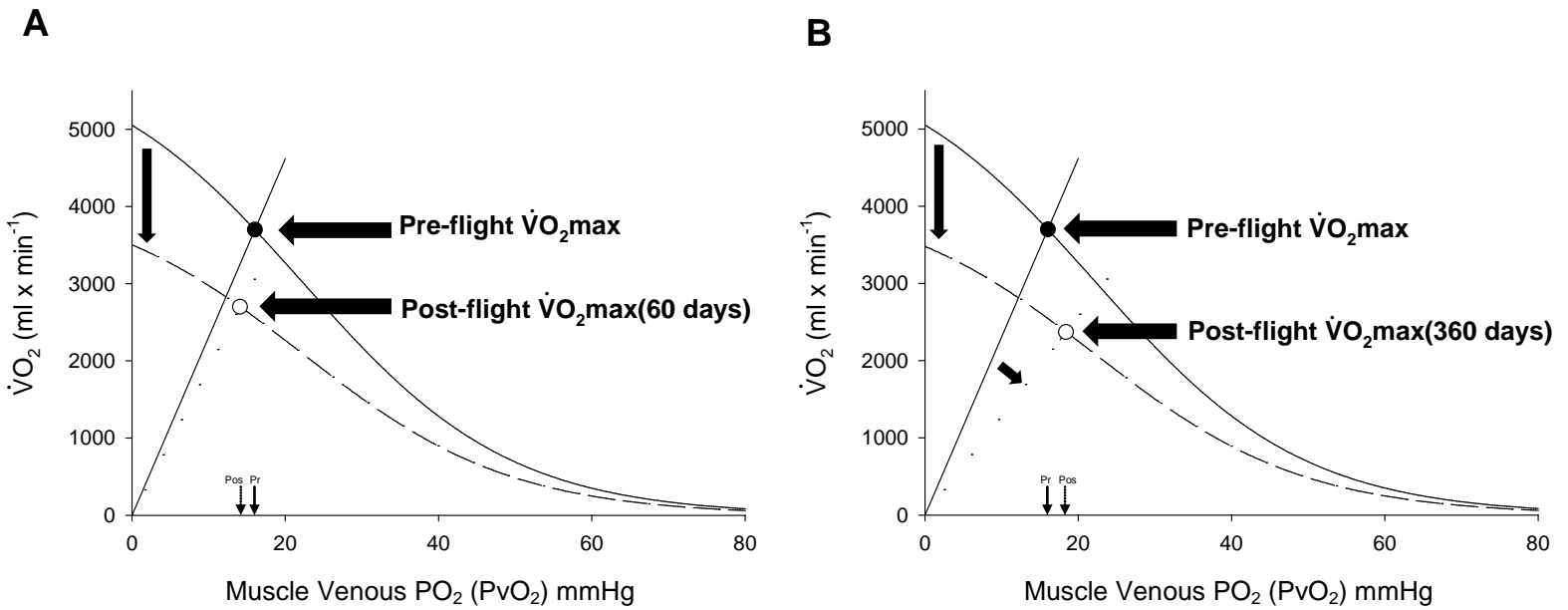
Figure 5-5. Schematic illustration of the effects of microgravity on the distribution of blood volume.

Note the head ward shift in blood volume and pressure. This redistribution increases transcapillary filtration leading to a decrease in plasma volume. During HDBR, the caudal translocation of blood volume distends the cardiac chambers and increases diuresis and naturesis via the Henry-Gaur reflex.

Chapter 6 - Conclusions

Following integration of the investigations described in this dissertation, we concluded that the cardiorespiratory adaptations to exercise conditioning and microgravity deconditioning are widespread and are in part mediated by alterations in the hemodynamic forces placed on the cardiovascular system. Specifically, the increased ventricular volume load achieved via exercise training in the hea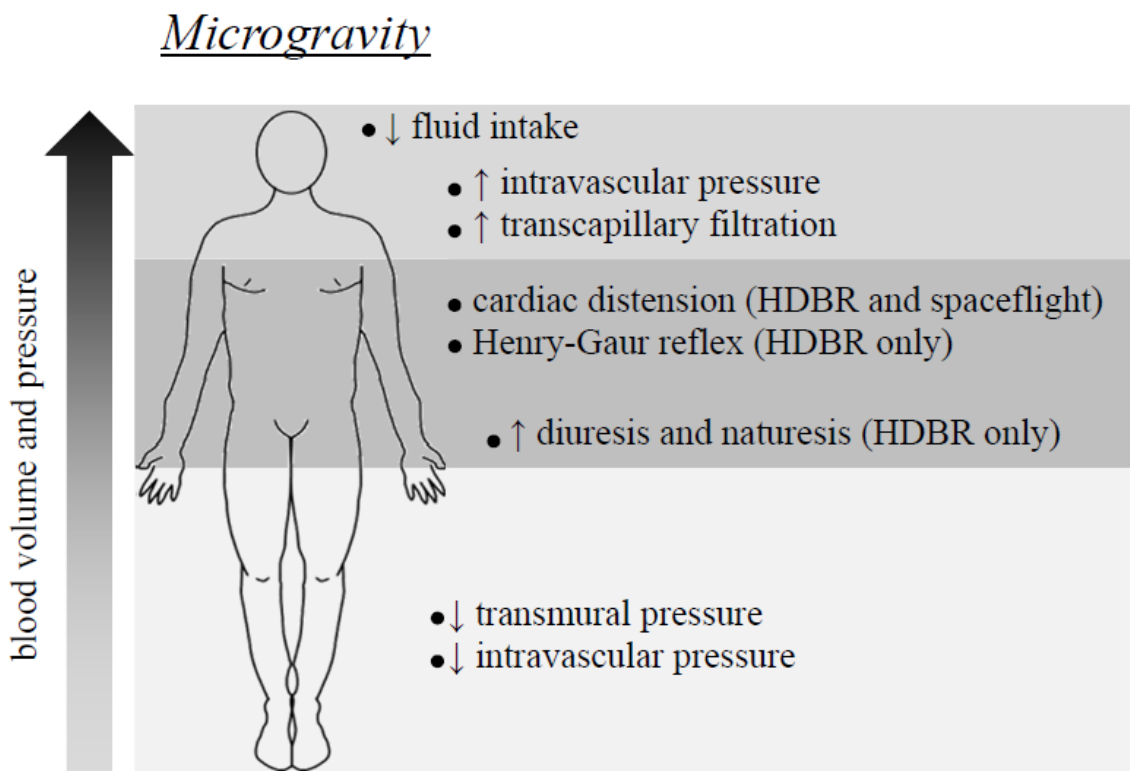d down tilt posture increases cardiac performance and maximal O_2 consumption ($\dot{V}O_2max$). Conversely, mechanical unloading of the heart via sustained microgravity exposure decreases cardiac mass and function thus contributing to a significant decrease in maximal cardiac output, convective O_2 delivery, and ultimately $\dot{V}O_2max$ following microgravity exposure. Our data also demonstrated that the hemodynamic environment within the peripheral circulation significantly impacts vascular function. With the gained knowledge that blood moves with an appropriate quasi-parabolic velocity profile we demonstrated that prior exposure to a high antegrade shear rate increases endothelial function as assessed via flow-mediated dilation and the kinetics of the on-transient vasodilator response to exercise. These findings suggest that one potential mechanism for vascular adaptation, like that achieved with exercise conditioning, is exposure to elevations in antegrade shear. On the other hand, as reviewed in Chapter 5, the stress imposed by sustained microgravity exposure decreases vascular function by some undefined mechanism. A chronic low shear stress has been implicated as a contributing factor, but direct scientific investigations have not been performed. Collectively, the current dissertation extends our understanding of the stress that initiates cardiorespiratory and vascular function. Important preventative and therapeutic applications arise from these investigations when considering that exercise conditioning can be used to positively impact cardiovascular health across multiple populations. Furthermore, the review of microgravity deconditioning highlights the adverse effects of an environment lacking the necessary stimuli for maintenance of healthy cardiorespiratory function and control.

Chapter 7 - References

1. **(LSAH) LSoAH**. Physiological Variables of EVA Participants (LSAHNEWSV7.2.3) National Aeronautics and Space Administration.

2. **Ade CJ, Broxterman RM, Gadbury GL, Schinstock D, Warren S, and Barstow TJ**. Standardized Exercise Test to Evaluate Planetary Mission Readiness. In: *NASA Humans Research Program Workshop*. Houston, TX: 2012.

3. **Ade CJ, Broxterman RM, Wong BJ, and Barstow TJ**. Anterograde and retrograde blood velocity profiles in the intact human cardiovascular system. *Exp Physiol* 97: 849-860, 2012.

4. **Alfrey CP, Udden MM, Huntoon CL, and Driscoll T**. Destruction of newly released red blood cells in space flight. *Med Sci Sports Exerc* 28: S42-44, 1996.

5. **Alfrey CP, Udden MM, Leach-Huntoon C, Driscoll T, and Pickett MH**. Control of red blood cell mass in spaceflight. *J Appl Physiol* 81: 98-104, 1996.

6. **Antonutto G, and di Prampero PE**. Cardiovascular deconditioning in microgravity: some possible countermeasures. *Eur J Appl Physiol* 90: 283-291, 2003.

7. **Barakat A, and Lieu D**. Differential responsiveness of vascular endothelial cells to different types of fluid mechanical shear stress. *Cell Biochem Biophys* 38: 323-343, 2003.

8. **Beaver WL, Wasserman K, and Whipp BJ**. A new method for detecting anaerobic threshold by gas exchange. *J Appl Physiol* 60: 2020-2027, 1986.

9. **Behnke BJ, Delp MD, Dougherty PJ, Musch TI, and Poole DC**. Effects of aging on microvascular oxygen pressures in rat skeletal muscle. *Respir Physiol Neurobiol* 146: 259-268, 2005.

10. **Behnke BJ, Zawieja DC, Gashev AA, Ray CA, and Delp MD**. Diminished mesenteric vaso- and venoconstriction and elevated plasma ANP and BNP with simulated microgravity. *J Appl Physiol* 104: 1273-1280, 2008.

11. **Berg HE, Dudley GA, Hather B, and Tesch PA**. Work capacity and metabolic and morphologic characteristics of the human quadriceps muscle in response to unloading. *Clin Physiol* 13: 337-347, 1993.

12. **Bevegard S, Freyschuss U, and Strandell T**. Circulatory adaptation to arm and leg exercise in supine and sitting position. *J Appl Physiol* 21: 37-46, 1966.

13. **Bevegard S, Holmgren A, and Jonsson B**. The effect of body position on the circulation at rest and during exercise, with special reference to the influence on the stroke volume. *Acta Physiol Scand* 49: 279-298, 1960.

14. **Bishop JJ, Nance PR, Popel AS, Intaglietta M, and Johnson PC**. Effect of erythrocyte aggregation on velocity profiles in venules. *Am J Physiol Heart Circ Physiol* 280: H222-236, 2001.

15. **Blair SN, and Morris JN**. Healthy hearts--and the universal benefits of being physically active: physical activity and health. *Ann Epidemiol* 19: 253-256, 2009.

16. **Blomqvist CG, Nixon JV, Johnson RL, Jr., and Mitchell JH**. Early cardiovascular adaptation to zero gravity simulated by head-down tilt. *Acta Astronaut* 7: 543-553, 1980.

17. **Blomqvist CG, and Saltin B**. Cardiovascular adaptations to physical training. *Annu Rev Physiol* 45: 169-189, 1983.

18. **Bock O, Weigelt C, and Bloomberg JJ**. Cognitive demand of human sensorimotor performance during an extended space mission: a dual-task study. *Aviat Space Environ Med* 81: 819-824, 2010.

19. **Boushel R, Langberg H, Olesen J, Gonzales-Alonzo J, Bulow J, and Kjaer M**. Monitoring tissue oxygen availability with near infrared spectroscopy (NIRS) in health and disease. *Scand J Med Sci Sports* 11: 213-222, 2001.

20. **Bringard A, Pogliaghi S, Adami A, De Roia G, Lador F, Lucini D, Pizzinelli P, Capelli C, and Ferretti G**. Cardiovascular determinants of maximal oxygen consumption in upright and supine posture at the end of prolonged bed rest in humans. *Respir Physiol Neurobiol* 172: 53-62, 2010.

21. **Buckey JC, Jr., Gaffney FA, Lane LD, Levine BD, Watenpaugh DE, Wright SJ, Yancy CW, Jr., Meyer DM, and Blomqvist CG**. Central venous pressure in space. *J Appl Physiol* 81: 19-25, 1996.

22. **Buckey JC, Jr., Lane LD, Levine BD, Watenpaugh DE, Wright SJ, Moore WE, Gaffney FA, and Blomqvist CG**. Orthostatic intolerance after spaceflight. *J Appl Physiol* 81: 7-18, 1996.

23. **Buderer MC, Rummel JA, Michel EL, Mauldin DG, and Sawin CF**. Exercise cardiac output following Skylab missions: the second manned Skylab mission. *Aviat Space Environ Med* 47: 365-372, 1976.

24. **Capelli C, Antonutto G, Kenfack MA, Cautero M, Lador F, Moia C, Tam E, and Ferretti G**. Factors determining the time course of VO_2max decay during bedrest: implications for VO_2max limitation. *Eur J Appl Physiol* 98: 152-160, 2006.

25. **Carrick-Ranson G, Hastings JL, Bhella PS, Shibata S, and Levine BD**. The effect of exercise training on left ventricular relaxation and diastolic suction at rest and during orthostatic stress after bed rest. *Exp Physiol* 98: 501-513, 2013.

26. **Casey DP, Mohamed EA, and Joyner MJ**. Role of nitric oxide and adenosine in the onset of vasodilation during dynamic forearm exercise. *Eur J Appl Physiol* 113: 295-303, 2013.

27. **Chappell DC, Varner SE, Nerem RM, Medford RM, and Alexander RW**. Oscillatory shear stress stimulates adhesion molecule expression in cultured human endothelium. *Circ Res* 82: 532-539, 1998.

28. **Chase GA, Grave C, and Rowell LB**. Independence of changes in functional and performance capacities attending prolonged bed rest. *Aerosp Med* 37: 1232-1238, 1966.

29. **Chobanian AV, Lille RD, Tercyak A, and Blevins P**. The metabolic and hemodynamic effects of prolonged bed rest in normal subjects. *Circulation* 49: 551-559, 1974.

30. **Christ F, Gamble J, Baranov V, Kotov A, Chouker A, Thiel M, Gartside IB, Moser CM, Abicht J, and Messmer K**. Changes in microvascular fluid filtration capacity during 120 days of 6 degrees head-down tilt. *J Appl Physiol* 91: 2517-2522, 2001.

31. **Clifford PS, and Hellsten Y**. Vasodilatory mechanisms in contracting skeletal muscle. *J Appl Physiol* 97: 393-403, 2004.

32. **Cogoli A**. Hematological and immunological changes during space flight. *Acta Astronaut* 8: 995-1002, 1981.

33. **Colleran PN, Behnke BJ, Wilkerson MK, Donato AJ, and Delp MD**. Simulated microgravity alters rat mesenteric artery vasoconstrictor dynamics through an intracellular Ca(2+) release mechanism. *Am J Physiol Regul Integr Comp Physiol* 294: R1577-1585, 2008.

34. **Convertino V**. Exercise and adaptation to microgravity environments. In: *Handbook of Physiology: Section 4 Environmental Physiology, vol 3*, edited by Fregly MJ, and Blatteis CM. New York: Oxford University, 1996, p. 815-843.

35. **Convertino V, Hung J, Goldwater D, and DeBusk RF**. Cardiovascular responses to exercise in middle-aged men after 10 days of bedrest. *Circulation* 65: 134-140, 1982.

36. **Convertino VA**. Cardiovascular consequences of bed rest: effect on maximal oxygen uptake. *Med Sci Sports Exerc* 29: 191-196, 1997.

37. **Convertino VA, Goldwater DJ, and Sandler H**. Bedrest-induced peak VO_2 reduction associated with age, gender, and aerobic capacity. *Aviat Space Environ Med* 57: 17-22, 1986.

38. **Convertino VA, Karst GM, Kirby CR, and Goldwater DJ**. Effect of simulated weightlessness on exercise-induced anaerobic threshold. *Aviat Space Environ Med* 57: 325-331, 1986.

39. **Convertino VA, Sandler H, Webb P, and Annis JF**. Induced venous pooling and cardiorespiratory responses to exercise after bed rest. *J Appl Physiol* 52: 1343-1348, 1982.

40. **Convertino VA, Stremel RW, Bernauer EM, and Greenleaf JE**. Cardiorespiratory responses to exercise after bed rest in men and women. *Acta Astronaut* 4: 895-905, 1977.

41. **Copp SW, Hirai DM, Sims GE, Fels RJ, Musch TI, Poole DC, and Kenney MJ**. Neuronal nitric oxide synthase inhibition and regional sympathetic nerve discharge: Implications for peripheral vascular control. *Respir Physiol Neurobiol* 186: 285-289, 2013.

42. **Copp SW, Holdsworth CT, Ferguson SK, Hirai DM, Poole DC, and Musch TI**. Muscle fibre-type dependence of neuronal nitric oxide synthase-mediated vascular control in the rat during high speed treadmill running. *J Physiol* 2013.

43. **Coyle EF**. Integration of the physiological factors determining endurance performance ability. *Exerc Sport Sci Rev* 23: 25-63, 1995.

44. **Coyle EF**. Physiological determinants of endurance exercise performance. *J Sci Med Sport* 2: 181-189, 1999.

45. **Credeur DP, Dobrosielski DA, Arce-Esquivel AA, and Welsch MA**. Brachial artery retrograde flow increases with age: relationship to physical function. *Eur J Appl Physiol* 107: 219-225, 2009.

46. **Davies PF**. Flow-mediated endothelial mechanotransduction. *Physiol Rev* 75: 519-560, 1995.

47. **Davis ML, and Barstow TJ**. Estimated contribution of hemoglobin and myoglobin to near infrared spectroscopy. *Respir Physiol Neurobiol* 186: 180-187, 2013.

48. **Davis SL, Fadel PJ, Cui J, Thomas GD, and Crandall CG**. Skin blood flow influences near-infrared spectroscopy-derived measurements of tissue oxygenation during heat stress. *J Appl Physiol* 100: 221-224, 2006.

49. **DeLorey DS, Kowalchuk JM, and Paterson DH**. Relationship between pulmonary O_2 uptake kinetics and muscle deoxygenation during moderate-intensity exercise. *J Appl Physiol* 95: 113-120, 2003.

50. **Delp MD**. Arterial adaptations in microgravity contribute to orthostatic tolerance. *J Appl Physiol* 102: 836, 2007.

51.   **Delp MD**. Effects of exercise training on endothelium-dependent peripheral vascular responsiveness. *Med Sci Sports Exerc* 27: 1152-1157, 1995.

52.   **Delp MD**. Myogenic and vasoconstrictor responsiveness of skeletal muscle arterioles is diminished by hindlimb unloading. *J Appl Physiol* 86: 1178-1184, 1999.

53.   **Delp MD, Colleran PN, Wilkerson MK, McCurdy MR, and Muller-Delp J**. Structural and functional remodeling of skeletal muscle microvasculature is induced by simulated microgravity. *Am J Physiol Heart Circ Physiol* 278: H1866-1873, 2000.

54.   **Delp MD, and Laughlin MH**. Regulation of skeletal muscle perfusion during exercise. *Acta Physiol Scand* 162: 411-419, 1998.

55.   **Desjardins C, and Duling BR**. Microvessel hematocrit: measurement and implications for capillary oxygen transport. *Am J Physiol* 252: H494-503, 1987.

56.   **Desplanches D, Kayar SR, Sempore B, Flandrois R, and Hoppeler H**. Rat soleus muscle ultrastructure after hindlimb suspension. *J Appl Physiol* 69: 504-508, 1990.

57.   **Dibski DW, Smith DJ, Jensen R, Norris SR, and Ford GT**. Comparison and reliability of two non-invasive acetylene uptake techniques for the measurement of cardiac output. *Eur J Appl Physiol* 94: 670-680, 2005.

58.   **Diederich ER, Behnke BJ, McDonough P, Kindig CA, Barstow TJ, Poole DC, and Musch TI**. Dynamics of microvascular oxygen partial pressure in contracting skeletal muscle of rats with chronic heart failure. *Cardiovasc Res* 56: 479-486, 2002.

59.   **DiMenna FJ, Bailey SJ, and Jones AM**. Influence of body position on muscle deoxy[Hb+Mb] during ramp cycle exercise. *Respir Physiol Neurobiol* 173: 138-145, 2010.

60.   **Dorfman TA, Levine BD, Tillery T, Peshock RM, Hastings JL, Schneider SM, Macias BR, Biolo G, and Hargens AR**. Cardiac atrophy in women following bed rest. *J Appl Physiol* 103: 8-16, 2007.

61.   **Dorfman TA, Rosen BD, Perhonen MA, Tillery T, McColl R, Peshock RM, and Levine BD**. Diastolic suction is impaired by bed rest: MRI tagging studies of diastolic untwisting. *J Appl Physiol* 104: 1037-1044, 2008.

62.   **Downey AE, Chenoweth LM, Townsend DK, Ranum JD, Ferguson CS, and Harms CA**. Effects of inspiratory muscle training on exercise responses in normoxia and hypoxia. *Respir Physiol Neurobiol* 156: 137-146, 2007.

63.   **Drummer C, Heer M, Dressendorfer RA, Strasburger CJ, and Gerzer R**. Reduced natriuresis during weightlessness. *Clin Investig* 71: 678-686, 1993.

64. **Drummer C, Hesse C, Baisch F, Norsk P, Elmann-Larsen B, Gerzer R, and Heer M**. Water and sodium balances and their relation to body mass changes in microgravity. *Eur J Clin Invest* 30: 1066-1075, 2000.

65. **Egana M, Green S, Garrigan EJ, and Warmington S**. Effect of posture on high-intensity constant-load cycling performance in men and women. *Eur J Appl Physiol* 96: 1-9, 2006.

66. **Egana M, O'Riordan D, and Warmington SA**. Exercise performance and VO_2 kinetics during upright and recumbent high-intensity cycling exercise. *Eur J Appl Physiol* 110: 39-47, 2010.

67. **Egana M, Smith S, and Green S**. Revisiting the effect of posture on high-intensity constant-load cycling performance in men and women. *Eur J Appl Physiol* 99: 495-501, 2007.

68. **Ekblom B**. Effect of physical training on oxygen transport system in man. *Acta Physiol Scand Suppl* 328: 1-45, 1968.

69. **Elliott AR, Prisk GK, Guy HJ, and West JB**. Lung volumes during sustained microgravity on Spacelab SLS-1. *J Appl Physiol* 77: 2005-2014, 1994.

70. **Evans DH**. On the measurement of the mean velocity of blood flow over the cardiac cycle using Doppler ultrasound. *Ultrasound Med Biol* 11: 735-741, 1985.

71. **Ferreira LF, Koga S, and Barstow TJ**. Dynamics of noninvasively estimated microvascular O_2 extraction during ramp exercise. *J Appl Physiol* 103: 1999-2004, 2007.

72. **Ferreira LF, Padilla DJ, Williams J, Hageman KS, Musch TI, and Poole DC**. Effects of altered nitric oxide availability on rat muscle microvascular oxygenation during contractions. *Acta Physiol (Oxf)* 186: 223-232, 2006.

73. **Ferreira LF, Townsend DK, Lutjemeier BJ, and Barstow TJ**. Muscle capillary blood flow kinetics estimated from pulmonary O_2 uptake and near-infrared spectroscopy. *J Appl Physiol* 98: 1820-1828, 2005.

74. **Ferretti G, Antonutto G, Denis C, Hoppeler H, Minetti AE, Narici MV, and Desplanches D**. The interplay of central and peripheral factors in limiting maximal O_2 consumption in man after prolonged bed rest. *J Physiol* 501 (Pt 3): 677-686, 1997.

75. **Ferretti G, and Capelli C**. Maximal O_2 consumption: Effects of gravity withdrawal and resumption. *Respir Physiol Neurobiol* 169 Suppl 1: S50-54, 2009.

76. **Ferretti G, Girardis M, Moia C, and Antonutto G**. Effects of prolonged bed rest on cardiovascular oxygen transport during submaximal exercise in humans. *Eur J Appl Physiol Occup Physiol* 78: 398-402, 1998.

77.   **Fitts RH, Trappe SW, Costill DL, Gallagher PM, Creer AC, Colloton PA, Peters JR, Romatowski JG, Bain JL, and Riley DA**. Prolonged space flight-induced alterations in the structure and function of human skeletal muscle fibres. *J Physiol* 588: 3567-3592, 2010.

78.   **Fitzpatrick R, Taylor JL, and McCloskey DI**. Effects of arterial perfusion pressure on force production in working human hand muscles. *J Physiol* 495 (Pt 3): 885-891, 1996.

79.   **Friman G**. Effect of clinical bed rest for seven days on physical performance. *Acta Med Scand* 205: 389-393, 1979.

80.   **Gaehtgens P, Meiselman HJ, and Wayland H**. Velocity profiles of human blood at normal and reduced hematocrit in glass tubes up to 130 diameter. *Microvasc Res* 2: 13-23, 1970.

81.   **Gaffney FA, Nixon JV, Karlsson ES, Campbell W, Dowdey AB, and Blomqvist CG**. Cardiovascular deconditioning produced by 20 hours of bedrest with head-down tilt (-5 degrees) in middle-aged healthy men. *Am J Cardiol* 56: 634-638, 1985.

82.   **Gauer OH, and Henry JP**. Neurohormonal control of plasma volume. *Int Rev Physiol* 9: 145-190, 1976.

83.   **Green DJ**. Exercise training as vascular medicine: direct impacts on the vasculature in humans. *Exerc Sport Sci Rev* 37: 196-202, 2009.

84.   **Green DJ, Maiorana A, O'Driscoll G, and Taylor R**. Effect of exercise training on endothelium-derived nitric oxide function in humans. *J Physiol* 561: 1-25, 2004.

85.   **Green DJ, O'Driscoll G, Joyner MJ, and Cable NT**. Exercise and cardiovascular risk reduction: time to update the rationale for exercise? *J Appl Physiol* 105: 766-768, 2008.

86.   **Greenleaf JE, Bernauer EM, Ertl AC, Trowbridge TS, and Wade CE**. Work capacity during 30 days of bed rest with isotonic and isokinetic exercise training. *J Appl Physiol* 67: 1820-1826, 1989.

87.   **Guinet P, Schneider SM, Macias BR, Watenpaugh DE, Hughson RL, Le Traon AP, Bansard JY, and Hargens AR**. WISE-2005: effect of aerobic and resistive exercises on orthostatic tolerance during 60 days bed rest in women. *Eur J Appl Physiol* 106: 217-227, 2009.

88.   **Gunga HC, Kirsch K, Baartz F, Maillet A, Gharib C, Nalishiti W, Rich I, and Rocker L**. Erythropoietin under real and simulated microgravity conditions in humans. *J Appl Physiol* 81: 761-773, 1996.

89.   **Gunga HC, Kirsch K, and Rocker L**. Erythropoietin in blood volume regulation under real and simulated micro-g conditions. *J Gravit Physiol* 3: 1-4, 1996.

90. **Hahn C, and Schwartz MA**. Mechanotransduction in vascular physiology and atherogenesis. *Nat Rev Mol Cell Biol* 10: 53-62, 2009.

91. **Hale JF, Mc DD, and Womersley JR**. Velocity profiles of oscillating arterial flow, with some calculations of viscous drag and the Reynolds numbers. *J Physiol* 128: 629-640, 1955.

92. **Halliwill JR, and Minson CT**. Retrograde shear: backwards into the future? *Am J Physiol Heart Circ Physiol* 298: H1126-1127, 2010.

93. **Haram PM, Adams V, Kemi OJ, Brubakk AO, Hambrecht R, Ellingsen O, and Wisloff U**. Time-course of endothelial adaptation following acute and regular exercise. *Eur J Cardiovasc Prev Rehabil* 13: 585-591, 2006.

94. **Hargens AR, and Richardson S**. Cardiovascular adaptations, fluid shifts, and countermeasures related to space flight. *Respir Physiol Neurobiol* 169 Suppl 1: S30-33, 2009.

95. **Harper AJ, Ferreira LF, Lutjemeier BJ, Townsend DK, and Barstow TJ**. Human femoral artery and estimated muscle capillary blood flow kinetics following the onset of exercise. *Exp Physiol* 91: 661-671, 2006.

96. **Hastings JL, Krainski F, Snell PG, Pacini EL, Jain M, Bhella PS, Shibata S, Fu Q, Palmer MD, and Levine BD**. Effect of rowing ergometry and oral volume loading on cardiovascular structure and function during bed rest. *J Appl Physiol* 112: 1735-1743, 2012.

97. **Hather BM, Adams GR, Tesch PA, and Dudley GA**. Skeletal muscle responses to lower limb suspension in humans. *J Appl Physiol* 72: 1493-1498, 1992.

98. **Hester RL, Eraslan A, and Saito Y**. Differences in EDNO contribution to arteriolar diameters at rest and during functional dilation in striated muscle. *Am J Physiol* 265: H146-151, 1993.

99. **Hoelting BD, Scheuermann BW, and Barstow TJ**. Effect of contraction frequency on leg blood flow during knee extension exercise in humans. *J Appl Physiol* 91: 671-679, 2001.

100. **Hoskins PR, Martin K, and Thrush A**. *Diagnostic ultrasound : physics and equipment*. Cambridge, UK ; New York: Cambridge University Press, p. xi, 263 p.

101. **Howell WH, Fulton JF, Ruch TC, and Patton HD**. *Physiology and biophysics*. Philadelphia: Saunders, 1973.

102. **Hughson RL, Cochrane JE, and Butler GC**. Faster O_2 uptake kinetics at onset of supine exercise with than without lower body negative pressure. *J Appl Physiol* 75: 1962-1967, 1993.

103. **Hughson RL, Shoemaker JK, Arbeille P, Dyson KS, Edgell H, Kerbeci P, Mattar L, Zuj K, and Greaves DK**. WISE 2005: vascular responses to 60-day bed rest in women. *J Gravit Physiol* 14: P53-54, 2007.

104. **Hughson RL, Shoemaker JK, Tschakovsky ME, and Kowalchuk JM**. Dependence of muscle VO$_2$ on blood flow dynamics at onset of forearm exercise. *J Appl Physiol* 81: 1619-1626, 1996.

105. **Hughson RL, Xing HC, Borkhoff C, and Butler GC**. Kinetics of ventilation and gas exchange during supine and upright cycle exercise. *Eur J Appl Physiol Occup Physiol* 63: 300-307, 1991.

106. **Hung J, Goldwater D, Convertino VA, McKillop JH, Goris ML, and DeBusk RF**. Mechanisms for decreased exercise capacity after bed rest in normal middle-aged men. *Am J Cardiol* 51: 344-348, 1983.

107. **Hwang J, Ing MH, Salazar A, Lassegue B, Griendling K, Navab M, Sevanian A, and Hsiai TK**. Pulsatile versus oscillatory shear stress regulates NADPH oxidase subunit expression: implication for native LDL oxidation. *Circ Res* 93: 1225-1232, 2003.

108. **Jeon BH, Chang SJ, Kim JW, Hong YM, Yoon SY, and Choe IS**. Effect of high blood flow on the expression of endothelial constitutive nitric oxide synthase in rats with femoral arteriovenous shunts. *Endothelium* 7: 243-252, 2000.

109. **Johansen LB, Gharib C, Allevard AM, Sigaudo D, Christensen NJ, Drummer C, and Norsk P**. Haematocrit, plasma volume and noradrenaline in humans during simulated weightlessness for 42 days. *Clin Physiol* 17: 203-210, 1997.

110. **Johnson BD, Mather KJ, and Wallace JP**. Mechanotransduction of shear in the endothelium: basic studies and clinical implications. *Vasc Med* 16: 365-377, 2011.

111. **Jones AM, Berger NJ, Wilkerson DP, and Roberts CL**. Effects of "priming" exercise on pulmonary O$_2$ uptake and muscle deoxygenation kinetics during heavy-intensity cycle exercise in the supine and upright positions. *J Appl Physiol* 101: 1432-1441, 2006.

112. **Jones AM, and Carter H**. The effect of endurance training on parameters of aerobic fitness. *Sports Med* 29: 373-386, 2000.

113. **Joyner MJ, and Green DJ**. Exercise protects the cardiovascular system: effects beyond traditional risk factors. *J Physiol* 587: 5551-5558, 2009.

114. **Kakurin LI, Kuzmin MP, Matsnev EI, and Mikhailov VM**. Physiological effects induced by antiorthostatic hypokinesia. *Life Sci Space Res* 14: 101-108, 1976.

115. **Kakurin LI, Lobachik VI, Mikhailov VM, and Senkevich YA**. Antiorthostatic hypokinesia as a method of weightlessness simulation. *Aviat Space Environ Med* 47: 1083-1086, 1976.

116.	**Katkovskiy BS, Machinskiy GV, Toman PS, Danilova VI, and Demida BF**. Man's physical performance after thirty-day hypokinesia with countermeasures. *Space and biology and aerospace medicine* 8: 62-68, 1974.

117.	**Kato M, Tsutsumi T, Yamaguchi T, Kurakane S, and Chang H**. Characteristics of maximum performance of pedaling exercise in recumbent and supine positions. *J Sports Sci Med* 10: 491-497, 2011.

118.	**Kindig CA, and Poole DC**. A comparison of the microcirculation in the rat spinotrapezius and diaphragm muscles. *Microvasc Res* 55: 249-259, 1998.

119.	**Kindig CA, Richardson TE, and Poole DC**. Skeletal muscle capillary hemodynamics from rest to contractions: implications for oxygen transfer. *J Appl Physiol* 92: 2513-2520, 2002.

120.	**Klitzman B, and Duling BR**. Microvascular hematocrit and red cell flow in resting and contracting striated muscle. *Am J Physiol* 237: H481-490, 1979.

121.	**Koga S, Kano Y, Barstow TJ, Ferreira LF, Ohmae E, Sudo M, and Poole DC**. Kinetics of muscle deoxygenation and microvascular PO_2 during contractions in rat: comparison of optical spectroscopy and phosphorescence-quenching techniques. *J Appl Physiol* 112: 26-32, 2012.

122.	**Koga S, Shiojiri T, Shibasaki M, Kondo N, Fukuba Y, and Barstow TJ**. Kinetics of oxygen uptake during supine and upright heavy exercise. *J Appl Physiol* 87: 253-260, 1999.

123.	**Kooijman M, Thijssen DH, de Groot PC, Bleeker MW, van Kuppevelt HJ, Green DJ, Rongen GA, Smits P, and Hopman MT**. Flow-mediated dilatation in the superficial femoral artery is nitric oxide mediated in humans. *J Physiol* 586: 1137-1145, 2008.

124.	**Koppo K, and Bouckaert J**. Prior arm exercise speeds the VO_2 kinetics during arm exercise above the heart level. *Med Sci Sports Exerc* 37: 613-619, 2005.

125.	**Kowalchuk JM, Rossiter HB, Ward SA, and Whipp BJ**. The effect of resistive breathing on leg muscle oxygenation using near-infrared spectroscopy during exercise in men. *Exp Physiol* 87: 601-611, 2002.

126.	**Kremkau F**. *Diagnostic Ultrasound: Principles and Practice*. Philadelphia: Saunders, 1998.

127.	**Kuchan MJ, and Frangos JA**. Role of calcium and calmodulin in flow-induced nitric oxide production in endothelial cells. *Am J Physiol* 266: C628-636, 1994.

128.	**Laughlin MH**. Skeletal muscle blood flow capacity: role of muscle pump in exercise hyperemia. *Am J Physiol* 253: H993-1004, 1987.

129. **Laughlin MH, Davis MJ, H. NS, van Lieshout JJ, Arce-Esquivel AA, Simmons GH, Bender SB, Padilla DJ, Bache RJ, Merkus D, and Duncker DJ**. Peripheral Circulation. *Comprehensive Physiology* 2: 321-447, 2012.

130. **Laughlin MH, and Joyner M**. Closer to the edge? Contractions, pressures, waterfalls and blood flow to contracting skeletal muscle. *J Appl Physiol* 94: 3-5, 2003.

131. **Laughlin MH, Newcomer SC, and Bender SB**. Importance of hemodynamic forces as signals for exercise-induced changes in endothelial cell phenotype. *J Appl Physiol* 104: 588-600, 2008.

132. **Leach CS, Alfrey CP, Suki WN, Leonard JI, Rambaut PC, Inners LD, Smith SM, Lane HW, and Krauhs JM**. Regulation of body fluid compartments during short-term spaceflight. *J Appl Physiol* 81: 105-116, 1996.

133. **Leach CS, and Johnson PC**. Influence of spaceflight on erythrokinetics in man. *Science* 225: 216-218, 1984.

134. **Lee SM, Schneider SM, Boda WL, Watenpaugh DE, Macias BR, Meyer RS, and Hargens AR**. LBNP exercise protects aerobic capacity and sprint speed of female twins during 30 days of bed rest. *J Appl Physiol* 106: 919-928, 2009.

135. **Lee SM, Schneider SM, Boda WL, Watenpaugh DE, Macias BR, Meyer RS, and Hargens AR**. Supine LBNP exercise maintains exercise capacity in male twins during 30-d bed rest. *Med Sci Sports Exerc* 39: 1315-1326, 2007.

136. **Levine BD, Lane LD, Buckey JC, Friedman DB, and Blomqvist CG**. Left ventricular pressure-volume and Frank-Starling relations in endurance athletes. Implications for orthostatic tolerance and exercise performance. *Circulation* 84: 1016-1023, 1991.

137. **Levine BD, Lane LD, Watenpaugh DE, Gaffney FA, Buckey JC, and Blomqvist CG**. Maximal exercise performance after adaptation to microgravity. *J Appl Physiol* 81: 686-694, 1996.

138. **Levine BD, Zuckerman JH, and Pawelczyk JA**. Cardiac atrophy after bed-rest deconditioning: a nonneural mechanism for orthostatic intolerance. *Circulation* 96: 517-525, 1997.

139. **Leyk D, Essfeld D, Hoffmann U, Baum K, and Stegemann J**. Influence of body position and pre-exercise activity on cardiac output and oxygen uptake following step changes in exercise intensity. *Eur J Appl Physiol Occup Physiol* 65: 499-506, 1992.

140. **Liu Y, Menold E, Dullenkopf A, Reissnecker S, Lormes W, Lehmann M, and Steinacker JM**. Validation of the acetylene rebreathing method for measurement of cardiac output at rest and during high-intensity exercise. *Clin Physiol* 17: 171-182, 1997.

141. **Ludbrook J**. Should we use one-sided or two-sided P values in tests of significance? *Clin Exp Pharmacol Physiol* 2013.

142. **Lunt MJ, Jenkinson DF, and Kerr D**. Transcranial Doppler blood velocity measurement--the effect of changes in velocity profile. *Ultrasound Med Biol* 26: 1145-1151, 2000.

143. **Lutjemeier BJ, Miura A, Scheuermann BW, Koga S, Townsend DK, and Barstow TJ**. Muscle contraction-blood flow interactions during upright knee extension exercise in humans. *J Appl Physiol* 98: 1575-1583, 2005.

144. **Mancini DM, Bolinger L, Li H, Kendrick K, Chance B, and Wilson JR**. Validation of near-infrared spectroscopy in humans. *J Appl Physiol* 77: 2740-2747, 1994.

145. **Martin WH, 3rd, Montgomery J, Snell PG, Corbett JR, Sokolov JJ, Buckey JC, Maloney DA, and Blomqvist CG**. Cardiovascular adaptations to intense swim training in sedentary middle-aged men and women. *Circulation* 75: 323-330, 1987.

146. **McCurdy MR, Colleran PN, Muller-Delp J, and Delp MD**. Effects of fiber composition and hindlimb unloading on the vasodilator properties of skeletal muscle arterioles. *J Appl Physiol* 89: 398-405, 2000.

147. **McDonald DA**. *Blood flow in arteries*. Baltimore,: Williams & Wilkins Co., 1960, p. 328 p.

148. **McDonald DA**. The relation of pulsatile pressure to flow in arteries. *J Physiol* 127: 533-552, 1955.

149. **McDonald KS, Delp MD, and Fitts RH**. Effect of hindlimb unweighting on tissue blood flow in the rat. *J Appl Physiol* 72: 2210-2218, 1992.

150. **McDonald KS, Delp MD, and Fitts RH**. Fatigability and blood flow in the rat gastrocnemius-plantaris-soleus after hindlimb suspension. *J Appl Physiol* 73: 1135-1140, 1992.

151. **McNally JS, Davis ME, Giddens DP, Saha A, Hwang J, Dikalov S, Jo H, and Harrison DG**. Role of xanthine oxidoreductase and NAD(P)H oxidase in endothelial superoxide production in response to oscillatory shear stress. *Am J Physiol Heart Circ Physiol* 285: H2290-2297, 2003.

152. **Meehan JP**. Investigation to determine the effects of long-term bed rest on G-tolerance and on psychomotor performance. edited by Administration NAaS. Manned Spacecraft Center; Houston, TX: 1966.

153. **Miller VM, and Burnett JC, Jr.** Modulation of NO and endothelin by chronic increases in blood flow in canine femoral arteries. *Am J Physiol* 263: H103-108, 1992.

154. **Minson CT, Halliwill JR, Young TM, and Joyner MJ**. Influence of the menstrual cycle on sympathetic activity, baroreflex sensitivity, and vascular transduction in young women. *Circulation* 101: 862-868, 2000.

155. **Montmerle S, Spaak J, and Linnarsson D**. Lung function during and after prolonged head-down bed rest. *J Appl Physiol* 92: 75-83, 2002.

156. **Moore AD, Lee SM, Stenger MB, and Platts SH**. Cardiovascular exercise in the U.S. space program: Past, present and future. *Acta Astronaut* 66: 974-988, 2010.

157. **Moore RL, and Brown DA**. The Cardiovascular System: Cardiac Function. In: *ACSM's Advanced Exercise Physiology*, edited by Farrell PA, Joyner M, and Caiozzo V, J. Baltimore, MD: 2012.

158. **Moore RL, Musch TI, Yelamarty RV, Scaduto RC, Jr., Semanchick AM, Elensky M, and Cheung JY**. Chronic exercise alters contractility and morphology of isolated rat cardiac myocytes. *Am J Physiol* 264: C1180-1189, 1993.

159. **Mora S, Cook N, Buring JE, Ridker PM, and Lee IM**. Physical activity and reduced risk of cardiovascular events: potential mediating mechanisms. *Circulation* 116: 2110-2118, 2007.

160. **Morganroth J, Maron BJ, Henry WL, and Epstein SE**. Comparative left ventricular dimensions in trained athletes. *Ann Intern Med* 82: 521-524, 1975.

161. **Musacchia XJ, Steffen JM, Fell RD, and Dombrowski MJ**. Skeletal muscle response to spaceflight, whole body suspension, and recovery in rats. *J Appl Physiol* 69: 2248-2253, 1990.

162. **Nadaud S, Philippe M, Arnal JF, Michel JB, and Soubrier F**. Sustained increase in aortic endothelial nitric oxide synthase expression in vivo in a model of chronic high blood flow. *Circ Res* 79: 857-863, 1996.

163. **Naylor LH, Carter H, FitzSimons MG, Cable NT, Thijssen DH, and Green DJ**. Repeated increases in blood flow, independent of exercise, enhance conduit artery vasodilator function in humans. *Am J Physiol Heart Circ Physiol* 300: H664-669, 2011.

164. **Newcomer SC, Thijssen DH, and Green DJ**. Effects of exercise on endothelium and endothelium/smooth muscle cross talk: role of exercise-induced hemodynamics. *J Appl Physiol* 111: 311-320, 2011.

165. **Nielsen HV**. Arterial pressure-blood flow relations during limb elevation in man. *Acta Physiol Scand* 118: 405-413, 1983.

166. **Nixon JV, Murray RG, Bryant C, Johnson RL, Jr., Mitchell JH, Holland OB, Gomez-Sanchez C, Vergne-Marini P, and Blomqvist CG**. Early cardiovascular adaptation to simulated zero gravity. *J Appl Physiol* 46: 541-548, 1979.

167. **Norcross JR, Lee LR, Clowers KG, Morency RM, Desantis L, De Witt JK, Jones JA, Vos JR, and Gernhardt ML**. Feasibility of Performing a Suited 10-km Ambulation on the Moon - Final Report of the EVA Walkback Test (EWT). edited by Administration NAaS2009.

168. **Noris M, Morigi M, Donadelli R, Aiello S, Foppolo M, Todeschini M, Orisio S, Remuzzi G, and Remuzzi A**. Nitric oxide synthesis by cultured endothelial cells is modulated by flow conditions. *Circ Res* 76: 536-543, 1995.

169. **Norsk P**. Cardiovascular and fluid volume control in humans in space. *Curr Pharm Biotechnol* 6: 325-330, 2005.

170. **Osada T, and Radegran G**. Alterations in the blood velocity profile influence the blood flow response during muscle contractions and relaxations. *J Physiol Sci* 56: 195-203, 2006.

171. **Osada T, and Radegran G**. Alterations in the rheological flow profile in conduit femoral artery during rhythmic thigh muscle contractions in humans. *Jpn J Physiol* 55: 19-28, 2005.

172. **Padilla J, Simmons GH, Bender SB, Arce-Esquivel AA, Whyte JJ, and Laughlin MH**. Vascular effects of exercise: endothelial adaptations beyond active muscle beds. *Physiology (Bethesda)* 26: 132-145, 2011.

173. **Padilla J, Simmons GH, Fadel PJ, Laughlin MH, Joyner MJ, and Casey DP**. Impact of aging on conduit artery retrograde and oscillatory shear at rest and during exercise: role of nitric oxide. *Hypertension* 57: 484-489, 2011.

174. **Padilla J, Young CN, Simmons GH, Deo SH, Newcomer SC, Sullivan JP, Laughlin MH, and Fadel PJ**. Increased muscle sympathetic nerve activity acutely alters conduit artery shear rate patterns. *Am J Physiol Heart Circ Physiol* 298: H1128-1135, 2010.

175. **Paffenbarger RS, Jr., Hyde RT, Wing AL, Lee IM, Jung DL, and Kampert JB**. The association of changes in physical-activity level and other lifestyle characteristics with mortality among men. *N Engl J Med* 328: 538-545, 1993.

176. **Parker BA, Trehearn TL, and Meendering JR**. Pick your Poiseuille: normalizing the shear stimulus in studies of flow-mediated dilation. *J Appl Physiol* 107: 1357-1359, 2009.

177. **Perhonen MA, Franco F, Lane LD, Buckey JC, Blomqvist CG, Zerwekh JE, Peshock RM, Weatherall PT, and Levine BD**. Cardiac atrophy after bed rest and spaceflight. *J Appl Physiol* 91: 645-653, 2001.

178. **Perktold K, Thurner E, and Kenner T**. Flow and stress characteristics in rigid walled and compliant carotid artery bifurcation models. *Med Biol Eng Comput* 32: 19-26, 1994.

179. **Platts SH, Strenger MB, Phillips TR, Natalia MA, Angela KB, Levine BD, and Summers R**. Evidence Based Review: Risk of Cardiac Rhythm Problems during Space Flight NASA Scientific and Technical Information Program Office, 2010.

180. **Poliner LR, Dehmer GJ, Lewis SE, Parkey RW, Blomqvist CG, and Willerson JT**. Left ventricular performance in normal subjects: a comparison of the responses to exercise in the upright and supine positions. *Circulation* 62: 528-534, 1980.

181. **Poole DC, Behnke BJ, and Padilla DJ**. Dynamics of muscle microcirculatory oxygen exchange. *Med Sci Sports Exerc* 37: 1559-1566, 2005.

182. **Poole DC, Copp SW, Hirai DM, and Musch TI**. Dynamics of muscle microcirculatory and blood-myocyte O_2 flux during contractions. *Acta Physiol (Oxf)* 202: 293-310, 2011.

183. **Poole DC, Hirai DM, Copp SW, and Musch TI**. Muscle oxygen transport and utilization in heart failure: implications for exercise (in)tolerance. *Am J Physiol Heart Circ Physiol* 302: H1050-1063, 2012.

184. **Poole DC, and Musch TI**. Muscle microcirculatory O_2 exchange in health and disease. *Adv Exp Med Biol* 662: 301-307, 2010.

185. **Porcelli S, Marzorati M, Lanfranconi F, Vago P, Pisot R, and Grassi B**. Role of skeletal muscles impairment and brain oxygenation in limiting oxidative metabolism during exercise after bed rest. *J Appl Physiol* 109: 101-111, 2010.

186. **Prisk GK**. Gas exchange under altered gravitational stress. *Compr Physiol* 1: 339-355, 2011.

187. **Prisk GK**. Microgravity. *Compr Physiol* 1: 485-497, 2011.

188. **Prisk GK**. Microgravity and the lung. *J Appl Physiol* 89: 385-396, 2000.

189. **Prisk GK**. Pulmonary circulation in extreme environments. *Compr Physiol* 1: 319-338, 2011.

190. **Prisk GK, Fine JM, Cooper TK, and West JB**. Lung function is unchanged in the 1 G environment following 6-months exposure to microgravity. *Eur J Appl Physiol* 103: 617-623, 2008.

191. **Prisk GK, Guy HJ, Elliott AR, Deutschman RA, 3rd, and West JB**. Pulmonary diffusing capacity, capillary blood volume, and cardiac output during sustained microgravity. *J Appl Physiol* 75: 15-26, 1993.

192. **Proctor DN, Sinning WE, Bredle DL, and Joyner MJ**. Cardiovascular and peak VO_2 responses to supine exercise: effects of age and training status. *Med Sci Sports Exerc* 28: 892-899, 1996.

193. **Pyke KE, Hartnett JA, and Tschakovsky ME**. Are the dynamic response characteristics of brachial artery flow-mediated dilation sensitive to the magnitude of increase in shear stimulus? *J Appl Physiol* 105: 282-292, 2008.

194. **Pyke KE, and Jazuli F**. Impact of repeated increases in shear stress via reactive hyperemia and handgrip exercise: no evidence of systematic changes in brachial artery FMD. *Am J Physiol Heart Circ Physiol* 300: H1078-1089, 2011.

195. **Pyke KE, and Tschakovsky ME**. Peak vs. total reactive hyperemia: which determines the magnitude of flow-mediated dilation? *J Appl Physiol* 102: 1510-1519, 2007.

196. **Pyke KE, and Tschakovsky ME**. The relationship between shear stress and flow-mediated dilatation: implications for the assessment of endothelial function. *J Physiol* 568: 357-369, 2005.

197. **Ranjan V, Xiao Z, and Diamond SL**. Constitutive NOS expression in cultured endothelial cells is elevated by fluid shear stress. *Am J Physiol* 269: H550-555, 1995.

198. **Ray CA, and Cureton KJ**. Interactive effects of body posture and exercise training on maximal oxygen uptake. *J Appl Physiol* 71: 596-600, 1991.

199. **Ray CA, Cureton KJ, and Ouzts HG**. Postural specificity of cardiovascular adaptations to exercise training. *J Appl Physiol* 69: 2202-2208, 1990.

200. **Reinke W, Johnson PC, and Gaehtgens P**. Effect of shear rate variation on apparent viscosity of human blood in tubes of 29 to 94 microns diameter. *Circ Res* 59: 124-132, 1986.

201. **Rerych SK, Scholz PM, Sabiston DC, Jr., and Jones RH**. Effects of exercise training on left ventricular function in normal subjects: a longitudinal study by radionuclide angiography. *Am J Cardiol* 45: 244-252, 1980.

202. **Roca J, Agusti AG, Alonso A, Poole DC, Viegas C, Barbera JA, Rodriguez-Roisin R, Ferrer A, and Wagner PD**. Effects of training on muscle O_2 transport at VO_2max. *J Appl Physiol* 73: 1067-1076, 1992.

203. **Rowell LB**. *Human cardiovascular control*. New York: Oxford University Press, 1993, p. xv, 500 p.

204. **Rubanyi GM, Romero JC, and Vanhoutte PM**. Flow-induced release of endothelium-derived relaxing factor. *Am J Physiol* 250: H1145-1149, 1986.

205. **Rummel JA, Michel EL, and Berry CA**. Physiological response to exercise after space flight--Apollo 7 to Apollo 11. *Aerosp Med* 44: 235-238, 1973.

206. **Rushmer RF**. Postural effects on the baselines of ventricular performance. *Circulation* 20: 897-905, 1959.

207. **Sadeh JS, Miller A, and Kukin ML**. Noninvasive measurement of cardiac output by an acetylene uptake technique and simultaneous comparison with thermodilution in ICU patients. *Chest* 111: 1295-1300, 1997.

208. **Salanova M, Schiffl G, Puttmann B, Schoser BG, and Blottner D**. Molecular biomarkers monitoring human skeletal muscle fibres and microvasculature following long-term bed rest with and without countermeasures. *J Anat* 212: 306-318, 2008.

209. **Saltin B, Blomqvist CG, Mitchell JH, Johnson RL, Wildenthal K, Chapman CB, Frenkel E, Norton W, Spiperstein M, Suki W, and Vastagh G**. A Longitudinal Study of Adaptive Changes in Oxygen Transport and Body Composition. *Circulation* 38: VII-1, 1968.

210. **Saltin B, Blomqvist G, Mitchell JH, Johnson RL, Jr., Wildenthal K, and Chapman CB**. Response to exercise after bed rest and after training. *Circulation* 38: VII1-78, 1968.

211. **Saltin B, Radegran G, Koskolou MD, and Roach RC**. Skeletal muscle blood flow in humans and its regulation during exercise. *Acta Physiol Scand* 162: 421-436, 1998.

212. **Salvadego D, Lazzer S, Marzorati M, Porcelli S, Rejc E, Simunic B, Pisot R, di Prampero PE, and Grassi B**. Functional impairment of skeletal muscle oxidative metabolism during knee extension exercise after bed rest. *J Appl Physiol* 111: 1719-1726, 2011.

213. **Sawin CF, Nicogossian AE, Rummel JA, and Michel EL**. Pulmonary function evaluation during the Skylab and Apollo-Soyuz missions. *Aviat Space Environ Med* 47: 168-172, 1976.

214. **Schmid-Schoenbein GW, and Zweifach BW**. RBC velocity profiles in arterioles and venules of the rabbit omentum. *Microvasc Res* 10: 153-164, 1975.

215. **Severinghaus JW**. Simple, accurate equations for human blood O_2 dissociation computations. *J Appl Physiol* 46: 599-602, 1979.

216. **Shibata S, Perhonen M, and Levine BD**. Supine cycling plus volume loading prevent cardiovascular deconditioning during bed rest. *J Appl Physiol* 108: 1177-1186, 2010.

217. **Shoemaker JK, Hogeman CS, Silber DH, Gray K, Herr M, and Sinoway LI**. Head-down-tilt bed rest alters forearm vasodilator and vasoconstrictor responses. *J Appl Physiol* 84: 1756-1762, 1998.

218. **Shykoff BE, Farhi LE, Olszowka AJ, Pendergast DR, Rokitka MA, Eisenhardt CG, and Morin RA**. Cardiovascular response to submaximal exercise in sustained microgravity. *J Appl Physiol* 81: 26-32, 1996.

219. **Simmons GH, Padilla J, Young CN, Wong BJ, Lang JA, Davis MJ, Laughlin MH, and Fadel PJ**. Increased brachial artery retrograde shear rate at exercise onset is abolished during prolonged cycling: role of thermoregulatory vasodilation. *J Appl Physiol* 110: 389-397.

220. **Spaak J, Montmerle S, Sundblad P, and Linnarsson D**. Long-term bed rest-induced reductions in stroke volume during rest and exercise: cardiac dysfunction vs. volume depletion. *J Appl Physiol* 98: 648-654, 2005.

221. **Stabley JN, Dominguez JM, 2nd, Dominguez CE, Mora Solis FR, Ahlgren J, Behnke BJ, Muller-Delp JM, and Delp MD**. Spaceflight reduces vasoconstrictor responsiveness of skeletal muscle resistance arteries in mice. *J Appl Physiol* 113: 1439-1445, 2012.

222. **Stenger MB, Evans JM, Knapp CF, Lee SM, Phillips TR, Perez SA, Moore AD, Jr., Paloski WH, and Platts SH**. Artificial gravity training reduces bed rest-induced cardiovascular deconditioning. *Eur J Appl Physiol* 112: 605-616, 2012.

223. **Stevens PM, Miller PB, Lynch TN, Gilbert CA, Johnson RL, and Lamb LE**. Effects of lower body negative pressure on physiologic changes due to four weeks of hypoxic bed rest. *Aerosp Med* 37: 466-474, 1966.

224. **Stremel RW, Convertino VA, Bernauer EM, and Greenleaf JE**. Cardiorespiratory deconditioning with static and dynamic leg exercise during bed rest. *J Appl Physiol* 41: 905-909, 1976.

225. **Taylor HL, and Henschel A**. Effects of bed rest on cardiovascular function and work performance. *J Appl Physiol* 2: 223-239, 1949.

226. **Thadani U, and Parker JO**. Hemodynamics at rest and during supine and sitting bicycle exercise in normal subjects. *Am J Cardiol* 41: 52-59, 1978.

227. **Thijssen DH, Black MA, Pyke KE, Padilla J, Atkinson G, Harris RA, Parker B, Widlansky ME, Tschakovsky ME, and Green DJ**. Assessment of flow-mediated dilation in humans: a methodological and physiological guideline. *Am J Physiol Heart Circ Physiol* 300: H2-12, 2011.

228. **Thijssen DH, Dawson EA, Black MA, Hopman MT, Cable NT, and Green DJ**. Brachial artery blood flow responses to different modalities of lower limb exercise. *Med Sci Sports Exerc* 41: 1072-1079, 2009.

229. **Thijssen DH, Dawson EA, Tinken TM, Cable NT, and Green DJ**. Retrograde flow and shear rate acutely impair endothelial function in humans. *Hypertension* 53: 986-992, 2009.

230. **Thijssen DH, Green DJ, and Hopman MT**. Blood vessel remodeling and physical inactivity in humans. *J Appl Physiol* 111: 1836-1845, 2011.

231. **Thijssen DH, Maiorana AJ, O'Driscoll G, Cable NT, Hopman MT, and Green DJ**. Impact of inactivity and exercise on the vasculature in humans. *Eur J Appl Physiol* 108: 845-875, 2010.

232. **Tinken TM, Thijssen DH, Hopkins N, Black MA, Dawson EA, Minson CT, Newcomer SC, Laughlin MH, Cable NT, and Green DJ**. Impact of shear rate modulation on vascular function in humans. *Hypertension* 54: 278-285, 2009.

233.   **Tinken TM, Thijssen DH, Hopkins N, Dawson EA, Cable NT, and Green DJ**. Shear stress mediates endothelial adaptations to exercise training in humans. *Hypertension* 55: 312-318, 2010.

234.   **Trappe S, Costill D, Gallagher P, Creer A, Peters JR, Evans H, Riley DA, and Fitts RH**. Exercise in space: human skeletal muscle after 6 months aboard the International Space Station. *J Appl Physiol* 106: 1159-1168, 2009.

235.   **Trappe SW, Trappe TA, Lee GA, Widrick JJ, Costill DL, and Fitts RH**. Comparison of a space shuttle flight (STS-78) and bed rest on human muscle function. *J Appl Physiol* 91: 57-64, 2001.

236.   **Trappe T, Trappe S, Lee G, Widrick J, Fitts R, and Costill D**. Cardiorespiratory responses to physical work during and following 17 days of bed rest and spaceflight. *J Appl Physiol* 100: 951-957, 2006.

237.   **Uematsu M, Ohara Y, Navas JP, Nishida K, Murphy TJ, Alexander RW, Nerem RM, and Harrison DG**. Regulation of endothelial cell nitric oxide synthase mRNA expression by shear stress. *Am J Physiol* 269: C1371-1378, 1995.

238.   **Verbandt Y, Wantier M, Prisk GK, and Paiva M**. Ventilation-perfusion matching in long-term microgravity. *J Appl Physiol* 89: 2407-2412, 2000.

239.   **Wagner PD**. Algebraic analysis of the determinants of VO_2max. *Respir Physiol* 93: 221-237, 1993.

240.   **Wagner PD**. Determinants of maximal oxygen transport and utilization. *Annu Rev Physiol* 58: 21-50, 1996.

241.   **Wagner PD**. Gas exchange and peripheral diffusion limitation. *Med Sci Sports Exerc* 24: 54-58, 1992.

242.   **Wagner PD**. Modeling O_2 transport as an integrated system limiting VO_2MAX. *Comput Methods Programs Biomed* 101: 109-114, 2011.

243.   **Wagner PD, Hoppeleer H, and Saltin B**. Determinants of maximal oxygen uptake. In: *The Lung: Scientific Foundations*. New York: Raven, 1997, p. 2033-2041.

244.   **Wasserman K**. *Principles of exercise testing and interpretation : including pathophysiology and clinical applications*. Philadelphia: Wolters Kluwer Health/Lippincott Williams & Wilkins, 2012, p. p.

245.   **Watenpaugh DE**. Fluid volume control during short-term space flight and implications for human performance. *J Exp Biol* 204: 3209-3215, 2001.

246.   **Watenpaugh DE, Ballard RE, Schneider SM, Lee SM, Ertl AC, William JM, Boda WL, Hutchinson KJ, and Hargens AR**. Supine lower body negative pressure exercise during bed rest maintains upright exercise capacity. *J Appl Physiol* 89: 218-227, 2000.

247. **Watenpaugh DE, and Hargens AR**. The cardiovascular system in microgravity. In: *Handbook of Physiology: Environmental Physiology*, edited by Fregly MJ, and Blatteis CM. New York: Oxford University Press, 1996, p. 631-674.

248. **West JB**. *Regional differences in the lung*. New York: Academic Press, 1977, p. xiv, 488 p.

249. **West JB**. *Respiratory physiology : the essentials*. Philadelphia: Wolters Kluwer Health/Lippincott Williams & Wilkins, 2008, p. ix, 186 p.

250. **West JB, Guy HJ, Elliott AR, and Prisk GK**. Respiratory System in Microgravity. In: *Handbook of Physiology, Environmental Physiology*. New York: Oxford University Press, 1996, p. 675-689.

251. **Williams DA, and Convertino VA**. Circulating lactate and FFA during exercise: effect of reduction in plasma volume following exposure to simulated microgravity. *Aviat Space Environ Med* 59: 1042-1046, 1988.

252. **Wilson AF, Savariryan S, James N, Mukai D, and Nishimura E**. Almost simultaneous measurement of cardiovascular and gas exchange variables during maximal exercise. *Med Sci Sports Exerc* 28: 436-443, 1996.

253. **Woodman CR, Muller JM, Rush JW, Laughlin MH, and Price EM**. Flow regulation of ecNOS and Cu/Zn SOD mRNA expression in porcine coronary arterioles. *Am J Physiol* 276: H1058-1063, 1999.

254. **Wright JR, McCloskey DI, and Fitzpatrick RC**. Effects of muscle perfusion pressure on fatigue and systemic arterial pressure in human subjects. *J Appl Physiol* 86: 845-851, 1999.

255. **Yeboah J, Folsom AR, Burke GL, Johnson C, Polak JF, Post W, Lima JA, Crouse JR, and Herrington DM**. Predictive value of brachial flow-mediated dilation for incident cardiovascular events in a population-based study: the multi-ethnic study of atherosclerosis. *Circulation* 120: 502-509, 2009.

256. **Young CN, Deo SH, Padilla J, Laughlin MH, and Fadel PJ**. Pro-atherogenic shear rate patterns in the femoral artery of healthy older adults. *Atherosclerosis* 211: 390-392, 2010.

257. **Yuan M, Coupe M, Bai Y, Gauquelin-Koch G, Jiang S, Aubry P, Wan Y, Custaud MA, Li Y, and Arbeille P**. Peripheral arterial and venous response to tilt test after a 60-day bedrest with and without countermeasures (ES-IBREP). *PLoS One* 7: e32854, 2012.

258. **Ziegler T, Bouzourene K, Harrison VJ, Brunner HR, and Hayoz D**. Influence of oscillatory and unidirectional flow environments on the expression of endothelin and nitric oxide synthase in cultured endothelial cells. *Arterioscler Thromb Vasc Biol* 18: 686-692, 1998.

Appendix A - Curriculum Vitae

Carl J. Ade

Department of Kinesiology   Phone: (785) 577-4098
Department of Anatomy & Physiology Fax: (785) 532-6486
Kansas State University   email: cade@ksu.edu
1A Natatorium
Manhattan, KS

Education

2008-	Ph.D. Candidate (ABD) (Anatomy & Physiology) Focus: Cardiorespiratory, Cardiovascular, and Gravitational Physiology Kansas State University Manhattan, KS
2009	Specialized Student (Radiologic Technology) Focus: Cardiac and Vascular Sonography University of Oklahoma Health Science Center Oklahoma City, OK
2006-2008	M.S. (Kinesiology) Kansas State University Manhattan, KS
2001-2004	B.S. (Biology, Chemistry minor) Kansas Wesleyan University Salina, KS

Teaching, Research and Employment

2008-	Research Assistant; Human Exercise Physiology Laboratory, Cardiovascular and Thermal Physiology Laboratory Department of Kinesiology Kanas State University; Manhattan, KS
2008-2012	Instructor Department of Science Cloud County Community College; Junction City, KS

2009-2011	Instructor
	Department of Science
	Manhattan Area Technical College; Manhattan, KS

2009-2011   Instructor
            Department of Science
            Manhattan Area Technical College; Manhattan, KS

2007-2008   Undergraduate Student Advisor
            Department of Kinesiology
            Kansas State University; Manhattan, KS

2006-2008   Teaching Assistant
            Department of Kinesiology
            Kanas State University; Manhattan, KS

2005-2006   Physical Therapy Technician
            Comcare Inc; Salina, KS

Research Grant Awards

Awarded

2013   National Aeronautics and Space Administration (NASA) NNJ12ZSA002N, "Determining the Effect of Spaceflight on the Incidence of Cardiovascular Risk Factors and Disease" Total Cost: $100,000. Co-PI: **CJ Ade**, Co-PI: TJ Barstow

2011-2013   National Aeronautics and Space Administration (NASA) NNX10AK60G "Standardized 'Pre-Flight' Exercise Tests to Predict Performance during Extravehicular Activities in a Lunar Environment", Total Cost: $1,200,000. PI: TJ Barstow, Co-I: **CJ Ade**, S Warren, D Schinstock

2009   National Aeronautics and Space Administration: Kansas Space Grant Consortium, Total Cost: $12,000. PI: BJ Wong, Student-Investigator **CJ Ade**

2009   Kansas State University Dr. Albert's Memorial Research Award, Total Cost $950, PI: **CJ Ade**

Declined

2013   National Aeronautics and Space Administration (NASA) NNJ12ZSA002N, "Innovative Bed Rest Protocol to Determine the Effects of Space Flight and Mars Gravity on exercise Analogs of EVA Performance" Total Cost: $100,000. PI: **CJ Ade**, Co-PI: TJ Barstow

2013   National Aeronautics and Space Administration (NASA) NNJ12ZSA002N, "Consequences of Microgravity and Simulated Space Suit on Muscle Activation and Metabolism" Total Cost: $100,000. PI: TJ Barstow, Co-PI: **CJ Ade**

Academic Awards:

2009   American Physiological Society "Exercise and Environmental Physiology –
                Space and Biomedical Research Institute's Gravitational Physiology Award for
                Young Investigators"

2010-2011   Kansas State University Graduate Student Travel Award

2012   Kanas State University College of Veterinary Medicine Travel Award

---

National Societies

American Physiological Society
American College of Sports Medicine

Teaching Experience

2008-2013   Cloud County Community College
                        Anatomy & Physiology I (Lecture and Laboratory)
                        Anatomy & Physiology II (Lecture and Laboratory)

2009-2011   Manhattan Area Technical College
                        Anatomy & Physiology (Lecture and Laboratory)
                        Microbiology (Lecture and Laboratory)

2006-2008   Kansas State University
                        Exercise Testing & Prescription (Laboratory)
                        Biomechanics (Laboratory)
                        Cardiovascular Physiology (Guest Lecture)

2008   Kansas State University
                        American College of Sports Medicine Health and Fitness Instructor
                        Workshop (Lecture)

Journals Reviewed

Journal of Applied Physiology
European Journal of Applied Physiology
Experimental Physiology

Peer-Reviewed Publications

---

1. **Ade CJ** and Wong BJ. Invited Commentary. Viewpoint: Is left-ventricular volume
   during diastasis the real equilibrium volume and, what is its relationship to diastolic
   suction? *J Appl Physiol*, 2008 Sep; 105(3): 1017

134

2. **Ade CJ**, Broxterman RM, Wong BJ, Barstow TJ. Critical Velocity and Maximal Lactate Steady State: Better Determinants of 2-hour marathon. *J Appl Physiol*, 2011 Jan; 110(1): 278-93

3. **Ade CJ**, R.M Broxterman, B.J. Wong, T.J. Barstow. Antegrade and Retrograde Blood Velocity Profiles in the Intact Human Cardiovascular System. *Exp Physiol* 2012 Jul; 97(7):849-60

4. Dana G, Broxterman R, **Ade CJ**, Barstow T, Nelson T, Song W, Warren S. "Automated Hand-Forearm Ergometer Data Collection System," *34th Annual International Conference of the IEEE Engineering in Medicine and Biology Society*, Hilton Bayfront Hotel, San Diego, CA, USA, August 28 – September 1, 2012.

5. Song W, **Ade CJ**, Barstow T, Barstow T, Nelson T, Warren S. "Activity Recognition in Planetary Navigation Field Tests Using Classification Algorithms Applied to Accelerometer Data," *34th Annual International Conference of the IEEE Engineering in Medicine and Biology Society*, Hilton Bayfront Hotel, San Diego, CA, USA, August 28 – September 1, 2012.

6. Broxterman R.M, **Ade C.J.**, Harms C.A., Poole D.C., Barstow T.J. A Single Test for the Determination of Parameters of the Speed-time Relationship for running. *Respir Physiol Neurobiol*, 185 (2), 380-5, 2013

7. **Ade, CJ,** Broxterman, RM, Barstow, TJ**.** Effects of body posture and exercise training on cardiorespiratory responses to exercise. *Resp Phys Neurobiol* 188, 39-48, 2013

8. **Ade, CJ,** Broxterman, RM, Craig J, Schlup SJ, Wilcox SL, Barstow, TJ**.** Influence of prior sustained antegrade shear rate on the vascular responses during dynamic forearm exercise. *Exp Physiol*. In review

9. Smith JR, **Ade CJ**, Broxterman RM, Skutnik BC, Barstow TJ, Wong BJ, Harms CA. Influence of respiratory muscle fatigue on brachial artery blood flow during cycling exercise. *J Physiol*. In review

---

<div align="center">Scientific Presentations</div>

---

1. **C.J. Ade**, C. McClain, C.A. Harms, T.I. Musch, T.J. Barstow. Effects of Upright, Supine and -6° Head-down tilt Posture on Cardiovascular and Exercise Performance. Central States Chapter of American College of Sports Medicine. Kansas City. October 2008

2. **C.J. Ade**. Influence of a Negative Hydrostatic Column and Central Fluid Shift via -6° Head-down Tilt Posture on Cardiovascular Performance. Anatomy & Physiology Department Seminar, Kansas State University. 2009

3. **C.J. Ade**. Effects of Fish Oil Supplementation of Airway Inflammation. Anatomy & Physiology Department Seminar, Kansas State University. 2010

4. C.M Bopp, B.J. Wong, **C.J. Ade**, R.M. Broxterman, S. Wilcox, T.J. Barstow. Ibuprofen Alters Initial Time Course of Hyperemic Response within Skeletal Muscle, but not Cutaneous Microvasculature during Post-Occlusive Reactive Hyperemia. American College of Sports Medicine. Denver. June 2011.

5. **C.J. Ade**, R.M Broxterman, G.L. Gadbury, D. Schinstock, S. Warren, T.J. Barstow. Physiologic Responses during Simulated Planetary Field Tests. American College of Sports Medicine. San Francisco 2012

6. R.M Broxterman, **C.J Ade**, G.L. Gadbury, D. Schinstock, S. Warren, T.J. Barstow. Gender differences in laboratory assessment and simulated EVA performance. NASA HRP Presentation. Glaveston 2013

Abstracts

1. **C.J. Ade**, C.A. Harms, T.I. Musch, T.J. Barstow. Influence of a Negative Hydrostatic Column and Central Fluid Shift via -6° Head-down-tilt Posture on Cardiovascular Performance. Experimental Biology. New Orleans. April 2009

2. **C.J. Ade**, B.J. Wong, R.M Broxterman, T.J. Barstow, Brachial and Femoral Artery Blood Velocity Profiles are Quasi-Parabolic during Physiologic Stress. Experimental Biology, Washington DC. April 2011

3. **C.J. Ade**, SK Rosenkranz, C.A. Harms. An anti-inflammatory role for fish oil supplementation. Experimental Biology. Washington DC. April 2011

4. **C.J. Ade**, R.M Broxterman, S. Warren, R.D. Taylor, T.J. Barstow. Development of Standardized Exercise Tests for Planetary Task Performance. IAA Humans in Space Symposium. Houston. April 2011

5. Broxterman R.M, **Ade C.J.**, Barstow T.J., A Single Test for the Determination of Critical Velocity, American College of Sports Medicine. Denver. June 2011

6. **C.J Ade**, SK Rosenkranz, C.A. Harms. Fish oil supplementation protects against airway inflammation following a high fat meal. American College of Sports Medicine. Denver. June 2011

7. **C.J. Ade**, R.M. Broxterman, G.L. Gadbury, D. Schinstock, S. Warren, T.J. Barstow. Standardized Exercise Test to Evaluate Planetary Mission Readiness. NASA Humans Research Program Workshop. Houston. February 2012

8. Broxterman R.M, **Ade C.J.**, Gadbury G.L., Schinstock D., Warren S., Barstow T.J. Standardized Exercise Test to Evaluate Planetary Mission Readiness. NASA Humans Research Program Workshop. Houston. February 2012

9. Broxterman R.M, **Ade C.J.**, Gadbury G.L., Schinstock D., Warren S., Barstow T.J. Predictors of 10-Kilometer Performance. American College of Sports Medicine. San Francisco 2012

10. **Ade CJ**, Broxternam RM, SJ Schlup, Wilcox SL, Barstow TJ. Influence of duty cycle on muscle deoxy-[Hb+Mb] during ramp hand grip exercise. APS Intersociety Meeting: Integrative Biology of Exercise. Westminster. October 2012

11. Broxternam RM, **Ade CJ**, Wilcox SL, SJ Schlup, Barstow TJ. Influence of altered duty cycle on critical power during hand grip exercise. APS Intersociety Meeting: Integrative Biology of Exercise. Westminster. October 2012

12. **Ade CJ**, Broxternam RM, Schlup SJ, Wilcox SL, Craig JC, Bernard J, Barstow TJ. Effects of Retrograde Shear on the Kinetics of Blood Flow to Hand Grip Exercise. American College of Sports Medicine. Indianapolis. June 2013

13. Broxternam RM, **Ade CJ**, Wilcox SL, Schlup SJ, Mendoza Y, Barstow TJ. Influence Of Oxygen Delivery On The Parameters Of The Power-duration Relationship. American College of Sports Medicine. Indianapolis. June 2013

14. Schlup SJ, **Ade CJ**, Broxternam RM, Wilcox SL, Craig JC, Barstow TJ. Kinetics Of Leg And Capillary Blood Flow Response To Knee Extension Exercise. Indianapolis. June 2013

15. Smith JR, **Ade CJ**, Broxternam RM, Skutnik BC, Harms CA. The Influence of Respiratory Muscle Fatigue on Inactive Arm Blood Flow during Cycling Exercise. American College of Sports Medicine. Indianapolis. June 2013

16. Craig JC, **Ade CJ**, Broxternam RM, Wilcox SL, Schlup SJ, Mendoza Y, Chavez L, , Barstow TJ. The Relationship Between Critical Speed and the Respiratory Compensation Point. American College of Sports Medicine. Indianapolis. June 2013

17. Wilcox SL, Broxternam RM, **Ade CJ**, Schlup SJ, Craig JC, Chavez L, Mendoza Y, Barstow TJ. The Relationship between Physiologic Parameters in Upper versus Lower Body Exercise. American College of Sports Medicine. Indianapolis. June 2013